SHORELINE EVOLUTION MODEL WITH A GROIN STRUCTURE WITH BREAKING WAVE CREST IMPACT

PIDOK UNYAPOTI

A THESIS SUBMITTED IN PARTIAL FULFILLMENT OF THE REQUIREMENT FOR
THE DEGREE OF DOCTOR OF PHILOSOPHY IN APPLIED MATHEMATICS
DEPARTMENT OF MATHEMATICS SCHOOL OF SCIENCE
KING MONGKUT'S INSTITUTE OF TECHNOLOGY LADKRABANG
2023

KMITL-2023-SC-D-001-014

Thesis Title	Shoreline Evolution Model with a Groin Structure with Breaking Wave Crest Impact
Student Name	Mr.Pidok Unyapoti
Student ID	63605005
Degree	Doctor of Philosophy (Applied Mathematics)
Department	Mathematics
Year	2023
Thesis Advisor	Assoc.Prof.Dr.Nopparat Pochai

Abstract

Beach erosion is a natural process that occurs when conveying sediment away from the shoreline is not balanced by depositing new material on the shoreline. This is a problem that is causing beach areas to decline. To avoid beach erosion and flooding, a sea wall and groin have been built. Shoreline evolution prediction is used to investigate the beach topography in the future. There are three phenomena give a large effect to the coastal structure such as the erosion, the accretion and the water level changes. To investigate of beach erosion and beach deposition is needed qualitative understanding of idealized shoreline response to the governing process. The first part of this research we introduce a governing equation of a one-dimensional shoreline evolution model when a couple of groins is added. The manipulation of physical parameters for the model is introduced. The setting method of the initial condition and the boundary conditions techniques when a couple of groin structure effect are also proposed. The proposed simulation can be used to predict the efficiency of a groin system construction in a local beach. The second part of this research, we present a one-dimensional mathematical model of shoreline evolution, and the parameters that influence this model are described monthly over a period of one year. Consideration is given to the wave crest impact model for evaluating the impact of the wave crest at that stage. It focuses on the evolution of the shoreline in environments where groins are installed on both sides. The initial and boundary conditions setting techniques are proposed by the groins and their environmental parameters. The non-uniform influence of the crest of the breaking wave is so often considered.

Keywords : shoreline evolution, groin system, explicit finite method, wave crest impact, mathematical model.

Acknowledgements

I would like to thank the many people who helped me reach this point. My advisor Assoc. Prof. Dr. Nopparat Pochai, for taking me on as a student, introducing me to mathematics and methodology knowledge and enduring my frequent tardiness. Assoc. Prof. Dr. Nopparat Pochai, for give me a scholarship. My family no matter where I have gone, home has always been with you. My classmate for our friendship, supportiveness and helping me find my way through graduate.

Pidok Unyapoti

Table of Contents

List of Tables

Table **Page**

List of Figures

Figure **Page**

Chapter 1

Introduction

1.1 Research Motivation

The beach area is an area with potential for development and use in various fields. whether it is an industrial, tourist, or residential area. It is also important in the ecosystem and in the natural habitats of various types of animals and plants. In Thailand, beaches are important to the economy in terms of tourism. And the marine area is known for being abundant and beautiful, thus generating income and creating careers in nearby communities. Therefore, if the beach area is lost, it will affect income and occupation in the community, and it will also affect the economy.

(a) Pattaya beach *(b)* phuket beach

Figure 1.1: Famous beach in Thailand [3]

Beach deposition and erosion are two major phenomena that have an impact on beach areas. Beach deposition and beach erosion are natural processes that occur whenever the transport of material away from the beach is not balanced by new material being deposited on the beach. Beach deposition, which is the transport of material away from the beach, is less than new material being deposited onto the beach. Beach erosion is the transport of material away from the beach, more than new material being deposited on the beach.

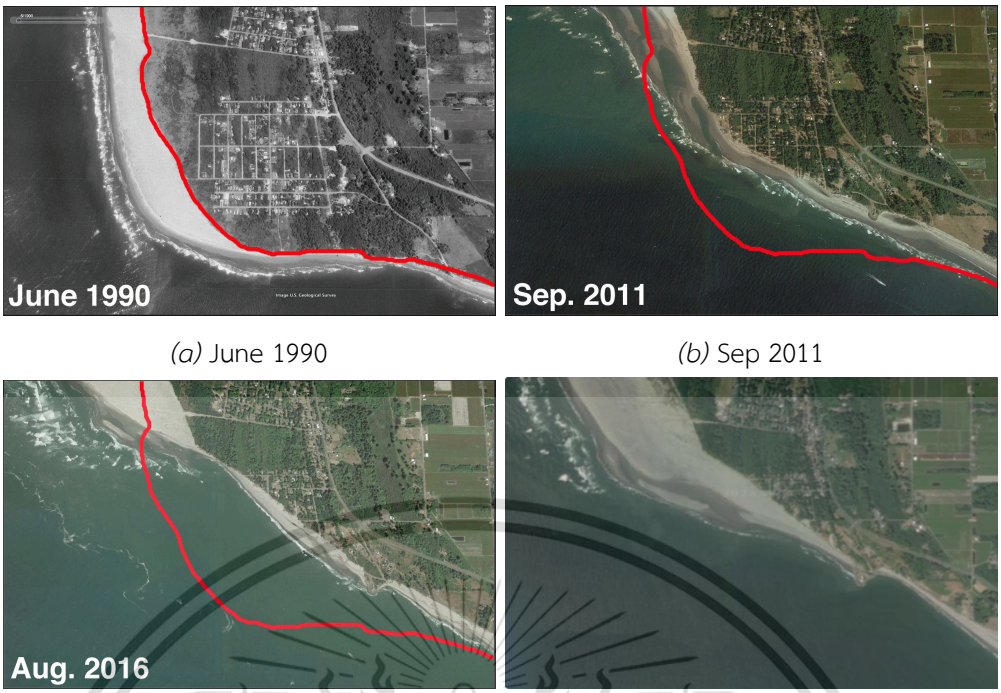

(a) June 1990 *(b)* Sep 2011

(c) Aug 2016 *(d)* 2022

Figure 1.2*:* Washaway Beach shoreline [1].

Many countries have lost beach areas due to beach erosion. Beach erosion affects more than just beaches. Sometimes it affects the buildings along the shore. And many people have lost their living space as a result of beach erosion. This makes beach erosion a major problem in many countries.

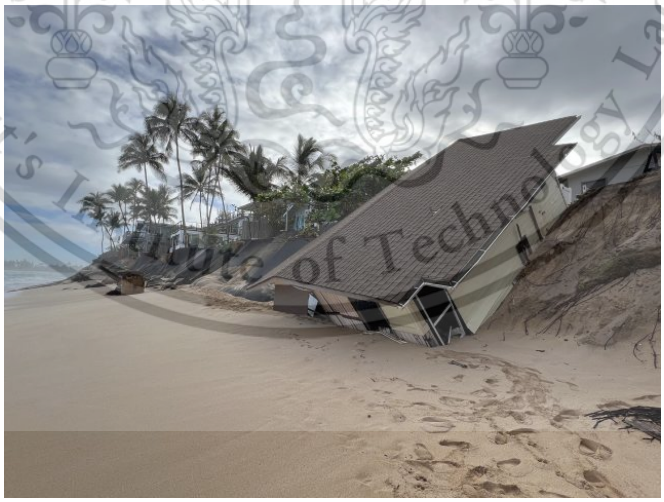

Figure 1.3*:* Oahu's North Shore in March 2022 [2].

Thailand has more than 3,000 kilometers of shoreline covering 23 provinces and over 800 kilometers of that shoreline are currently suffering from coastal erosion. The entire coastal area of Thailand has been eroded by 180.8672 square kilometers in the past 30 years. The rate of coastal erosion on the Gulf of Thailand and the

Andaman average is more than 5.0 meters per year.

(a) 2015 *(b)* 2017

Figure 1.4*:* Haad Kaew Resort, Songkhla, Thailand From Google earth

To protect the beach area from beach erosion. As a result, various methods have been invented, as have many different structures.

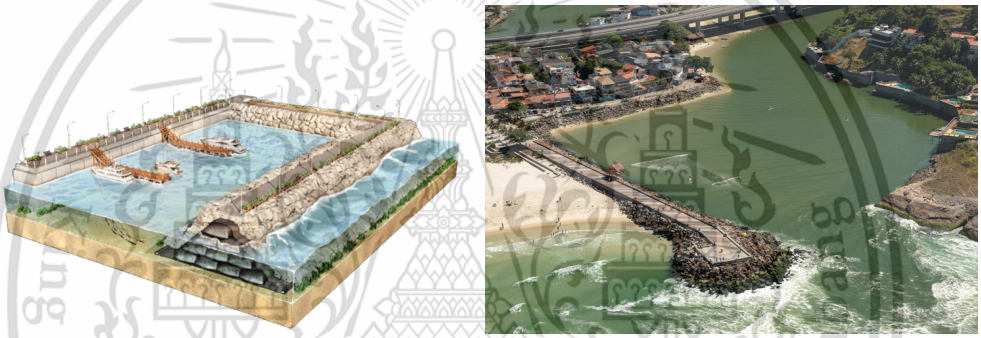

Figure 1.5*:* Breakwater [5],[6].

A breakwater is a permanent structure constructed in a coastal area to create a safe harbor, marina, or anchorage for fishing vessels, and protect against tides, currents, waves, and storm surges.

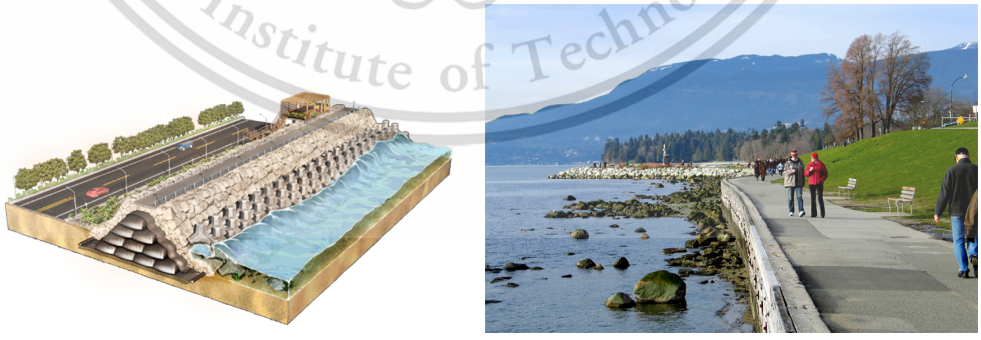

Figure 1.6*:* Seawall [5],[6].

A seawall is a large barrier built along the shoreline. The purpose of a seawall is to protect areas of human habitation, conservation, and leisure activities from the action of tides, waves.

Figure 1.7*:* Detached Breakwater [5],[6].

A detached Breakwaters are primarily installed near the surf zone to mitigate swift water currents that scour coastlines.

Figure 1.8*:* Groin [5],[6].

(a) 1991. *(b)* 2004.

Figure 1.9*:* Cape May Point [7].

A groin is a medium-sized artificial structure built on a shoreline or a riverbank to interrupt water flow and limit sediment movement.

1.2 Literature Review

In [8], they presented realistic cost-benefit scenarios for important stakeholders and policy-makers in order to prioritize and allocate costs and benefits from a "beach governance" perspective, based on the Integrated Coastal Management (ICM) framework. The empirical investigation presented here uses the highly touristic coastal city of Rethymnon on the island of Crete as the study area. In [9], They demonstrated a novel approach that combines citizen science with low-cost unmanned aerial vehicles to produce survey-grade morphological data that can be used to model sediment dynamics from event to annual scales. The high-energy wave-dominated coast of Victoria in south-eastern Australia is used as a field laboratory to test the reliability of our protocol and develop a set of indices to study multi-scale erosional dynamics.

To prevent beach erosion and beach deposition so it has devised a sea wall and groin. In [11], they presented a description of the observed behavior and evolution of beaches with seawalls subjected to raised water levels, investigated the potential influence of wave climate (erosive versus accretionary), and proposed a new methodology for predicting profile evolution due to sea level rise (SLR) at seawalls. The experiments were carried out in a 44 m (L) x 1.2 m (W) x 1.6 m (D) wave flume to study the effect of coastal armoring in the form of seawalls on coastal response to SLR. In [12], they presented sediment transport and erosion-deposition patterns near a detached, low-crested breakwater protecting Carey Island's cohesive shore in Malaysia. Their study found that the conductivity of the breakwater structure is essential to reducing erosion issues on Carey Island's cohesive coasts and to the effectiveness of mangrove rehabilitation initiatives in the area. In [13], they predicted the most likely total water level scenarios that result in overtopping at Santos Bay beaches and examined overtopping events in 2016. The prediction shows that the wider and flatter profiles in the western portion of Santos and Itararé provide greater protection from storm events, while the steeper eastern stretch of Santos Beach is more vulnerable to overtopping events. Their research focuses on beaches in Santos and So Vicente (So Paulo, Brazil). A seawall surrounds the entire 7 kilometer stretch of shoreline.

Many authors have achieved an analytical solution to the evolution of the shoreline using a basic mathematical method. Many authors have developed one-line theory, and several contributors include [14], [15], [16], [17], [18], [19], and [20] in the analytical solution of the evolution of the shoreline. Analytical solutions cannot be assumed to present quantitatively precise solutions to the problems containing complex boundary conditions and wave inputs.

A numerical model of shoreline evolution would be more fitting in the actual case. A general expression for the long-shore sand transport rate was developed by [21]. The empirical predictive formula for the amplitude of the long-shore sand

transport rate presented by [22]. In [23], they have examined and presented two numerical schemes of shoreline evolution for simplified configuration beach.

In this research, the governing equation of a one-dimensional shoreline evolution model is introduced. We will also propose techniques for initial conditions and boundary conditions when a couple of groins and a couple of T-heads are added. We will propose a wave crest impact model for a couple of groins. Finite difference techniques will be used to approximate the model solution.

1.3 Objectives of the study

1) We will introduce a governing equation for a one-dimensional shoreline evolution when a couple of groins are added to the model.
2) We will introduce a governing equation for a one-dimensional shoreline evolution when a couple of T-head groins are added to the model.
3) We will introduce the manipulation of physical parameters for the shoreline evolution model.
4) We will propose the setting method for the initial and the boundary conditions techniques when a couple of groins are added.
5) We will propose the setting method for the initial and the boundary conditions techniques when a couple of T-head groins are added.
6) We will propose the wave crest impact model for evaluating the impact of the wave crest when a couple of groins are added.
7) We will propose the wave crest impact model for evaluating the impact of the wave crest when a couple of T-head groins are added.
8) We will propose the setting method for the initial and the boundary conditions techniques of the wave crest impact modal when a couple of groins are added.
9) We will propose the setting method for the initial and the boundary conditions techniques of the wave crest impact modal when a couple of T-head groins are added.
10) We will propose numerical methods that are employed to approximate the incremental model in each year.

1.4 Scopes of the study

1) Study the shoreline evolution model when a couple of groins are added.
2) Study the shoreline evolution model when a couple of T-head groins are added.

3) Study the influence of wave crest impact models when a couple of groins are added to shoreline evolution.

4) Study the influence of wave crest impact models when a couple of T-head groins are added to shoreline evolution.

5) Study the parameters for use in the Gulf of Thailand.

6) Study the comparison of both numerical techniques.

7) The wave crest impact will be considered.

1.5 Methodology

1) Study the wave group velocity and the wave height measurement by GISTDA.

2) Generated the parameters of a mathematical model for use in the Gulf of Thailand.

3) Generated a mathematical model of shoreline evolution with groin structure.

4) Generated a mathematical model of shoreline evolution with T-head groin structure.

5) Generated a mathematical model of non-uniform wave crest impact with groin structure.

6) Generated a mathematical model of non-uniform wave crest impact with T-head groin structure.

7) Define the initial condition and boundary condition consistent with the problem of a mathematical model of non-uniform wave crest impact with groin structure.

8) Define the initial condition and boundary condition consistent with the problem of a mathematical model of non-uniform wave crest impact with T-head groin structure.

9) Define the initial condition and boundary condition consistent with the problem of a mathematical model of shoreline evolution with groin structure.

10) Define the initial condition and boundary condition consistent with the problem of a mathematical model of shoreline evolution with T-head groin structure.

11) Using numerical methods to approximate the solution problem of shoreline evolution with groin structure.

1.6 Benefits of the study

1) We can forecast the efficiency of groin contraction in a local beach.
2) We can forecast the effect of two groins types on a local beach.
3) We can measure the shoreline evolution for monthly of each year consistency non-uniform of the wave crest impact.
4) We can forecast the long-term shoreline evolution.

Chapter 2

Governing Equations

2.1 Shoreline evolution model

In the one-line model, the beach profile is assumed to move landward and seaward while retaining the same shape, implying that all bottom contours are parallel. Consequently, under this assumption it is sufficient to specify the horizontal location of the profile with respect to baseline, and one contour line can be used to describe changes in the beach plan shape and volume as the beach erodes and accretes. The major assumption of the model is the sand is transported alongshore between two well-defined limiting elevations on the profile. One contribution to the volume change results if there is a difference in the alongshore sand transport rate at the lateral sides of the section and the associated the sand continuity. The principles of mass conservation must apply to the system at all times. By considering above definitions, the following differential equation for shoreline evolution is obtained,

$$\frac{\partial y}{\partial t} = \frac{1}{D_B + D_C}\left(-\frac{\partial Q}{\partial x}\right), \tag{2.1}$$

where x is the alongshore coordinate (m); y is the shoreline positions (m) and perpendicular to x-axis; t is time (day); Q is the long-shore sand transport rate (m^3/day); D_B is the average berm height (m) and D_C is the closure depth(m) as show in Fig 2.2.

In order to solve the Eq (2.1), necessary to specify an expression for the long-shore sand transport rate, Q . This quantity is considered to be generated by the wave obliquely incident to the shoreline. A general expression for the long-shore sand transport rate was developed by the US Army Corp [26] :

$$Q = Q_0 \sin(2\alpha_b), \tag{2.2}$$

where Q_0 is the amplitude of the long-shore sand transport rate. α_b is the angle between breaking wave crest impact angle and local shoreline. The empirical predictive formula for the amplitude of the long-shore sand transport rate is [22] :

$$Q_0 = \frac{\rho}{16}(H_b^2 c_{gb})\frac{K}{(\rho_s - \rho)(1-n)}, \tag{2.3}$$

where the subscript b denotes value at the point of breaking, $c_g$is the wave group velocity, H is the wave height, ρ_s is the density of the sediment (kg/m^3), ρ is the density of the sea water, n is the porosity and K is the dimensionless coefficient which is a function of particle size. The quantity α_b is the angle between breaking wave crest and local shoreline, and may be written as :

$$\alpha_b = \alpha_0 - \tan^{-1}\left(\frac{\partial y}{\partial x}\right), \tag{2.4}$$

where α_0 is the angle between breaking wave crests and the x-axis. For beaches with mild slope, it can be assumed that breaking wave angle to the shoreline is small. In this case,

$$\sin(2\alpha_b) \approx 2\alpha_b, \tag{2.5}$$

and

$$\tan^{-1}\left(\frac{\partial y}{\partial x}\right) \approx \frac{\partial y}{\partial x}. \tag{2.6}$$

Substituting Eq (2.4) into the Eq (2.2), and assuming the beach with mild slope yields :

$$Q = Q_0\left(2\alpha_b - 2\frac{\partial y}{\partial x}\right), \tag{2.7}$$

Substituting Eq (2.7) into the Eq (2.1) and neglecting the sources or sinks along the coast gives :

$$\frac{\partial y}{\partial x} = D\frac{\partial^2 y}{\partial x^2}, \tag{2.8}$$

for all$(x,t) \in (L,T)$, where

$$D = \frac{2Q_0}{D_B + D_C}. \tag{2.9}$$

Eq (2.8) is analogous to the one-dimensional heat diffusion equation, it can be solved analytically for various initial and boundary conditions.

2.2 Physical parameters

Physical parameter of the model can be illustrated as show in Figures 2.1-2.2 that are listed below.

α_0 is the impact angle between breaking wave crests angle with the x-axis.

Q_0 is the amplitude of the long-shore sand transport rate.

D_B is the average berm height.

D_C is the average closure depth.

L is alongshore.

T is time of simulation.

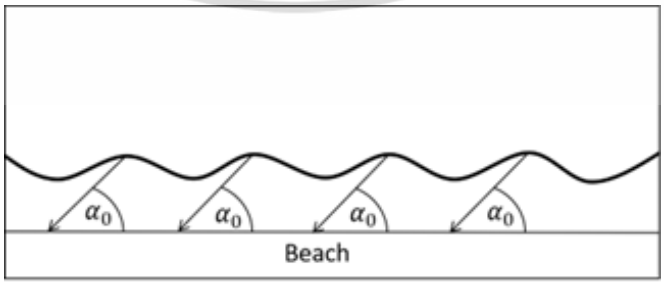

Figure 2.1*:* Breaking wave crests impact angle

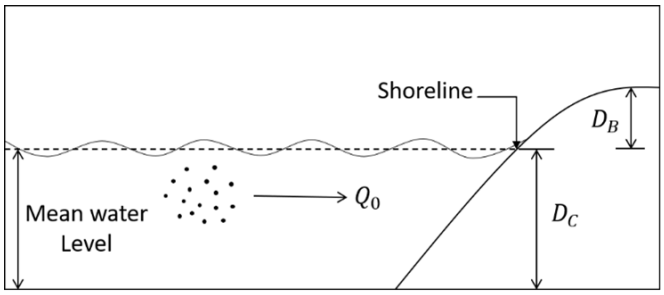

Figure 2.2*:* Shoreline physical parameters

2.3 Physical parameters setting techniques

Assuming that the density of the sediment (ρ_s) [27], the density of sea water (ρ) [28], the porosity (n) [29], the dimensionless coefficient which is a function of particle size (K) [30], the averaged berm height (D_B) and the closure depth (D_C) are listed belows.

Table 2.1*:* Parameters of sand transport rate [27], [28], [29], [30].

The density of the sediment (ρ_s (kg/m^3))	1700
The density of sea water (ρ (kg/m^3))	1020
The porosity (n)	0.406
The dimensionless coefficient which is a function of particle size (K)	0.375
The averaged berm height (D_B (m))	2
The closure depth (D_C (m))	28

The wave group velocity (c_g) and the wave height (H) in each month along a year is measured by field data at gulf of Thailand such that data are collected by Geo¬Informatics and Space Technology Development Agency (Public Organization) (GISTDA) [31] as listed belows.

Table 2.2*:* The wave group velocity and the wave height [31].

Month	$c_g\ (m/day)$	$H\ (m)$
Jan	8951.04	1.5
Feb	6998.4	1.5
Mar	5866.56	0.5
Apr	6920.64	1.5
May	5719.68	0.5
Jun	5546.88	0.5
Jul	8225.28	1.5
Aug	9357.12	1.5
Sep	13711.68	1.5
Oct	15085.44	2.5
Nov	10877.76	1.5
Dec	11396.16	1.5

The amplitude of the long¬shore transport rates (Q_0) are obtained by Eq (2.3) and the long-shore transport rates (D) are obtained by Eq (2.9) as listed belows.

Table 2.3*:* The amplitude of the long¬shore transport rates and the long¬shore transport rates.

Month	$Q_0\ (m/day)$	$D\ (m/day)$
Jan	1191.99	79.4659
Feb	931.96	62.1307
Mar	86.80	5.7869
Apr	921.61	61.4403
May	84.63	5.6420
Jun	82.07	5.4716
Jul	1095.34	73.0227
Aug	1246.07	83.071
Sep	1825.95	121.7301
Oct	5580.26	372.017
Nov	1448.57	96.5710
Dec	1517.60	101.1233

We setting parameters for use in the Gulf of Thailand.

2.4 Wave crest impact model

The hydrodynamic model is introduced to obtain the wave crest impact in the shoreline evolution model [32].

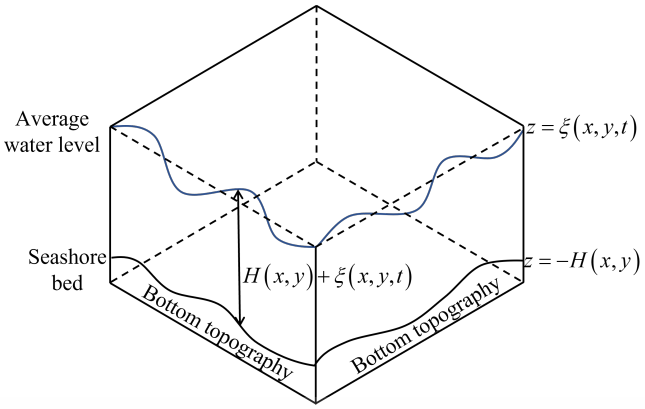

Figure 2.3: Water elevation and bottom topography.

The two-dimensional unstable water flows into and out of the seashore may be calculated using a system of shallow water equations, taking into consideration the mass conservation and the momentum conservation. The equations of this method should be derived from the vertical direction of the depth-averaging of the Navier-Stokes equations, neglecting the diffusion of momentum due to vibration and discarding the terms representing the effects of friction, surface wind, Coriolis factor, and shear stress. The equation of continuity is then expressed as follows:

$$\frac{\partial h}{\partial t}+\frac{\partial(xh)}{\partial x}+\frac{\partial(vh)}{\partial y}=0, \tag{2.10}$$

and the momentum equations are expressed as below:

$$\frac{\partial(uh)}{\partial t}+\frac{\partial(u^2h+\frac{1}{2}gh^2)}{\partial x}+\frac{\partial(uvh)}{\partial y}=0,\frac{\partial(uh)}{\partial t}+\frac{\partial(uvh)}{\partial x}+\frac{\partial(v^2h+\frac{1}{2}gh^2)}{\partial y}=0, \tag{2.11}$$

where $h(x,y,t)$ is the depth estimated from the average water surface to the seashore bed $(m)h=H+\xi$,

$\xi(x,y,t)$ is the elevation of the water surface from the average water level in the seashore (m),

$H(x,y)$ is the interpolated bottom topography function of the seashore (m),

$u(x,y,t)$ is the velocity in the direction of $x(m/s)$,

$v(x,y,t)$ is the velocity in the direction of $y(m/s)$,

g is a constant of gravity $(9.8m/s^2)$.

Such time (t), and two space coordinates, x and y are the independent variables. Likewise, the conserved quantities are mass, which is proportional to h, and momentum, which is proportional to (uh) and (vh). As taken with respect to the same term, the partial derivatives are grouped into vectors $(\partial x,\partial y,\partial t)$ and then rewritten as a partial differential hyperbolic equation as follows:

$$U = \begin{pmatrix} h \\ uh \\ vh \end{pmatrix}, F(U) = \begin{pmatrix} uh \\ u^2h + \frac{1}{2}gh^2 \\ uvh \end{pmatrix}, G(U) = \begin{pmatrix} vh \\ uvh \\ v^2h + \frac{1}{2}gh^2 \end{pmatrix}, \tag{2.12}$$

the hyperbolic PDE:

$$\frac{\partial U}{\partial t} + \frac{\partial F(U)}{\partial x} + \frac{\partial G(U)}{\partial y} = 0. \tag{2.13}$$

2.5 Numerical techniques

As in other mathematical problems, PDEs can be solved either analytically or numerically. Due to the complex nature of PDEs, various analytical techniques such as the method of separation of variables and the integral transforms can only be applied to some simple cases. Table 2.4 shows the nature of the analytical and numerical solutions.

Table 2.4*:* A comparison between analytical and numerical solution [34].

Analytical solution	Numerical solution
Solution is continuous, i.e. solution at any values of the independent variables can be found.	Solution can only be obtained at discrete grid points. Interpolations are necessary to obtain the solution between the grid points.
Exact or very accurate.	Approximate numerical errors have to be controlled properly for accuracy.
Provide physical insights into the problems. For instance, frequencies and mode shapes of vibrations can be obtained easily.	Physical information is more difficult to be obtained.
Do not exist for most of today's practical problems due to their complexities.	Can be obtained for complicated problems due to the advance in computer technology and the availability of more sophisticated numerical algorithms

The last difference, together with today's more economical computer technology, has made numerical methods important and indispensable. There are two main groups of numerical methods for solving PDEs - namely the finite-difference method and the finite-element method. The former is for general purpose while the latter is primarily for structural analysis problems although it was recently extended to other non-structural applications such as fluid flow problems and electromagnetism problems.

In our context, the finite-difference methods are mainly considered with the inclusion of the classical method of characteristics for hyperbolic equations which is neither a finite-difference method nor a finite-element method.

2.5.1 Even Grid System

Consider an even grid-spacing system in which Δx =constant= h and Δy =constant= k as shown in Figure 2.4

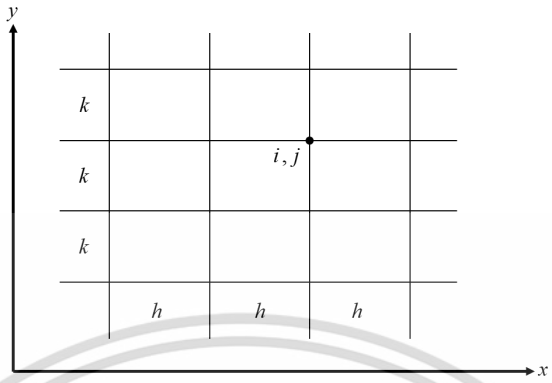

Figure 2.4: An even grid-spacing system.

The Taylor series for a function $u(x,y)$ expanded about x_i at (x_i+h) and (x_i-h) are respectively,

$$u(x+h,y) = u(x,y) + h\frac{\partial u(x,y)}{\partial x} + \frac{h^2}{2!}\frac{\partial^2 u(x,y)}{\partial x^2} + \frac{h^3}{3!}\frac{\partial^3 u(x,y)}{\partial x^3} + \ldots \tag{2.14}$$

$$u(x-h,y) = u(x,y) - h\frac{\partial u(x,y)}{\partial x} + \frac{h^2}{2!}\frac{\partial^2 u(x,y)}{\partial x^2} - \frac{h^3}{3!}\frac{\partial^3 u(x,y)}{\partial x^3} + \ldots \tag{2.15}$$

where h, called the grid size, grid spacing or step size, is sufficiently small for the series to be convergent.

Introducing the double-subscript notation in which the first subscript denotes the x-position and the second subscript denotes the y-position, the above expressions can be written as

$$u_{i+1,j} = u_{i,j} + h\frac{\partial u_{i,j}}{\partial x} + \frac{h^2}{2!}\frac{\partial^2 u_{i,j}}{\partial x^2} + \frac{h^3}{3!}\frac{\partial^3 u_{i,j}}{\partial x^3} + \ldots \tag{2.16}$$

$$u_{i-1,j} = u_{i,j} - h\frac{\partial u_{i,j}}{\partial x} + \frac{h^2}{2!}\frac{\partial^2 u_{i,j}}{\partial x^2} - \frac{h^3}{3!}\frac{\partial^3 u_{i,j}}{\partial x^3} + \ldots \tag{2.17}$$

From Eq 2.16,

$$\frac{\partial u_{i,j}}{\partial x} = \frac{u_{i+1,j} - u_{i,j}}{h} - \frac{h}{2!}\frac{\partial^2 u_{i,j}}{\partial x^2} - \frac{h^2}{3!}\frac{\partial^3 u_{i,j}}{\partial x^3} + \ldots \tag{2.18}$$

$$\frac{\partial u_{i,j}}{\partial x} = \frac{u_{i+1,j} - u_{i,j}}{h} + O(h) \tag{2.19}$$

Likewise, from Eq 2.17,

$$\frac{\partial u_{i,j}}{\partial x} = \frac{u_{i,j} - u_{i-1,j}}{h} - \frac{h}{2!}\frac{\partial^2 u_{i,j}}{\partial x^2} - \frac{h^2}{3!}\frac{\partial^3 u_{i,j}}{\partial x^3} + \ldots \tag{2.20}$$

$$\frac{\partial u_{i,j}}{\partial x} = \frac{u_{i,j} - u_{i-1,j}}{h} + O(h) \tag{2.21}$$

Hence, if the terms containing the second-order and higher-order derivatives are truncated in these expressions, we get the forward difference and backward difference approximations respectively for the first-order derivative. As h must be sufficiently small so that the series converge, the second and other truncated terms are

much smaller than the first truncated term and all truncated terms are thus written in terms of the order of magnitude of the first truncated term. Therefore the approximation errors, hence known as the truncation errors, in Eq 2.19 and Eq 2.21 are of the order of h and are written as $O(h)$. This implies that the truncation errors are approximately proportional to h because all derivatives are fixed for a given problem. The truncation errors are thus approximately halved if h is halved. These finite-difference expressions are said to be first-order accurate. Physically, the truncation error represents the difference between the exact value of the derivative and its finite-difference value.

If we take Eq 2.16 - Eq 2.17 and rearrange, we get the central difference

$$\frac{\partial u_{i,j}}{\partial x} = \frac{u_{i+1,j} - u_{i-1,j}}{2h} - \frac{h^2}{3!}\frac{\partial^3 u_{i,j}}{\partial x^3} + \ldots \tag{2.22}$$

$$\frac{\partial u_{i,j}}{\partial x} = \frac{u_{i+1,j} - u_{i-1,j}}{2h} + O(h^2) \tag{2.23}$$

and the truncation error is $O(h^2)$ and is approximately proportional to h^2. The central difference is second-order accurate. In this case, halving the grid size h would approximately reduce the truncation error to a quarter of the previous error. The central difference is thus more accurate than the forward or backward differences which may be seen geometrically in Figure 2.5 in which the central difference is closest to the actual tangent representing the first-order derivative.

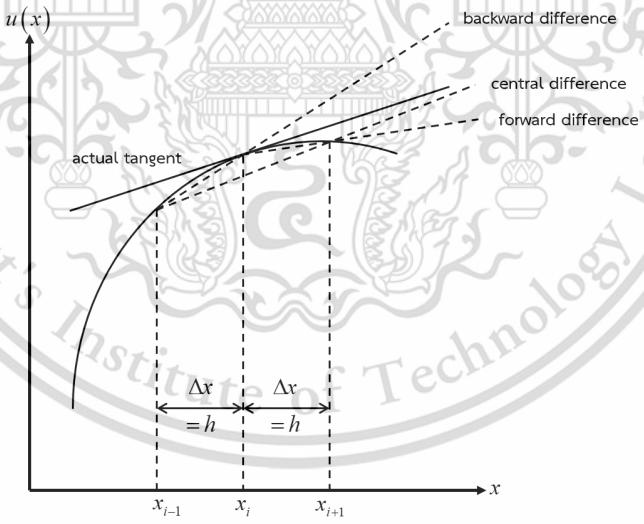

Figure 2.5*:* Direct approximations of derivatives.

If we take Eq 2.16 + Eq 2.17 and rearrange, we get the central difference for the second-order derivative

$$\frac{\partial^2 u_{i,j}}{\partial x^2} = \frac{u_{i+1,j} - 2u_{i,j} + u_{i-1,j}}{h^2} + \frac{2h^2}{4!}\frac{\partial^4 u_{i,j}}{\partial x^4} - \ldots \tag{2.24}$$

$$\frac{\partial^2 u_{i,j}}{\partial x^2} = \frac{u_{i+1,j} - 2u_{i,j} + u_{i-1,j}}{h^2} + O(h^2) \tag{2.25}$$

and the truncation error is $O(h^2)$.

Similarly,for the y-derivatives, we have

$$\frac{\partial u_{i,j}}{\partial y} = \frac{u_{i,j+1} - u_{i,j}}{k} + O(k) \tag{2.26}$$

$$\frac{\partial u_{i,j}}{\partial y} = \frac{u_{i,j} - u_{i,j-1}}{k} + O(k) \tag{2.27}$$

$$\frac{\partial u_{i,j}}{\partial y} = \frac{u_{i,j+1} - u_{i,j-1}}{2k} + O(k^2) \tag{2.28}$$

$$\frac{\partial^2 u_{i,j}}{\partial y^2} = \frac{u_{i,j+1} - 2u_{i,j} + u_{i,j-1}}{k^2} + O(k^2) \tag{2.29}$$

2.5.2 Traditional forward time centered space techniques

The forward time centered space schemes is employed. Consequently, the finite difference approximation becomes [34]

$$y \cong y_i^n, \tag{2.30}$$

$$\frac{\partial y}{\partial t} \cong \frac{y_i^{n+1} - y_i^n}{\Delta t}, \tag{2.31}$$

$$\frac{\partial y}{\partial x} \cong \frac{y_{i+1}^n - y_{i-1}^n}{2\Delta x}, \tag{2.32}$$

$$\frac{\partial^2 y}{\partial x^2} \cong \frac{y_{i+1}^n - 2y_i^n + y_{i-1}^n}{(\Delta x)^2}, \tag{2.33}$$

2.5.3 An unconditionally Saulyev finite difference techniques

The Saulyev scheme is employed. Consequently, the finite difference approximation becomes [35]

$$y \cong y_i^n, \tag{2.34}$$

$$\frac{\partial y}{\partial t} \cong \frac{y_i^{n+1} - y_i^n}{\Delta t}, \tag{2.35}$$

$$\frac{\partial^2 y}{\partial x^2} \cong \frac{y_{i+1}^n - y_i^n - y_i^{n+1} + y_{i-1}^{n+1}}{(\Delta x)^2}, \tag{2.36}$$

2.5.4 Numerical techniques for the wave crest impact model

The finite difference technique:

$$U_{i,j}^{n+1} = U_{i,j}^n - \frac{\Delta t}{\Delta x}\left(F_{i+\frac{1}{2},j}^{n+\frac{1}{2}} - F_{i-\frac{1}{2},j}^{n+\frac{1}{2}}\right) - \frac{\Delta t}{\Delta y}\left(G_{i,j+\frac{1}{2}}^{n+\frac{1}{2}} - G_{i,j-\frac{1}{2}}^{n+\frac{1}{2}}\right). \tag{2.37}$$

2.5.5 The wave crest impact

The wave crest impact becomes

$$\alpha\left(x_i, y_j, t\right) = \tan^{-1}\left(\frac{v\left(x_i, y_j, t\right)}{u\left(x_i, y_j, t\right)}\right), \tag{2.38}$$

the averaged wave crest impact is assumed by

$$\alpha_0\left(t\right) = \frac{\sum_{i=1}^{N_P} \alpha\left(x_i, 0, t\right)}{N_P}, \tag{2.39}$$

where $N_P$is several wave crest impact sample points along the shoreline.

Chapter 3

A Shoreline Evolution Model With the Wavelength Effect of Breaking Waves on Groin Structures

In this chapter, we present a one-dimensional mathematical model of shoreline evolution, and the parameters that influence this model are described on a monthly basis over a period of one year. Consideration is given to the wave crest impact model for evaluating the impact of the wave crest at that stage. It focuses on the evolution of the shoreline in environments where groins are installed on both sides. The initial and boundary condition setting techniques are proposed by the groins and their environmental parameters. The non-uniform influence of the crest of the breaking wave is so often considered. We then used the traditional forward time centered space technique and the Saulyev finite difference technique to estimate the monthly evolution of the shoreline for each year. The investigated area of shoreline evolution with a pair of groin structures is enlarged in this chapter to include the groin system and surrounding area. A more realistic shoreline evolution model has been presented, which takes into account the wavelength influence of breaking waves on groin constructions. The initial condition setting approach and boundary conditions techniques, as well as various groin structural impacts, are discussed. A wave crest impact model and five wavelength effects of breaking waves are introduced. Each year, the coastline evolution is approximated using the classical forward-time centered-space method and the unconditionally stable Saulyev finite differential methods. The estimated impacts of shoreline evolution were consistent with the wave crest impact model for five case wavelengths. For assessing long coastline evolution, the numerical models presented enable a reasonable simulation. The efficiency of building a groin system on a nearby beach might be predicted using the proposed modeling.

3.1 Traditional forward time centered space techniques applied to shoreline evolution model

Substituting Eqs (2.30)-(2.33) into Eq (2.8), we obtain,

$$\frac{y_i^{n+1} - y_i^n}{\Delta t} = D\left(\frac{y_{i+1}^n - 2y_i^n + y_{i-1}^n}{(\Delta x)^2}\right), \tag{3.1}$$

for $1 \le i \le M-1$ and $0 \le n \le N-1$. Eq (3.1) can be written in an explicit form of finite difference as follows,

$$y_i^{n+1} = Ay_{i+1}^n + (1-2A)y_i^n + Ay_{i-1}^n, \tag{3.2}$$

for $1 \le i \le M-1$ and $0 \le n \le N-1$.

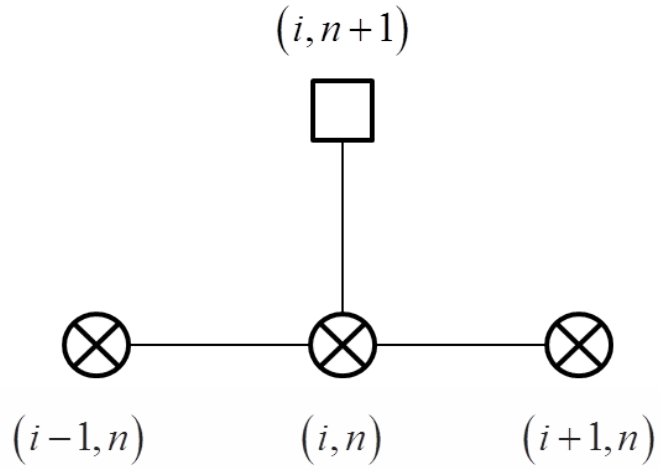

Figure 3.1*:* Stencil diagram of forward central space finite difference technique

3.2 An unconditionally Saulyev finite difference techniques applied to shoreline evolution model

Substituting Eqs (2.34)-(2.36) into Eq (2.8), we obtain

$$\frac{y_i^{n+1}-y_i^n}{\Delta t}=D\left(\frac{y_{i+1}^n-y_i^n-y_i^{n+1}+y_{i-1}^{n+1}}{(\Delta x)^2}\right), \tag{3.3}$$

for $1\le i\le M-1$ and $0\le n\le N-1$. Eq (3.3) can be written in an explicit form of finite difference as follows,

$$y_i^{n+1}=\frac{1}{1+A}(Ay_{i+1}^n+(1-A)y_i^n+Ay_{i-1}^{n+1}), \tag{3.4}$$

for $1\le i\le M-1$ and $0\le n\le N-1$.

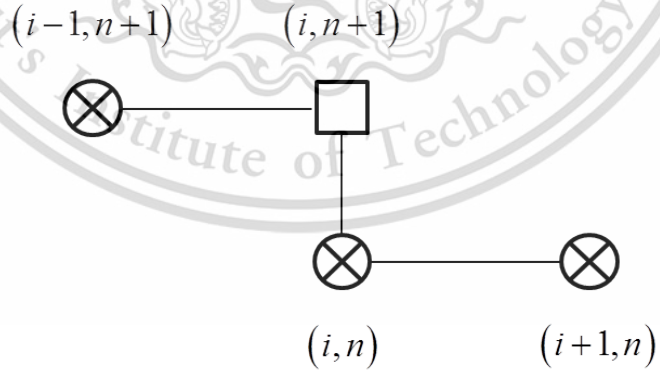

Figure 3.2*:* Stencil diagram of Saulyev finite difference technique

3.3 The employment of traditional forward time centered space techniques to the left and the right boundary conditions for Straight Impermeable twin-groin system

By substituting Eqs (2.30)-(2.33) into Eq (2.8), we obtain,

$$\frac{y_i^{n+1} - y_i^n}{\Delta t} = D\left(\frac{y_{i+1}^n - 2y_i^n + y_{i-1}^n}{(\Delta x)^2}\right), \tag{3.5}$$

For $i = 0$, substitution of the approximate unknown value of the left boundary by a traditional central difference approximation with the known derivative the left boundary condition gives

$$y_{-1}^n = y_1^n - 2(\Delta x)(-\tan(\alpha_0)), \tag{3.6}$$

Substituting Eq (3.6) into Eq (3.5), we obtain

$$y_i^{n+1} = (1-2A)y_i^n + 2Ay_{i+1}^n - 2A(\Delta x)(-\tan(\alpha_0)), \tag{3.7}$$

For $i = M$, substitution of the approximate unknown value of the right boundary by a traditional central difference approximation with the known derivative the right boundary condition gives

$$y_{M+1}^n = y_{M-1}^n + 2(\Delta x)(-\tan(-\alpha_0)), \tag{3.8}$$

Substituting Eq (3.8) into Eq (3.5), we obtain

$$y_i^{n+1} = 2Ay_{i-1}^n + (1-2A)y_i^n + 2A(\Delta x)(-\tan(-\alpha_0)), \tag{3.9}$$

The Eq (3.7) and Eq (3.9) can be used to calculate the values y_i^n on grid points of the solution domain.

3.4 Initial and boundary conditions setting

The initials shoreline is assumed to be parallel to the x-axis.

3.4.1 Straight Impermeable twin-groin system

Straight Impermeable twin-groin system as show in Figure 3.3. Assuming that the breaking wave angle α_0 to the shoreline is symmetric. It follows that the sand transport rate along the shoreline is uniform. The groin is instantaneously added at as show in Figure 3.4. These means that the initial condition becomes

$$y(x,0) = h_1(x), \tag{3.10}$$

boundary conditions are also assumed by

$$\frac{\partial y(0,t)}{\partial x} = -\tan(\alpha_0), \tag{3.11}$$

and

$$\frac{\partial y(L,t)}{\partial x} = -\tan(-\alpha_0), \tag{3.12}$$

when $h_1(x)$ is initial shoreline topography function.

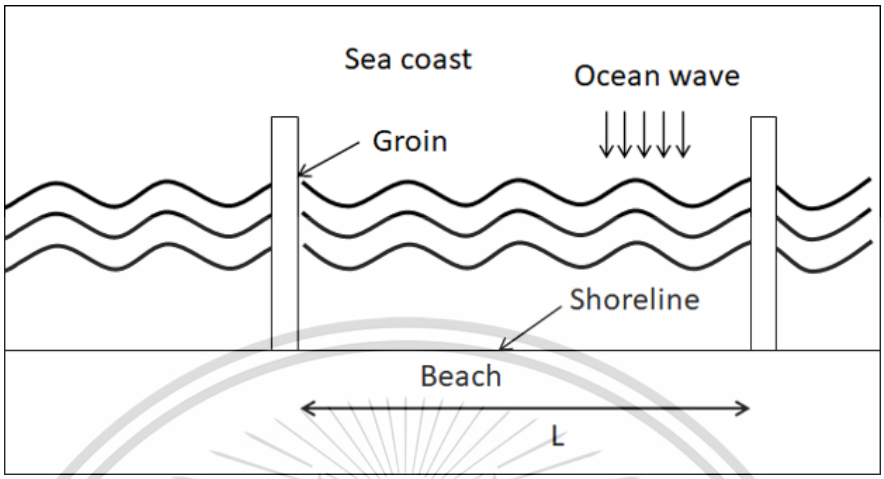

Figure 3.3: Initial shoreline with configuration straight impermeable twin-groin

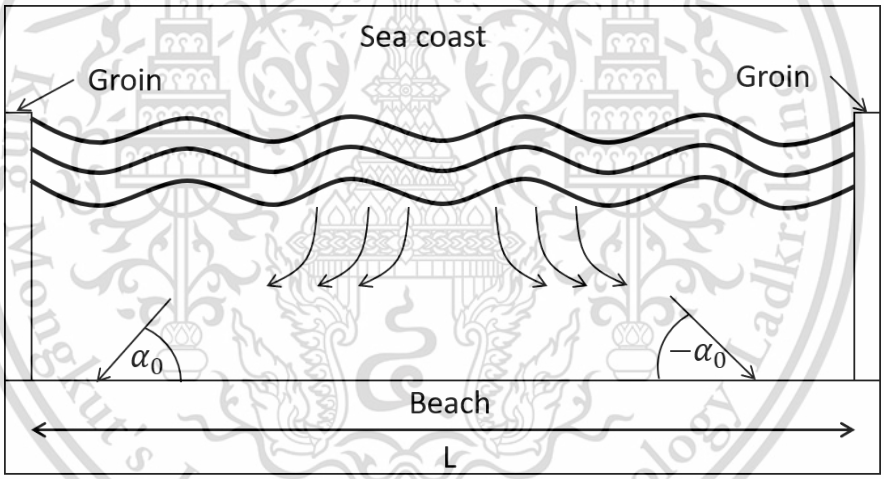

Figure 3.4: Initial shoreline

3.4.2 The initial and boundary condition for wave crest impact model with Straight Impermeable twin-groin system

The initial condition of the reservoir was as follows: the x and y velocity components were zero as well as the water elevation: $u = 0, v = 0$ and $\xi = 0$. Assuming that the breakwater is not a perfect barrier to water as it is made of an aggregate of rocks with large gaps.

The boundary condition was as follows:

(1) $u = 0, \frac{\partial v}{\partial y} = 0, \xi = f(x, y, t)$ for wave coming,

(2) $\frac{\partial u}{\partial x} = 0, v = 0, \frac{\partial \xi}{\partial x} = 0$ for left and right boundary,

(3) $u = 0, \frac{\partial v}{\partial y} = 0, \frac{\partial \xi}{\partial y} = 0$ for along the beach,
(4) $u = 0, \frac{\partial v}{\partial y} = 0, \frac{\partial \xi}{\partial y} = 0$ for top groin structure, and
(5) $\frac{\partial u}{\partial x} = 0, v = 0, \frac{\partial \xi}{\partial x} = 0$ for left and right groin structure. The boundary conditions are illustrated in Figure 3.5-3.6.

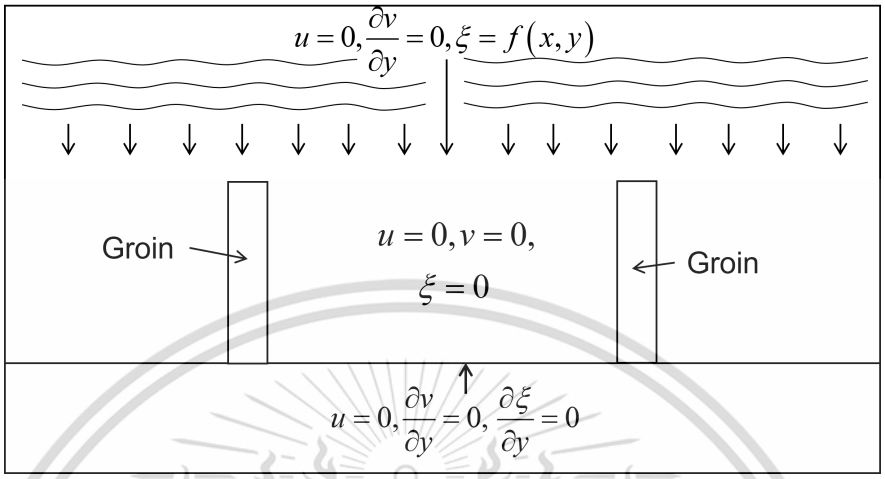

Figure 3.5: Initial and boundary conditions.

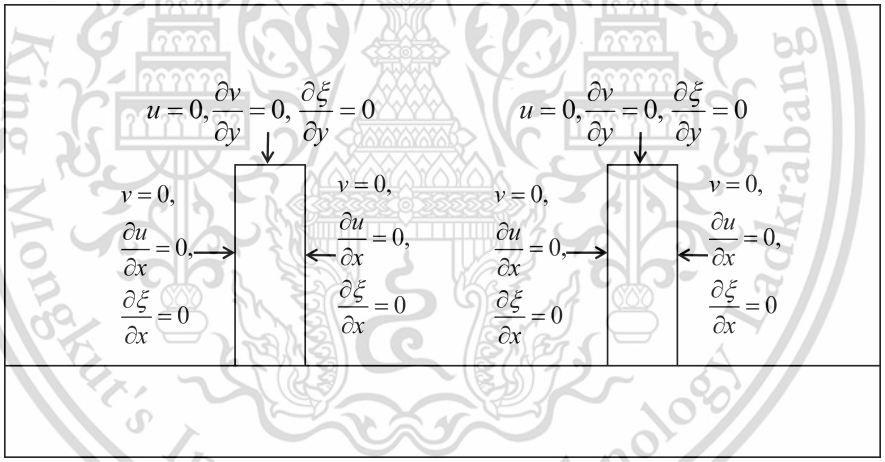

Figure 3.6: Initial and boundary conditions for groin structure.

3.5 Wavelength setting techniques

The simulation considers alongshore between groin are illustrated in Fig. 3.7. Table 3.1. shows the consideration of wavelengths. We assumed waves came in a function of wavelength $0.5\sin(t + \Lambda x)$.

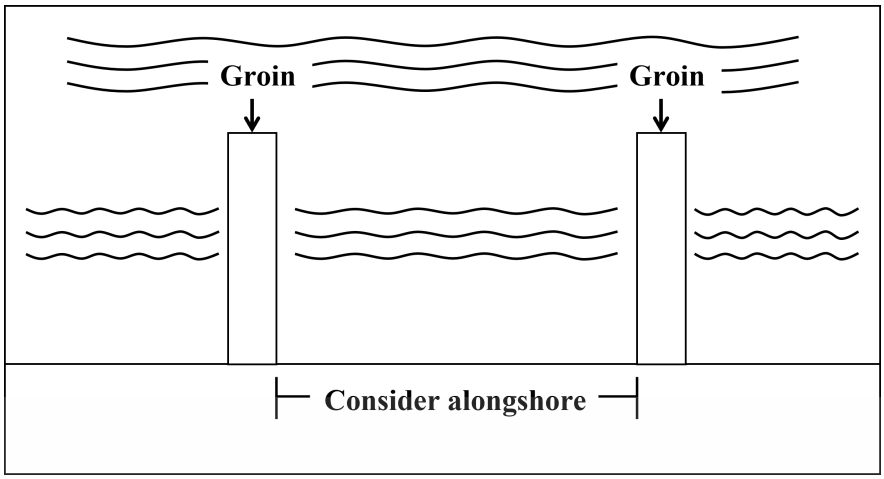

Figure 3.7: Consider alongshore.

Table 3.1: Wavelength setting.

Simulation	Λ	Wavelength
1	0.01	$0.5\sin(t+0.01x)$
2	0.02	$0.5\sin(t+0.02x)$
3	0.03	$0.5\sin(t+0.03x)$
4	0.04	$0.5\sin(t+0.04x)$
5	0.05	$0.5\sin(t+0.05x)$

We will employ the finite difference techniques to approximate the wave crest impact model solution for wavelengths $0.5\sin(t+0.01x)$, $0.5\sin(t+0.02x)$, $0.5\sin(t+0.03x)$, $0.5\sin(t+0.04x)$ and $0.5\sin(t+0.05x)$. The approximated wave crest impact model solutions for five case wavelengths are illustrated in Fig.3.8-3.12. The approximated vector fields of velocities for five case wavelengths are illustrated in Fig. 3.13-3.17.

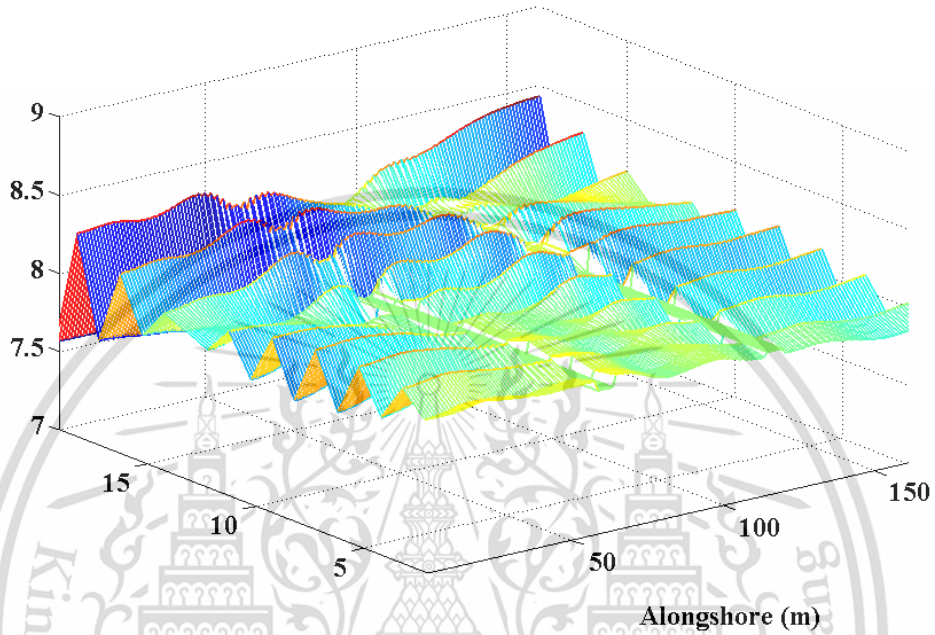

Figure 3.8: Wave crest impact in 15 years when wavelength $0.5\sin(t+0.01x)$.

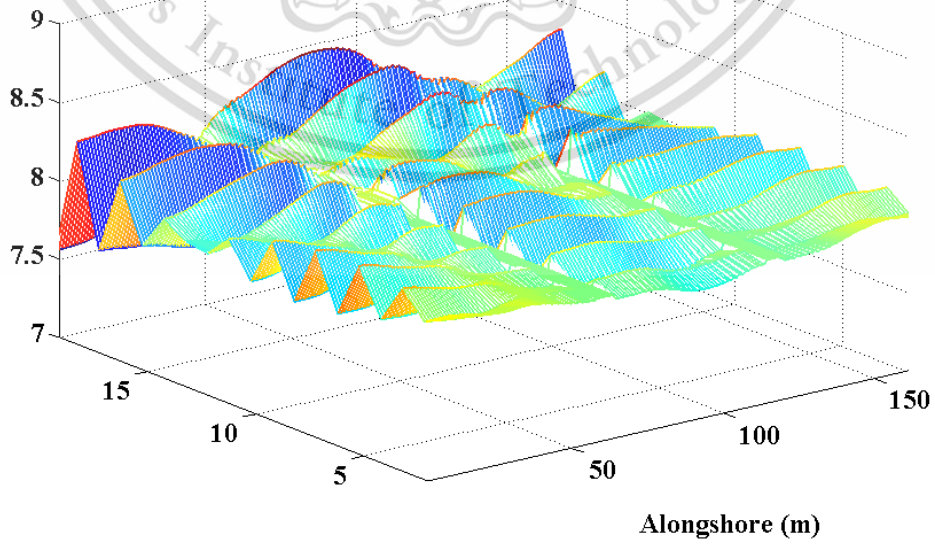

Figure 3.9: Wave crest impact in 15 years when wavelength $0.5\sin(t+0.02x)$.

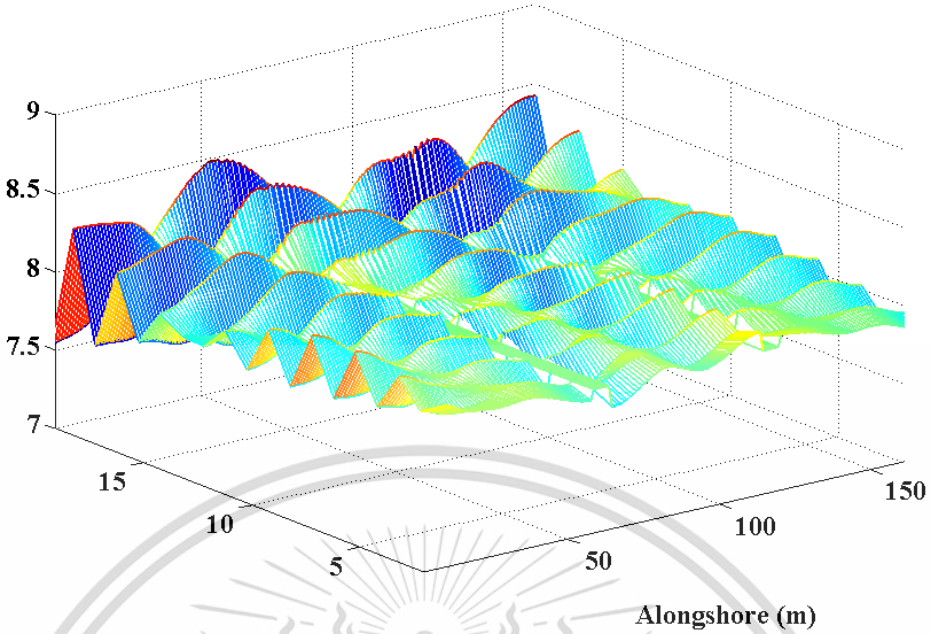

Figure 3.10: Wave crest impact in 15 years when wavelength $0.5\sin(t+0.03x)$.

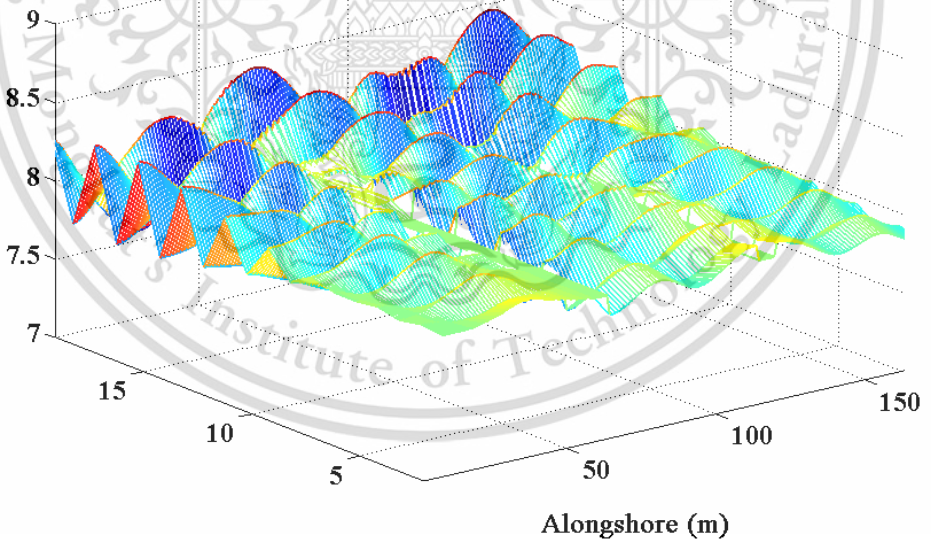

Figure 3.11: Wave crest impact in 15 years when wavelength $0.5\sin(t+0.04x)$.

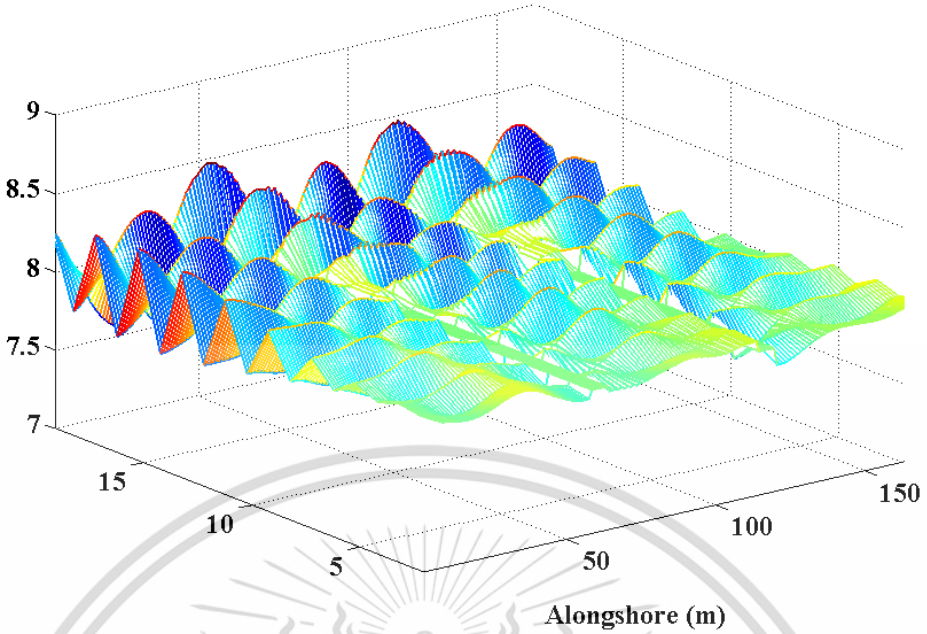

Figure 3.12: Wave crest impact in 15 years when wavelength $0.5\sin(t+0.05x)$.

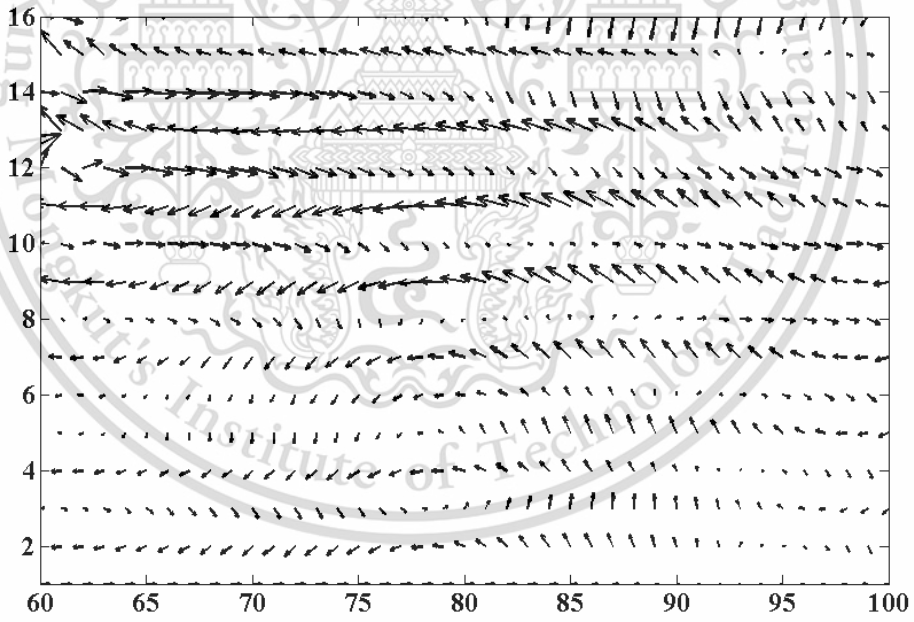

Figure 3.13: vector field of velocities between groin when wavelength $0.5\sin(t+0.01x)$.

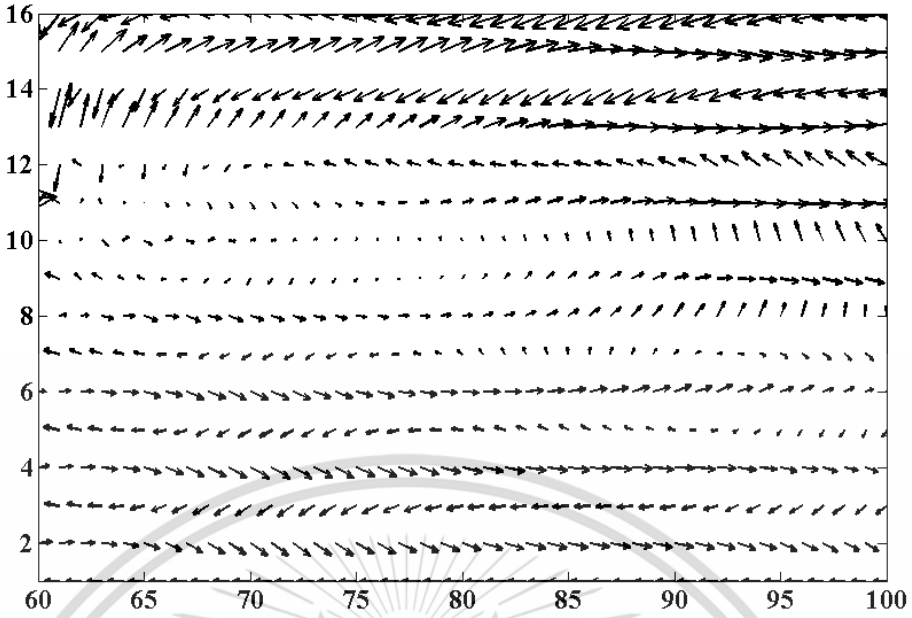

Figure 3.14*:* vector field of velocities between groin when wavelength $0.5\sin(t+0.02x)$.

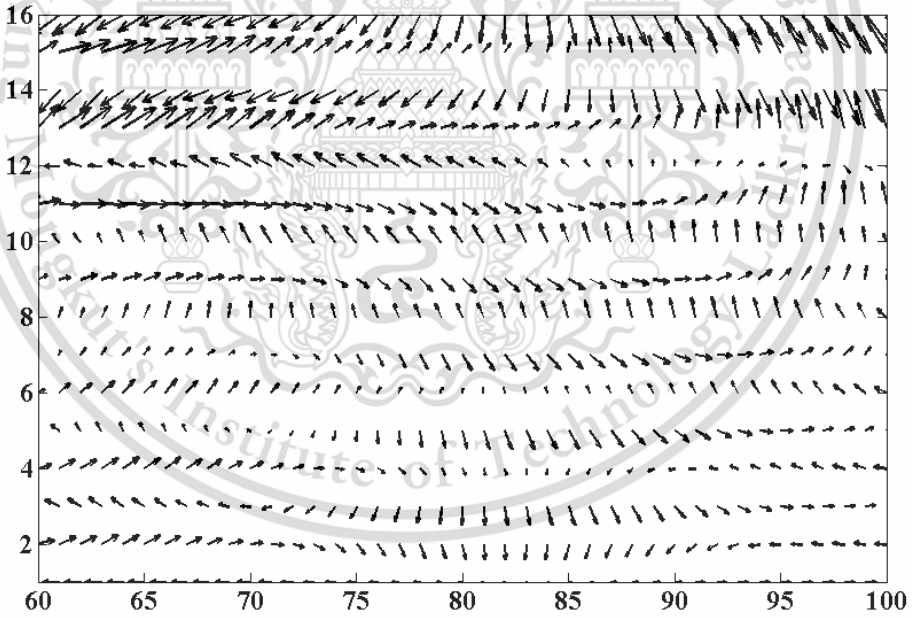

Figure 3.15*:* vector field of velocities between groin when wavelength $0.5\sin(t+0.03x)$.

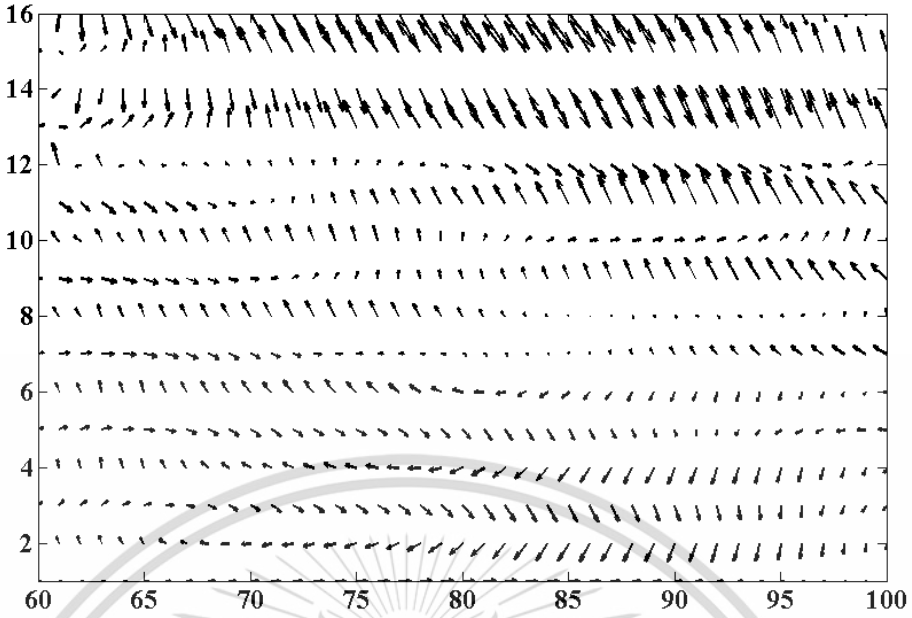

Figure 3.16*:* vector field of velocities between groin when wavelength $0.5\sin(t+0.04x)$.

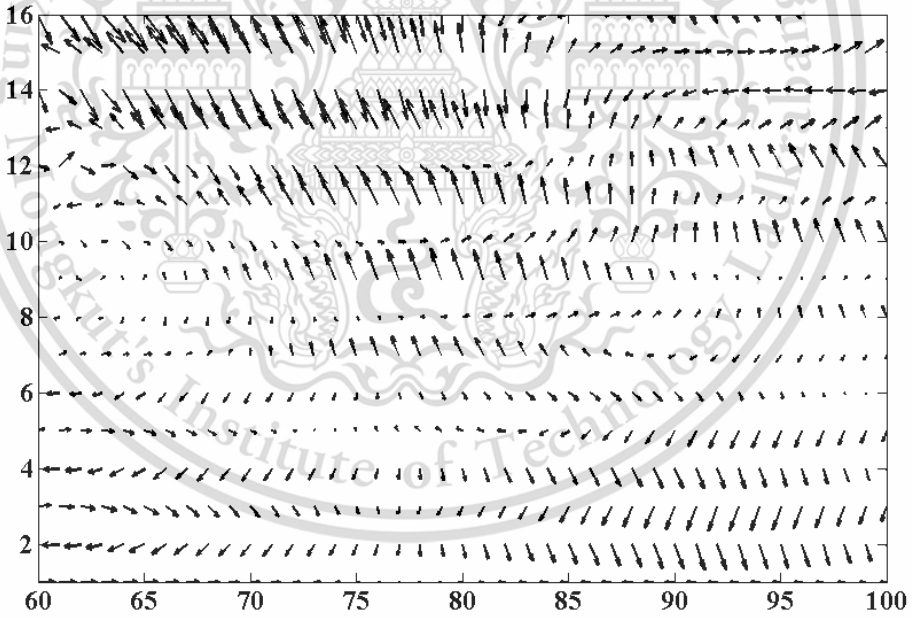

Figure 3.17*:* vector field of velocities between groin when wavelength $0.5\sin(t+0.05x)$.

Table 3.2-3.6 shows the averaged wave crest impact (α_0) as obtained by 2.39.

Table 3.2: The averaged wave crest impact 15 years when wavelength $0.5\sin(t+0.01x)$.

Time	Minute					
(Years)	0-15	15-30	30-45	45-60	60-75	75-90
1	0.0455	0.0448	0.0440	0.0433	0.0426	0.0419
5	-0.0400	-0.0419	-0.0439	-0.0459	-0.0480	-0.0501
10	-0.0705	-0.0721	-0.0737	-0.0754	-0.0770	-0.0786
15	0.0293	0.0284	0.0274	0.0264	0.0254	0.0244
Time	Minute					
(Years)	...	1365-1380	1380-1395	1395-1410	1410-1425	1425-1440
1	...	-0.0379	-0.0394	-0.0410	-0.0426	-0.0442
5	...	-0.0496	-0.1140	-0.1158	-0.1178	-0.1830
10	...	0.1472	0.1363	0.1881	0.1770	0.1658
15	...	0.1930	0.1961	0.1985	0.2003	0.2018

Table 3.3: The averaged wave crest impact 15 years when wavelength $0.5\sin(t+0.02x)$.

Time	Minute					
(Years)	0-15	15-30	30-45	45-60	60-75	75-90
1	0.1817	0.2377	0.2309	0.2241	0.2802	0.2734
5	0.3973	0.4493	0.3794	0.4342	0.4231	0.4109
10	-0.2747	-0.2215	-0.2315	-0.2418	-0.1899	-0.1385
15	-0.0364	-0.0478	0.0037	-0.0077	-0.0191	0.0323
Time	Minute					
(Years)	...	1365-1380	1380-1395	1395-1410	1410-1425	1425-1440
1	...	-0.0275	-0.038	-0.0485	0.0037	0.0559
5	...	0.1168	0.1154	0.1139	0.1124	0.1109
10	...	-0.1047	-0.1069	-0.1091	-0.1114	-0.1136
15	...	0.2057	0.2040	0.2024	0.2009	0.1993

Table 3.4: The averaged wave crest impact 15 years when wavelength $0.5\sin(t+0.03x)$.

Time	Minute					
(Years)	0-15	15-30	30-45	45-60	60-75	75-90
1	0.3715	0.3653	0.3595	0.3541	0.3489	0.3440
5	0.1662	0.1767	0.1243	0.1347	0.1449	0.1550
10	0.0148	0.0093	0.0039	-0.0015	-0.0070	-0.0123
15	0.1732	0.1821	0.1910	0.2000	0.2091	0.2182
Time	Minute					
(Years)	...	1365-1380	1380-1395	1395-1410	1410-1425	1425-1440
1	...	0.1182	0.0881	0.1162	0.0782	0.0951
5	...	-0.1423	-0.1392	-0.1361	-0.1330	-0.1300
10	...	0.1488	0.1398	0.1276	0.1550	0.1307
15	...	-0.0660	-0.0623	-0.0586	-0.0550	-0.0514

Table 3.5: The averaged wave crest impact 15 years when wavelength $0.5\sin(t+0.04x)$.

Time	Minute					
(Years)	0-15	15-30	30-45	45-60	60-75	75-90
1	-0.0060	-0.0017	0.0026	0.0068	0.0110	0.0151
5	-0.4238	-0.4291	-0.4346	-0.4403	-0.3833	-0.3894
10	0.3286	0.3249	0.3213	0.3177	0.3142	0.3108
15	-0.4203	-0.4178	-0.4781	-0.4754	-0.4728	-0.4701
Time	Minute					
(Years)	...	1365-1380	1380-1395	1395-1410	1410-1425	1425-1440
1	...	-0.2516	-0.2551	-0.2586	-0.2621	-0.2656
5	...	-0.0892	-0.0940	-0.0360	-0.0408	-0.0454
10	...	0.2663	0.2698	0.2104	0.2139	0.2175
15	...	-0.3283	-0.2725	-0.2801	-0.2880	-0.2960

Table 3.6: The averaged wave crest impact 15 years when wavelength $0.5\sin(t+0.05x)$.

Time	Minute					
(Years)	0-15	15-30	30-45	45-60	60-75	75-90
1	-0.1214	-0.1405	-0.1557	-0.1691	-0.1188	-0.1310
5	0.1536	0.1497	0.2085	0.2046	0.2006	0.1966
10	-0.0695	-0.0659	-0.0623	-0.0586	-0.0550	-0.0514
15	0.0316	0.0913	0.0882	0.0850	0.0818	0.0786
Time	Minute					
(Years)	...	1365-1380	1380-1395	1395-1410	1410-1425	1425-1440
1	...	0.2402	0.2359	0.2315	0.2271	0.2856
5	...	0.3529	0.3504	0.3479	0.4084	0.4060
10	...	-0.3659	-0.3637	-0.3616	-0.3595	-0.3574
15	...	0.3791	0.3757	0.3723	0.3690	0.3657

3.6 Numerical Experiment

In this section, the numerical results of the various beach scenarios are considered and the solution to the idealized problem is introduced. Assuming, during the experiments, that the length of the shoreline considered is $L = 100$ m and the averaged wave crest impact (α_0) of five case wavelengths. Table 3.7 shows the long-shore transport rate D . The simulation setting is illustrated in Fig. 3.18.

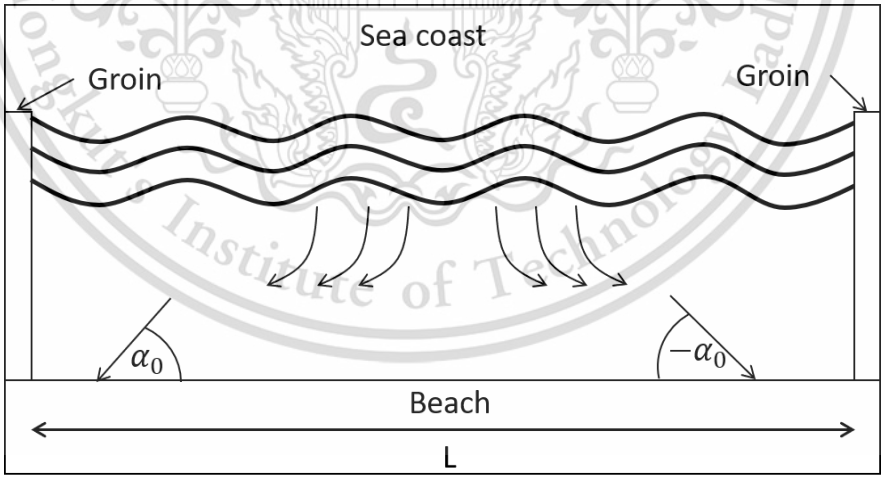

Figure 3.18: Initial shoreline.

Table 3.7: The long¬shore transport rates [37].

Month	$D\ (m/day)$
Jan	79.4659
Feb	62.1307
Mar	5.7869
Apr	61.4403
May	5.6420
Jun	5.4716
Jul	73.0227
Aug	83.071
Sep	121.7301
Oct	372.017
Nov	96.5710
Dec	101.1233

We are going to employ the traditional forward time centered space techniques 3.2, and the Saulyev finite difference techniques 3.4, to approximate the shoreline evolution model solution. The approximated solutions in each year are illustrated in Fig. 3.19-3.28. The approximated solutions in 5, 10 and 15 years are illustrated in Fig. 3.29-3.33. Table 3.8-3.16 shows the approximated solutions.

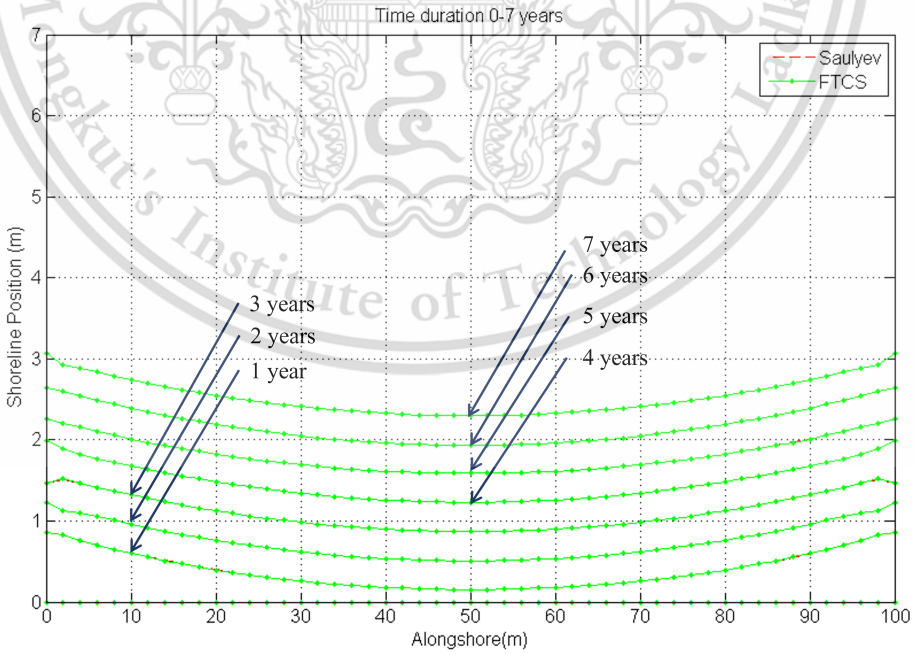

Figure 3.19: Shoreline evolution in 0-7 years when wavelength $0.5\sin(t+0.01x)$.

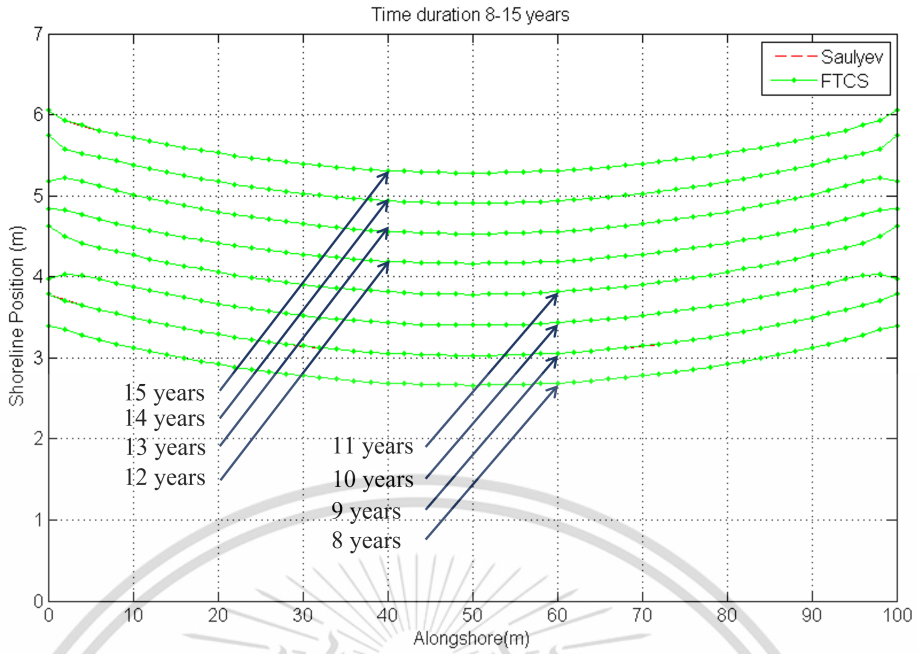

Figure 3.20: Shoreline evolution in 8-15 years when wavelength $0.5\sin(t + 0.01x)$.

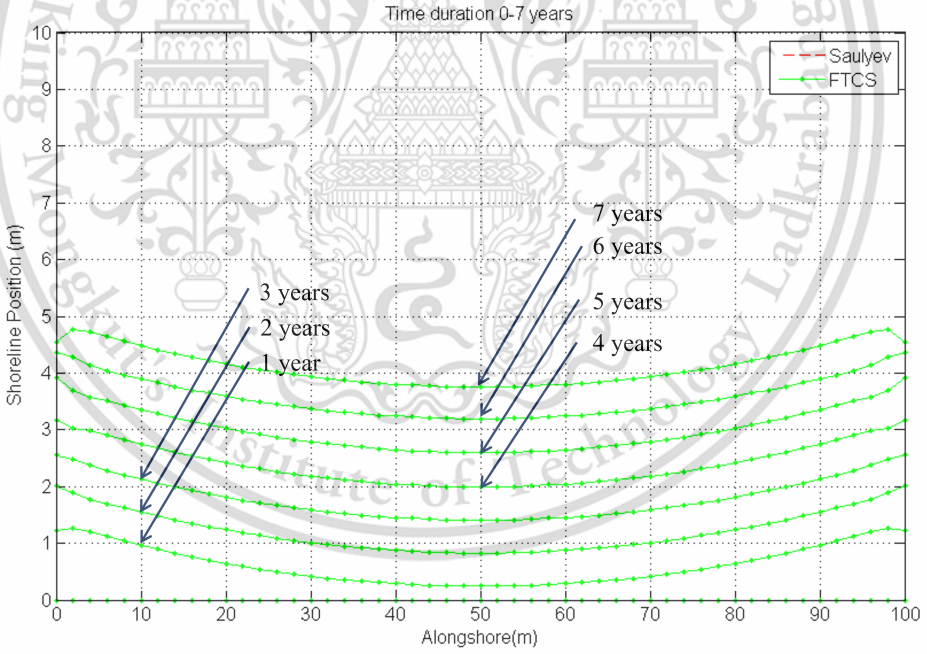

Figure 3.21: Shoreline evolution in 0-7 years when wavelength $0.5\sin(t + 0.02x)$.

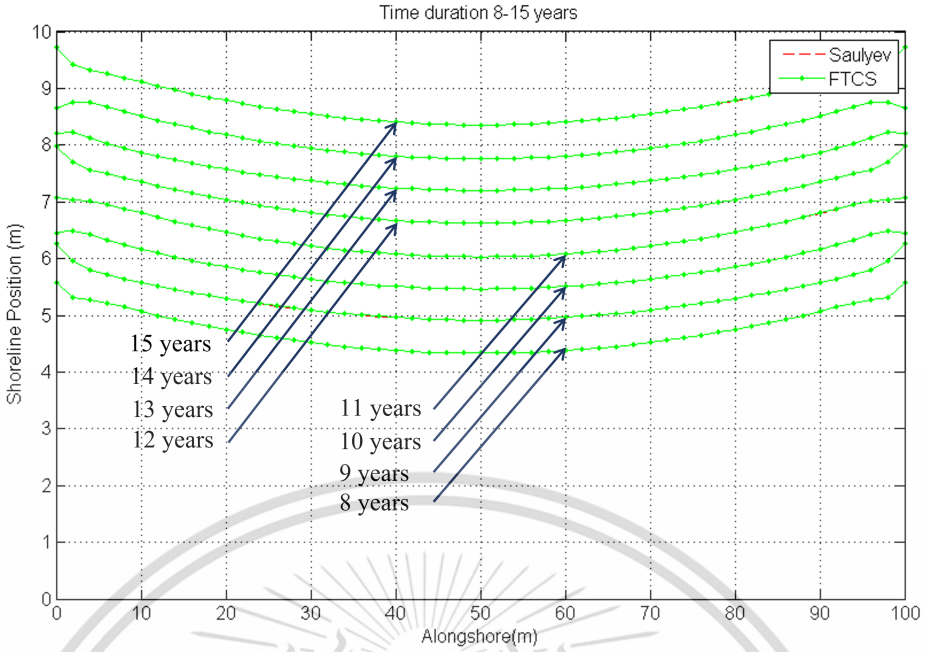

Figure 3.22: Shoreline evolution in 8-15 years when wavelength $0.5\sin(t+0.02x)$.

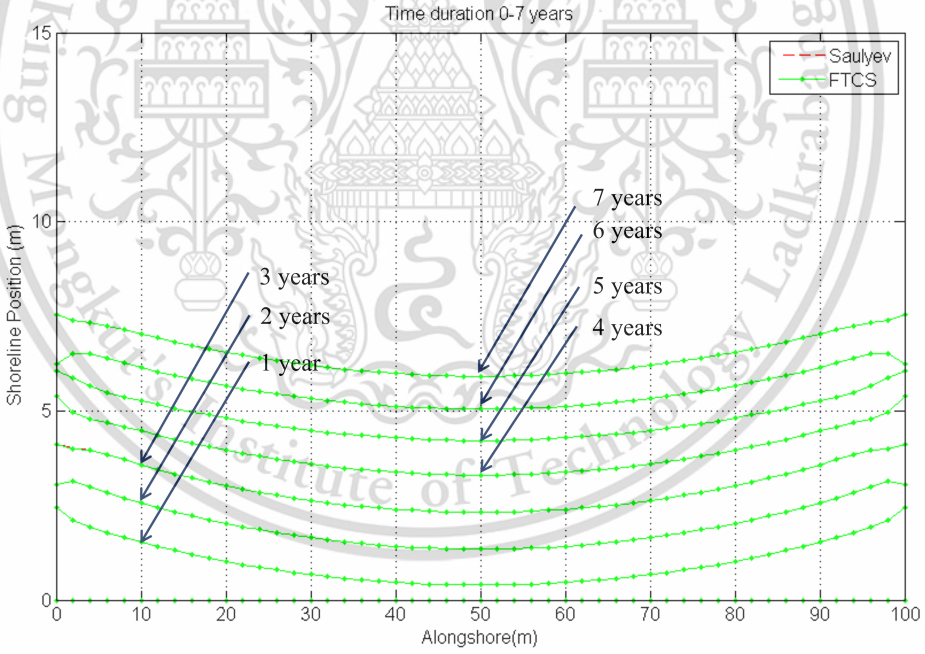

Figure 3.23: Shoreline evolution in 0-7 years when wavelength $0.5\sin(t+0.03x)$.

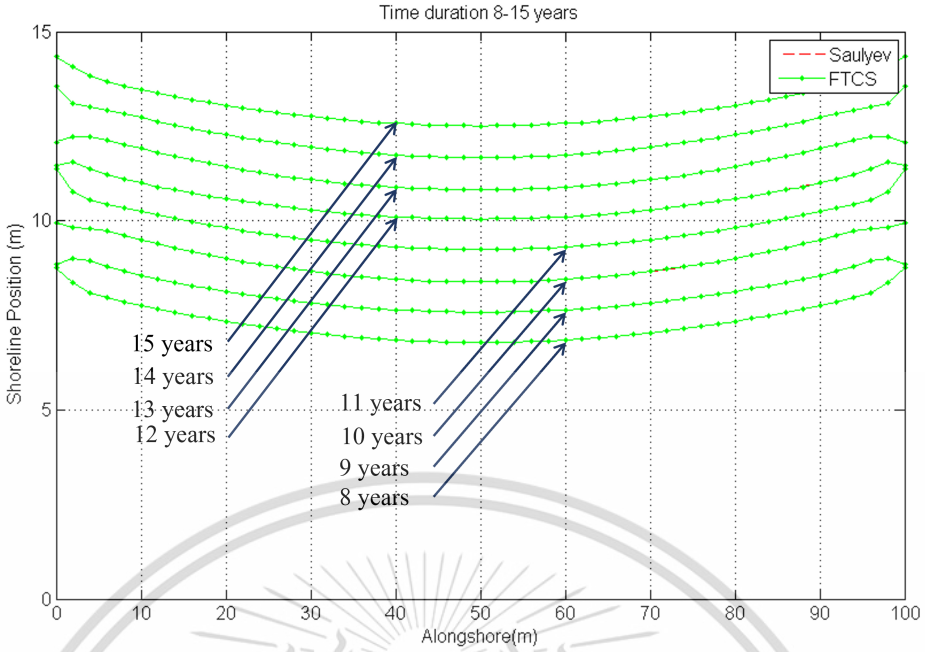

Figure 3.24: Shoreline evolution in 8-15 years when wavelength $0.5\sin(t+0.03x)$.

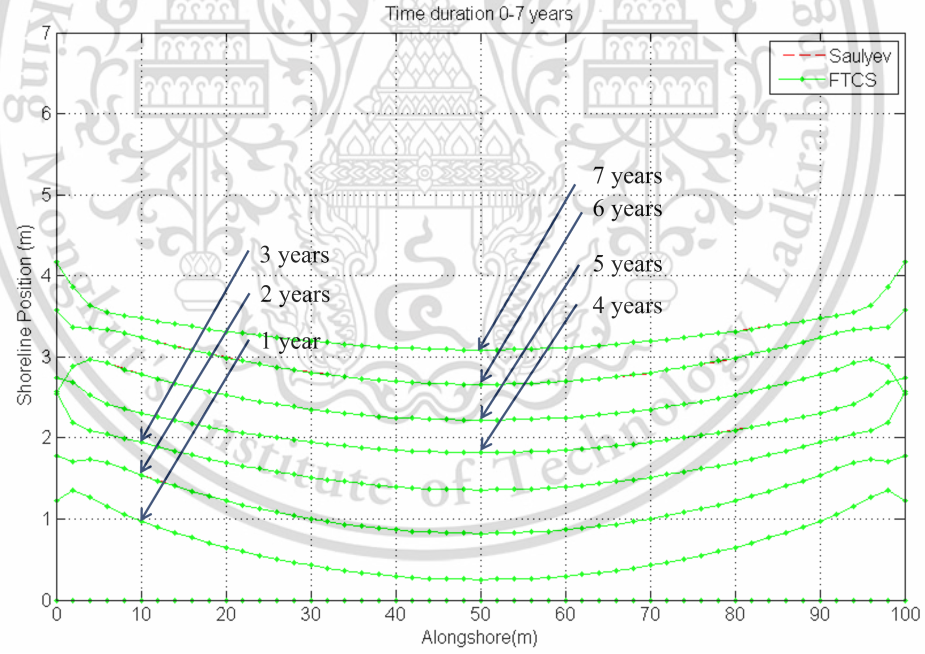

Figure 3.25: Shoreline evolution in 0-7 years when wavelength $0.5\sin(t+0.04x)$.

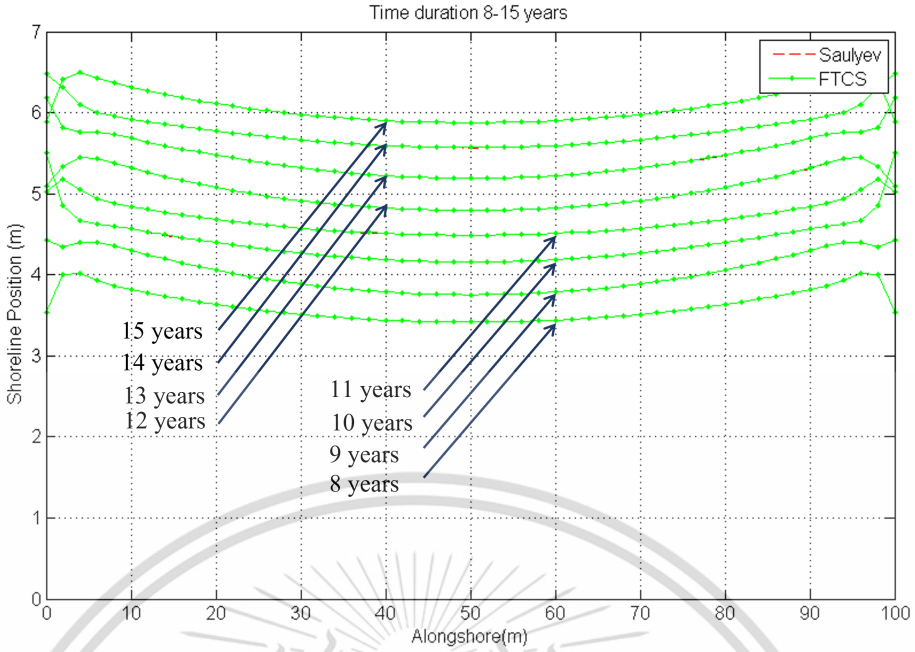

Figure 3.26: Shoreline evolution in 8-15 years when wavelength $0.5\sin(t+0.04x)$.

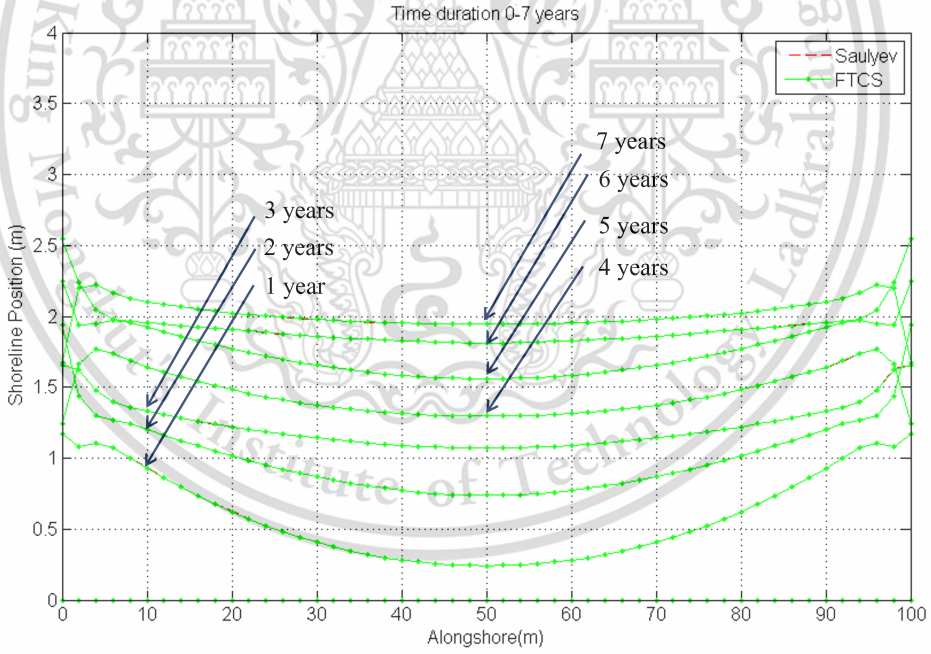

Figure 3.27: Shoreline evolution in 0-7 years when wavelength $0.5\sin(t+0.05x)$.

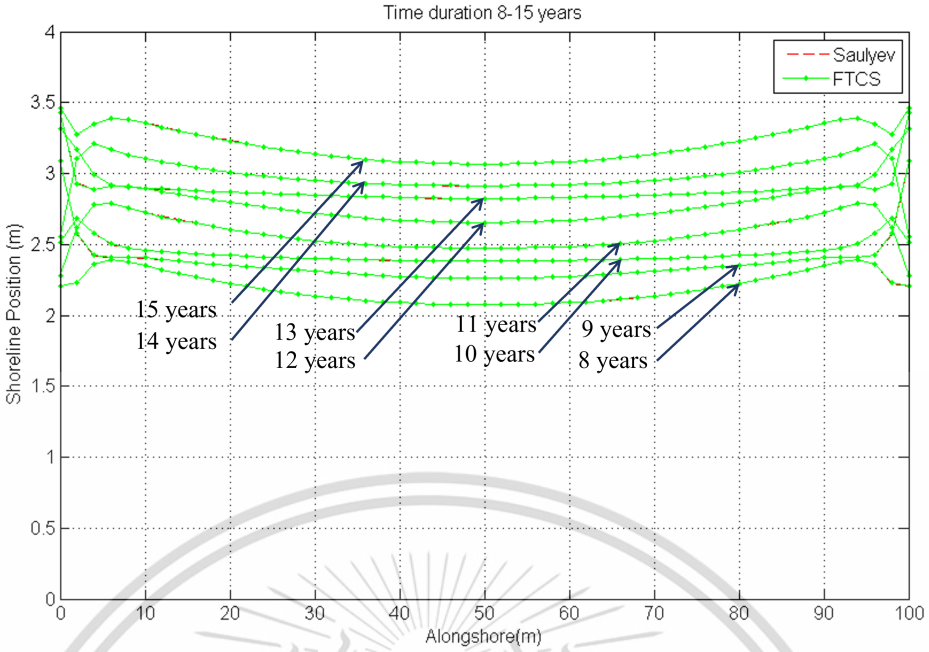

Figure 3.28: Shoreline evolution in 8-15 years when wavelength $0.5\sin(t+0.05x)$.

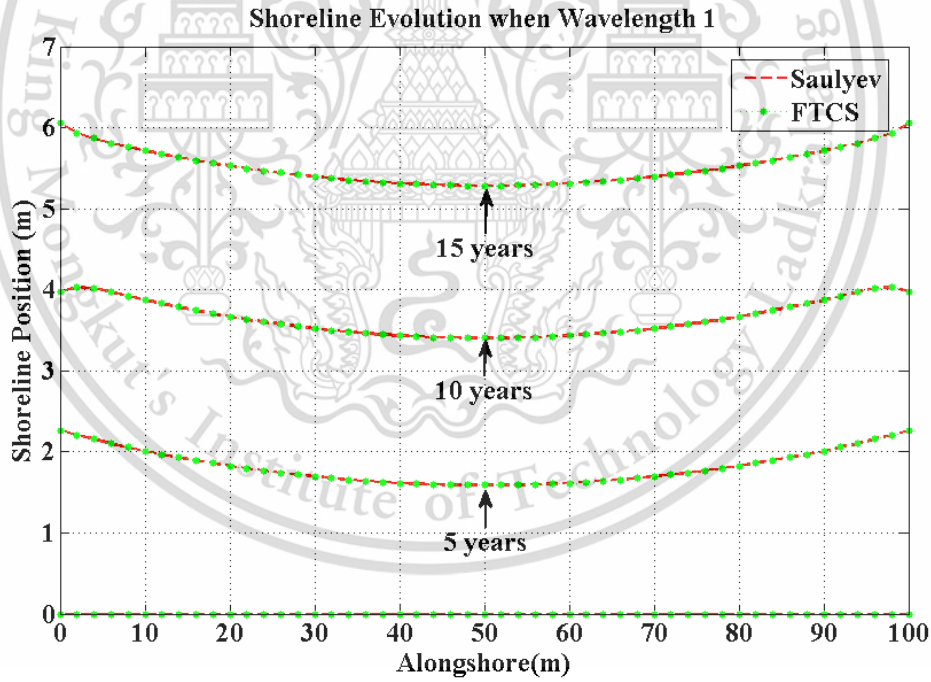

Figure 3.29: Shoreline evolution in 5, 10 and 15 years when wavelength $0.5\sin(t+0.01x)$.

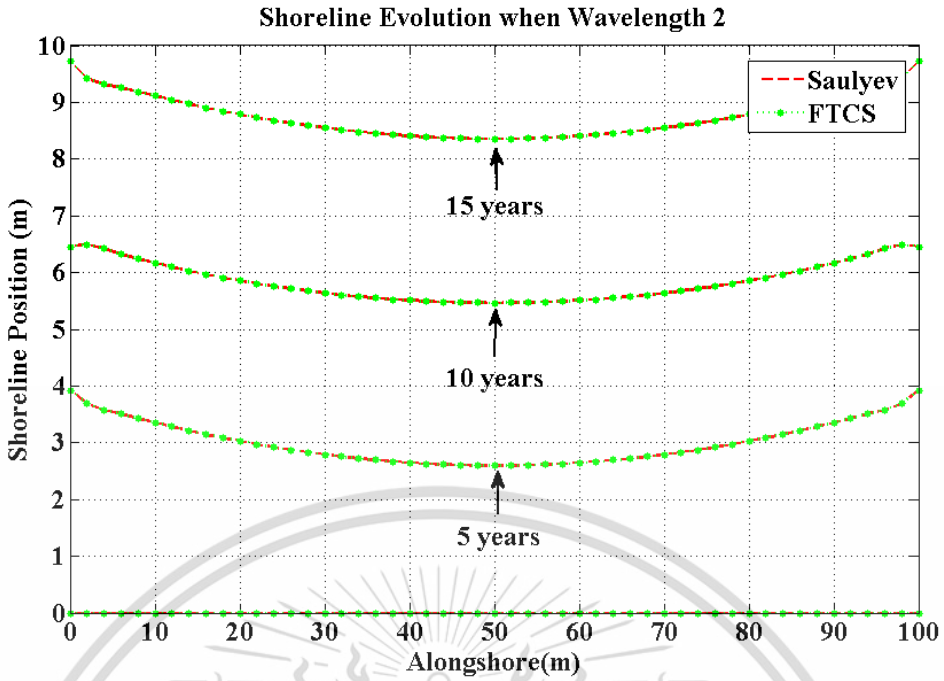

Figure 3.30: Shoreline evolution in 5, 10 and 15 years when wavelength $0.5\sin(t+0.02x)$.

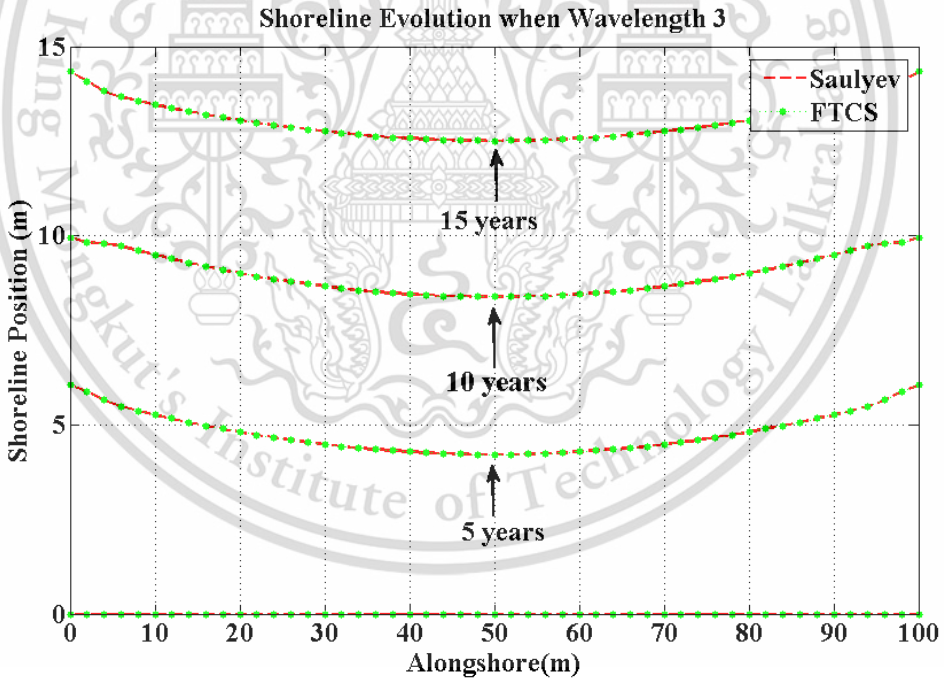

Figure 3.31: Shoreline evolution in 5, 10 and 15 years when wavelength $0.5\sin(t+0.03x)$.

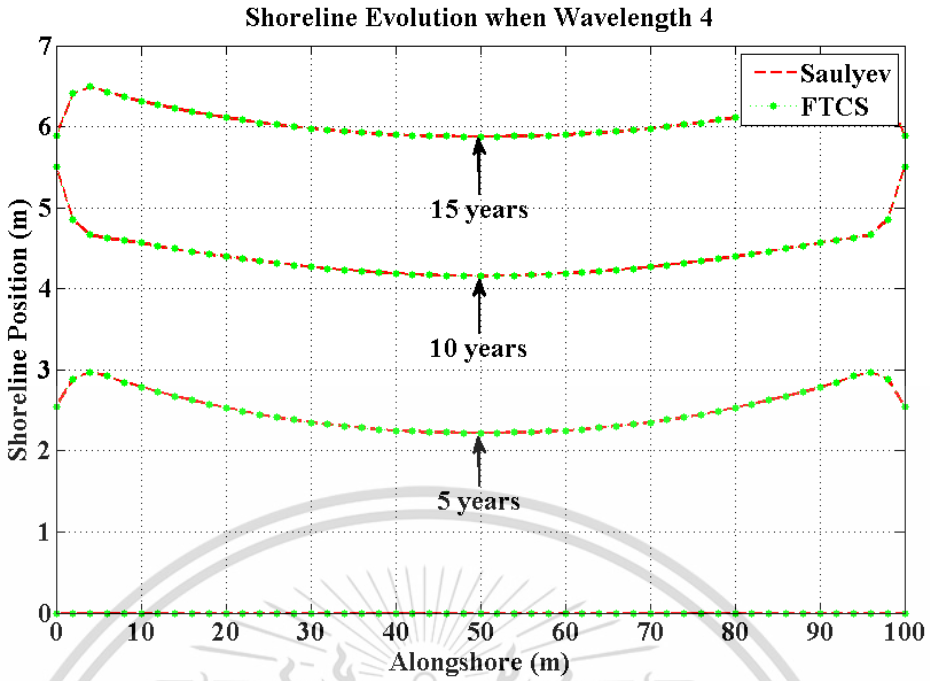

Figure 3.32: Shoreline evolution in 5, 10 and 15 years when wavelength $0.5\sin(t+0.04x)$.

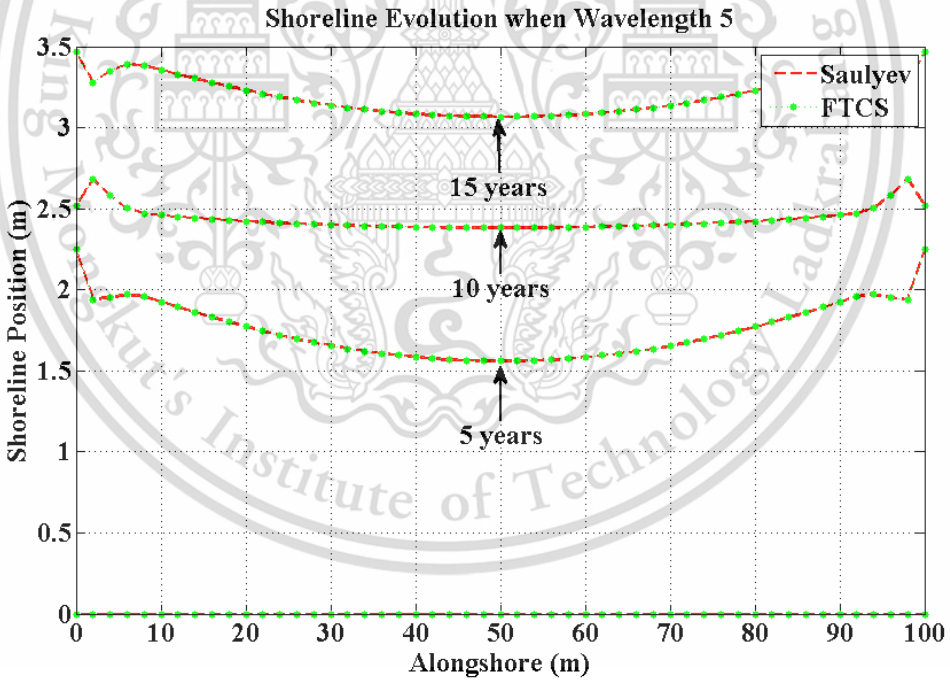

Figure 3.33: Shoreline evolution in 5, 10 and 15 years when wavelength $0.5\sin(t+0.05x)$.

Table 3.8: Approximated shoreline evolution along 15 years using the traditional forward time centered space techniques when wavelength $0.5\sin(t+0.01x)$.

Time	Distance (m)					
(Years)	0	20	40	60	80	100
1	0.8609	0.3967	0.1801	0.1801	0.3967	0.8609
5	2.2665	1.8264	1.6152	1.6152	1.8264	2.2665
10	3.9788	3.6680	3.4335	3.4335	3.6680	3.9788
15	6.0537	5.5284	5.3113	5.3113	5.5284	6.0537

Table 3.9: Approximated shoreline evolution along 15 years using the Saulyev finite difference techniques when wavelength $0.5\sin(t+0.01x)$.

Time	Distance (m)					
(Years)	0	20	40	60	80	100
1	0.8613	0.3969	0.1802	0.1800	0.3965	0.8606
5	2.2662	1.8588	1.6152	1.6152	1.8266	2.2667
10	3.9783	3.6679	3.4334	3.4334	3.6679	3.9788
15	6.0529	5.5280	5.3113	5.3113	5.5285	6.0538

Table 3.10: Approximated shoreline evolution along 15 years using the traditional forward time centered space techniques when wavelength $0.5\sin(t+0.02x)$.

Time	Distance (m)					
(Years)	0	20	40	60	80	100
1	1.2300	0.6412	0.2861	0.2861	0.6412	1.2300
5	3.9256	3.0263	2.6466	2.6466	3.0263	3.9256
10	6.4567	5.8539	5.5070	5.5070	5.8539	6.4567
15	9.7213	8.7855	8.4059	8.4059	8.7855	9.7213

Table 3.11: Approximated shoreline evolution along 15 years using the Saulyev finite difference techniques when wavelength $0.5\sin(t+0.02x)$.

Time	Distance (m)					
(Years)	0	20	40	60	80	100
1	1.2304	0.6416	0.2863	0.2860	0.6409	1.2296
5	3.9260	3.0264	2.6295	2.6466	3.0262	3.9255
10	6.4566	5.8537	5.5068	5.5071	5.8540	6.4568
15	9.7219	8.7857	8.4060	8.4058	8.7853	9.7212

Table 3.12: Approximated shoreline evolution along 15 years using the traditional forward time centered space techniques when wavelength $0.5\sin(t+0.03x)$.

Time	Distance (m)					
(Years)	0	20	40	60	80	100
1	2.4426	1.0204	0.4643	0.4643	1.0204	2.4426
5	6.0495	4.8087	4.2833	4.2833	4.8087	6.0495
10	9.9512	9.0056	8.4521	8.4521	9.0056	9.9512
15	14.3340	13.0512	12.5716	12.5716	13.0512	14.3340

Table 3.13: Approximated shoreline evolution along 15 years using the Saulyev finite difference techniques when wavelength $0.5\sin(t+0.03x)$.

Time	Distance (m)					
(Years)	0	20	40	60	80	100
1	2.4427	1.0205	0.4644	0.4641	1.0201	2.4423
5	6.0495	4.8082	4.2831	4.2833	4.8088	6.0495
10	9.9518	9.0062	8.4522	8.4521	9.0054	9.9509
15	14.3339	13.0507	12.5714	12.5715	13.0513	14.3341

Table 3.14: Approximated shoreline evolution along 15 years using the traditional forward time centered space techniques when wavelength $0.5\sin(t+0.04x)$.

Time	Distance (m)					
(Years)	0	20	40	60	80	100
1	1.2192	0.6492	0.2962	0.2962	0.6492	1.2192
5	2.5437	2.5297	2.2522	2.2522	2.5297	2.5437
10	5.5018	4.3970	4.1878	4.1878	4.3970	5.5018
15	5.8860	6.1114	5.9015	5.9015	6.1114	5.8860

Table 3.15: Approximated shoreline evolution along 15 years using the Saulyev finite difference techniques when wavelength $0.5\sin(t+0.04x)$.

Time	Distance (m)					
(Years)	0	20	40	60	80	100
1	1.2190	0.6492	0.2962	0.2961	0.6490	1.2189
5	2.5443	2.5302	2.2521	2.2522	2.5295	2.5434
10	5.5016	4.3967	4.1881	4.1879	4.3972	5.5022
15	5.8859	6.1116	5.9013	5.9015	6.1115	5.8859

Table 3.16: Approximated shoreline evolution along 15 years using the traditional forward time centered space techniques when wavelength $0.5\sin(t+0.05x)$.

Time	Distance (m)					
(Years)	0	20	40	60	80	100
1	1.1699	0.6231	0.2817	0.2817	0.6231	1.1699
5	2.2472	1.7718	1.5839	1.5839	1.7718	2.2472
10	2.5173	2.4222	2.3866	2.3866	2.4222	2.5173
15	3.4696	3.2305	3.0839	3.0839	3.2305	3.4696

Table 3.17: Approximated shoreline evolution along 15 years using the Saulyev finite difference techniques when wavelength $0.5\sin(t+0.05x)$.

Time	Distance (m)					
(Years)	0	20	40	60	80	100
1	1.1701	0.6235	0.2819	0.2816	0.6226	1.1696
5	2.2477	1.7722	1.5840	1.5837	1.7713	2.2466
10	2.5165	2.4214	2.3861	2.3865	2.4226	2.5175
15	3.4704	3.2312	3.0841	3.0837	3.2299	3.4691

We will compare the five wavelengths with time durations of 5, 10, and 15 years, as illustrated in Fig. 3.29-3.31.

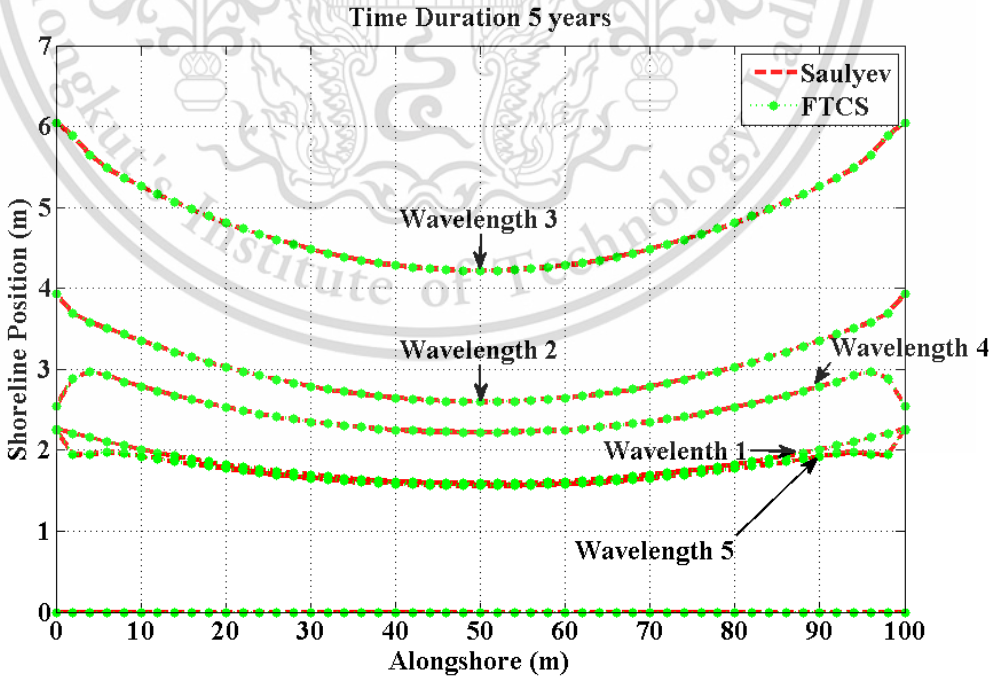

Figure 3.34: Wavelength Comparisons in 5 years.

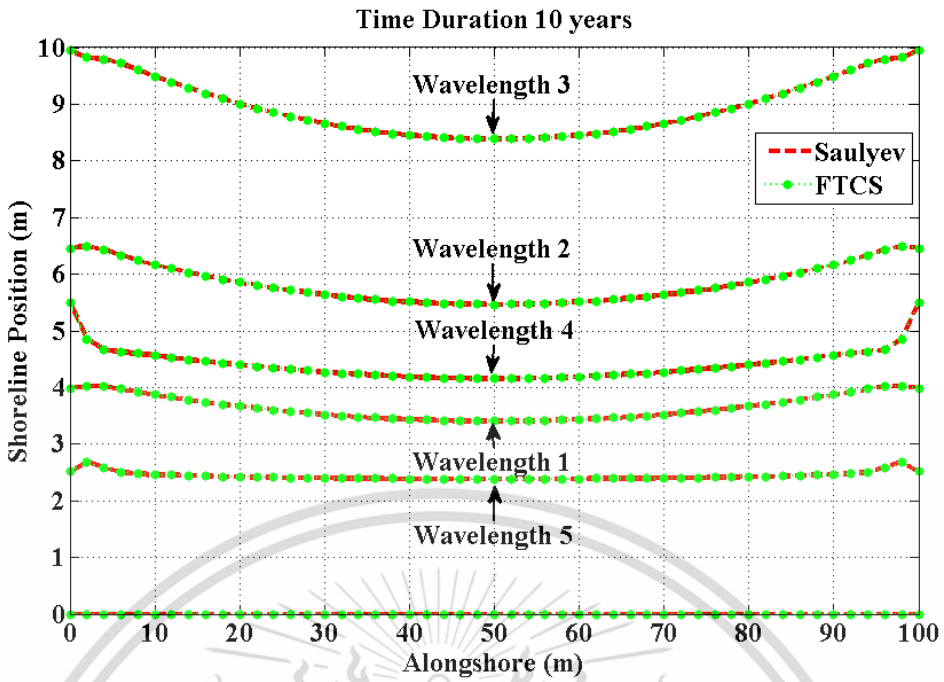

Figure 3.35: Wavelength Comparisons in 10 years.

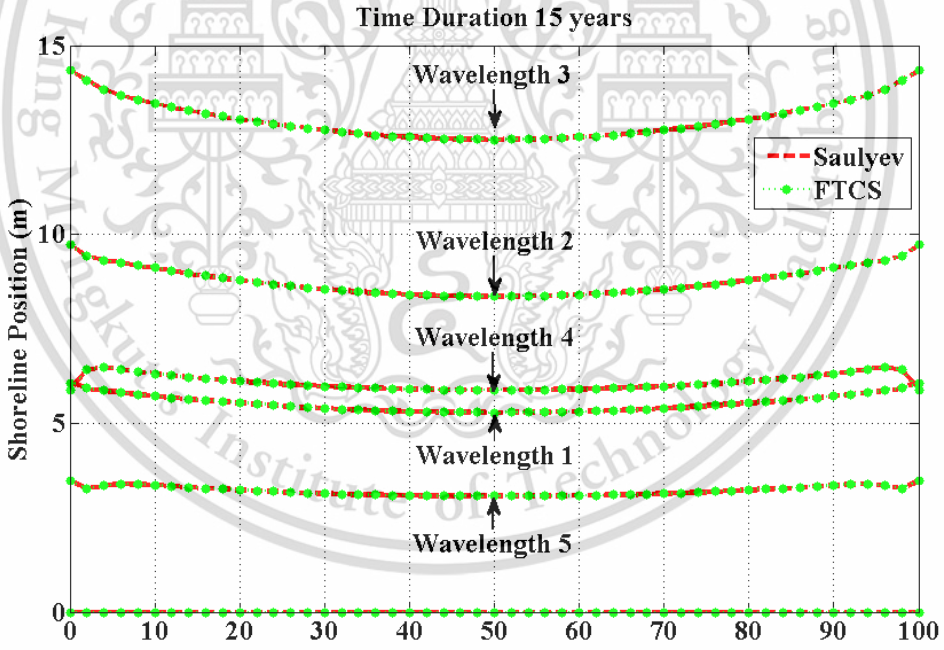

Figure 3.36: Wavelength Comparisons in 15 years.

Chapter 4

A Combination of A Shoreline Evolution Model and A Wave Crest Model on T-Head Groin Structures With the Breaking Wave Effect

In this chapter, we focus on the effects of the T-head groin structure on shoreline evolution. The average wave crest impact is analyzed for eight sizes of T-head groin construction. An initial condition setting technique and boundary conditions techniques, as well as the structural impacts of the T-head groin, are discussed. Each year, the shoreline evolution is approximated using the traditional forward time centered space techniques and the unconditionally stable Saulyev finite differential techniques. The calculated impacts of shoreline evolution for eight different T-head groin sizes were consistent with the wave crest impact model.

4.1 Traditional forward time centered space techniques applied to shoreline evolution model

Substituting Eqs (2.30)-(2.33) into Eq (2.8), we obtain,

$$\frac{y_i^{n+1}-y_i^n}{\Delta t}=D\left(\frac{y_{i+1}^n-2y_i^n+y_{i-1}^n}{(\Delta x)^2}\right), \tag{4.1}$$

for $1 \le i \le M-1$ and $0 \le n \le N-1$. Eq (4.1) can be written in an explicit form of finite difference as follows,

$$y_i^{n+1}=Ay_{i+1}^n+(1-2A)y_i^n+Ay_{i-1}^n, \tag{4.2}$$

for $1 \le i \le M-1$ and $0 \le n \le N-1$.

4.2 An unconditionally Saulyev finite difference techniques applied to shoreline evolution model

Substituting Eqs (2.34)-(2.36) into Eq (2.8), we obtain

$$\frac{y_i^{n+1}-y_i^n}{\Delta t}=D\left(\frac{y_{i+1}^n-y_i^n-y_i^{n+1}+y_{i-1}^{n+1}}{(\Delta x)^2}\right), \tag{4.3}$$

for $1 \le i \le M-1$ and $0 \le n \le N-1$. Eq (4.3) can be written in an explicit form of finite difference as follows,

$$y_i^{n+1}=\frac{1}{1+A}(Ay_{i+1}^n+(1-A)y_i^n+Ay_{i-1}^{n+1}), \tag{4.4}$$

for $1 \le i \le M-1$ and $0 \le n \le N-1$.

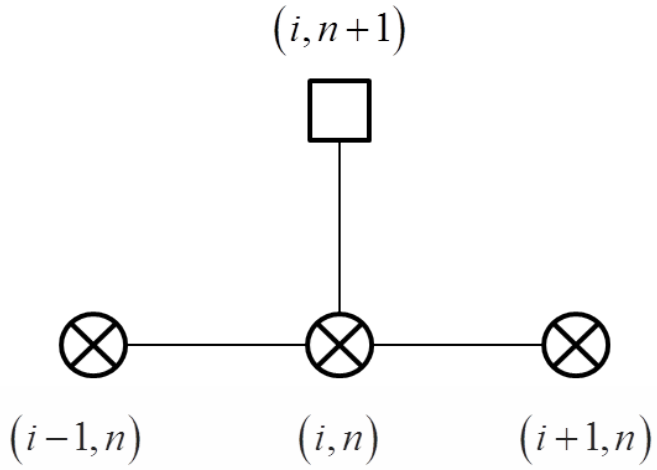

Figure 4.1: Stencil diagram of forward central space finite difference technique

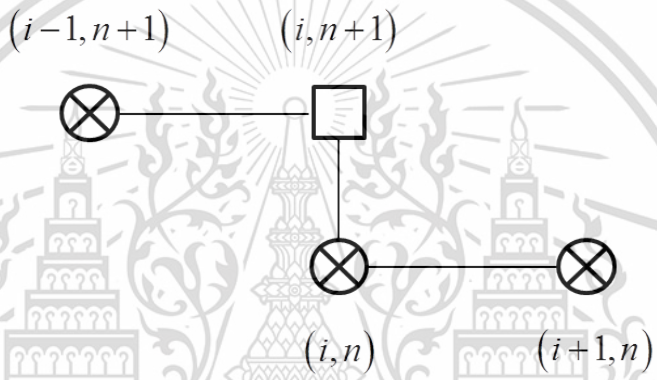

Figure 4.2: Stencil diagram of Saulyev finite difference technique

4.3 The employment of traditional forward time centered space techniques to the left and the right boundary conditions for Straight Impermeable T-head groin system

By substituting Eqs (2.30)-(2.33) into Eq (2.8), we obtain,

$$\frac{y_i^{n+1}-y_i^n}{\Delta t}=D\left(\frac{y_{i+1}^n-2y_i^n+y_{i-1}^n}{(\Delta x)^2}\right), \tag{4.5}$$

For $i=0$, substitution of the approximate unknown value of the left boundary by a traditional central difference approximation with the known derivative the left boundary condition gives

$$y_{-1}^n=y_1^n-2(\Delta x)(-\tan(\alpha_0)), \tag{4.6}$$

Substituting Eq (4.6) into Eq (4.5), we obtain

$$y_i^{n+1}=(1-2A)y_i^n+2Ay_{i+1}^n-2A(\Delta x)(-\tan(\alpha_0)), \tag{4.7}$$

For $i=M$, substitution of the approximate unknown value of the right boundary by a traditional central difference approximation with the known derivative the right

boundary condition gives

$$y_{M+1}^{n} = y_{M-1}^{n} + 2(\Delta x)(-\tan(-\alpha_0)), \tag{4.8}$$

Substituting Eq (4.8) into Eq (4.5), we obtain

$$y_i^{n+1} = 2Ay_{i-1}^{n} + (1-2A)y_i^{n} + 2A(\Delta x)(-\tan(-\alpha_0)), \tag{4.9}$$

The Eq (4.7) and Eq (4.9) can be used to calculate the values y_i^n on grid points of the solution domain.

4.4 Initial and boundary conditions setting

The initials shoreline is assumed to be parallel to the x-axis.

4.4.1 Straight Impermeable T-head groin system

Straight Impermeable twin-groin system as show in Figure 4.3. Assuming that the breaking wave angle α_0 to the shoreline is symmetric. It follows that the sand transport rate along the shoreline is uniform. The groin is instantaneously added at as show in Figure 4.4. These means that the initial condition becomes

$$y(x,0) = h_2(x), \tag{4.10}$$

boundary conditions are also assumed by

$$\frac{\partial y(0,t)}{\partial x} = -\tan(\alpha_0), \tag{4.11}$$

and

$$\frac{\partial y(L,t)}{\partial x} = -\tan(-\alpha_0), \tag{4.12}$$

when $h_2(x)$ is initial shoreline topography function.

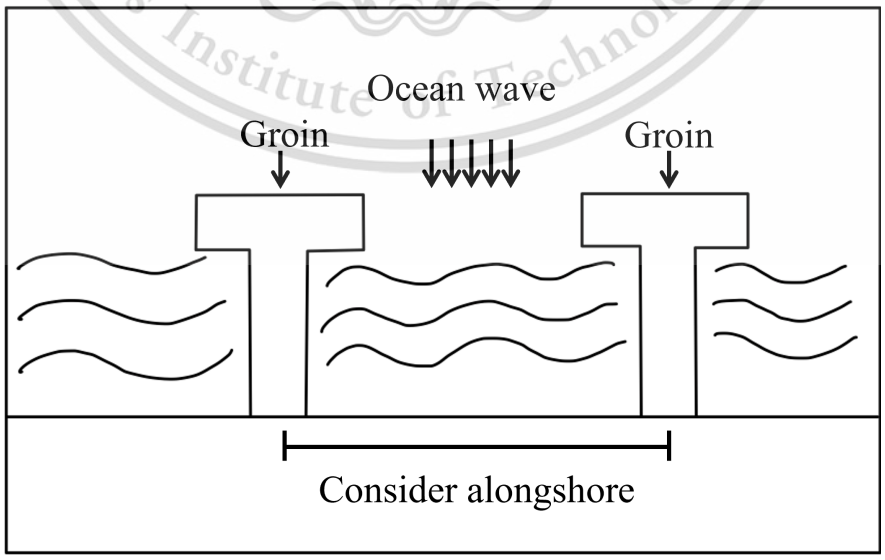

Figure 4.3*:* Initial shoreline with configuration straight impermeable T-head groins.

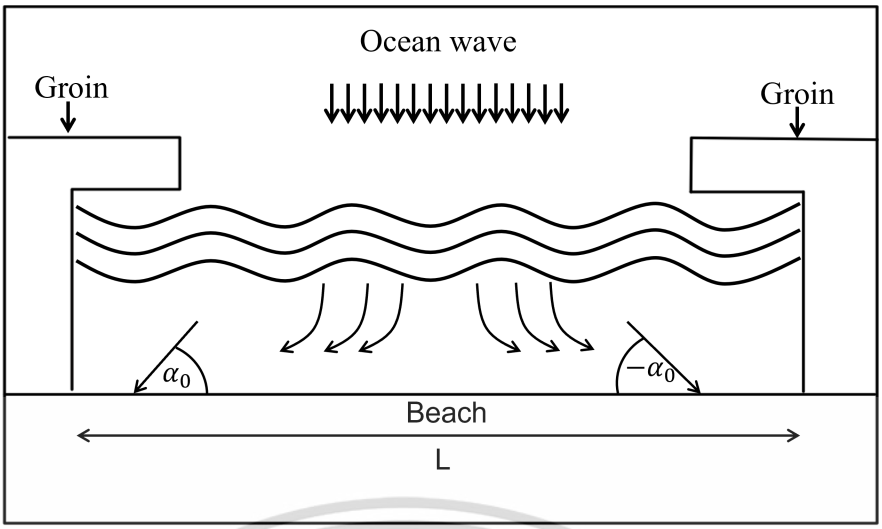

Figure 4.4: Initial shoreline with configuration straight impermeable T-head groins.

4.4.2 The initial and boundary condition for wave crest impact model with Straight Impermeable T-head groin system

The initial condition of the reservoir was as follows: the x and y velocity components were zero as well as the water elevation: $u = 0, v = 0$ and $\xi = 0$. Assuming that the breakwater is not a perfect barrier to water as it is made of an aggregate of rocks with large gaps.

The boundary condition was as follows:

(1) $u = 0, \frac{\partial v}{\partial y} = 0, \xi = f(x, y, t)$ for wave coming,

(2) $\frac{\partial u}{\partial x} = 0, v = 0, \frac{\partial \xi}{\partial x} = 0$ for left and right boundary,

(3) $u = 0, \frac{\partial v}{\partial y} = 0, \frac{\partial \xi}{\partial y} = 0$ for along the beach,

(4) $u = 0, \frac{\partial v}{\partial y} = 0, \frac{\partial \xi}{\partial y} = 0$ for top T-head groin structure,

(5) $u = 0, \frac{\partial v}{\partial y} = 0, \frac{\partial \xi}{\partial y} = 0$ for bottom T-head groin structure, and

(6) $\frac{\partial u}{\partial x} = 0, v = 0, \frac{\partial \xi}{\partial x} = 0$ for left and right T-head groin structure. The boundary conditions are illustrated in Figure 4.5-4.7.

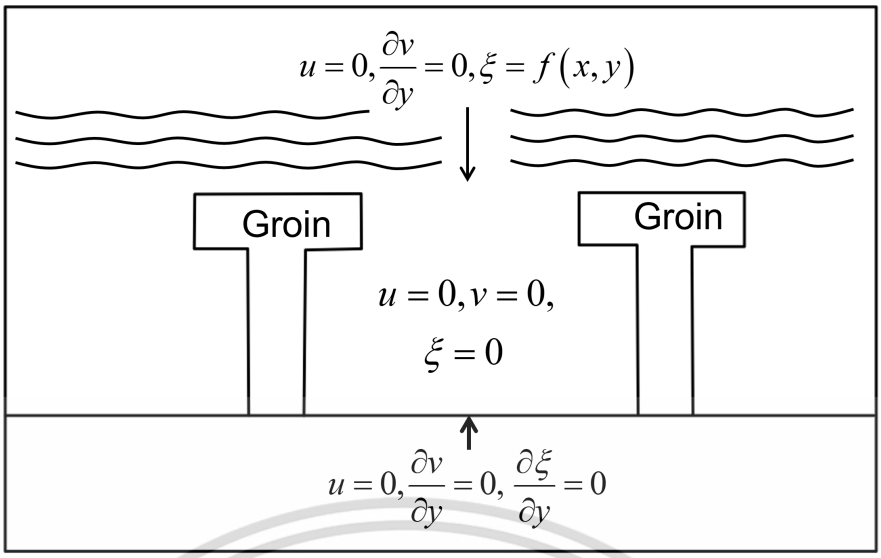

Figure 4.5: Initial and boundary conditions.

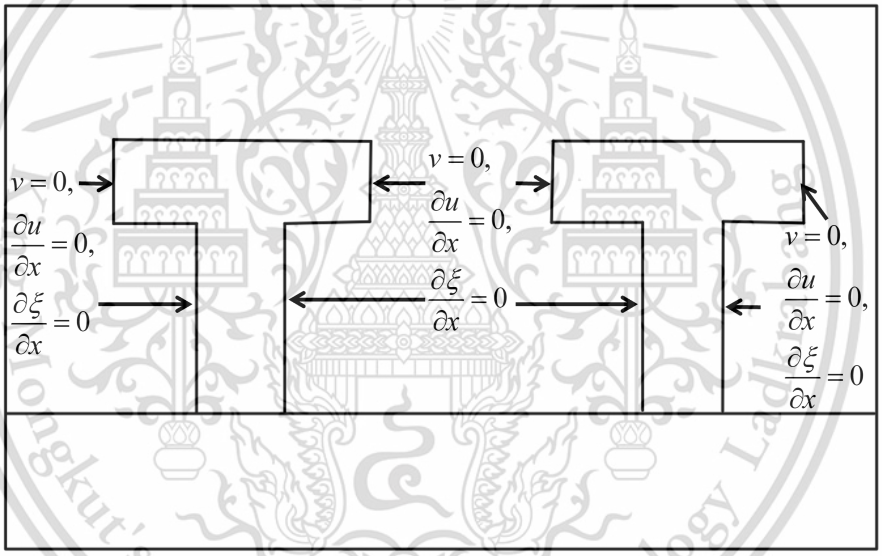

Figure 4.6: Initial and boundary conditions for T-head groin structure (1).

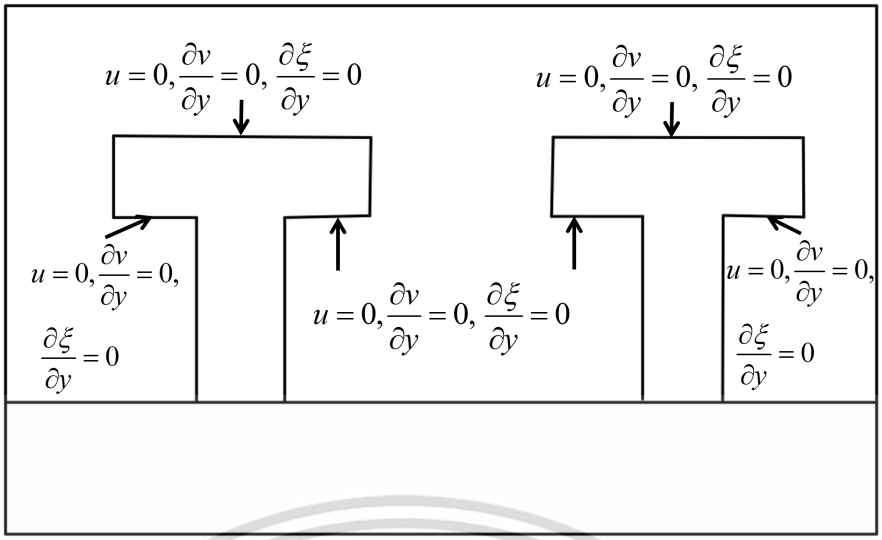

Figure 4.7*:* Initial and boundary conditions for T-head groin structure (2).

4.5 Groin Setting Techniques

We will consider eight lengths of considered T-head groin is 16, 18, 20, 22, 24, 26, 28, and 30 m. The consideration alongshore is illustrated in Fig 4.8.

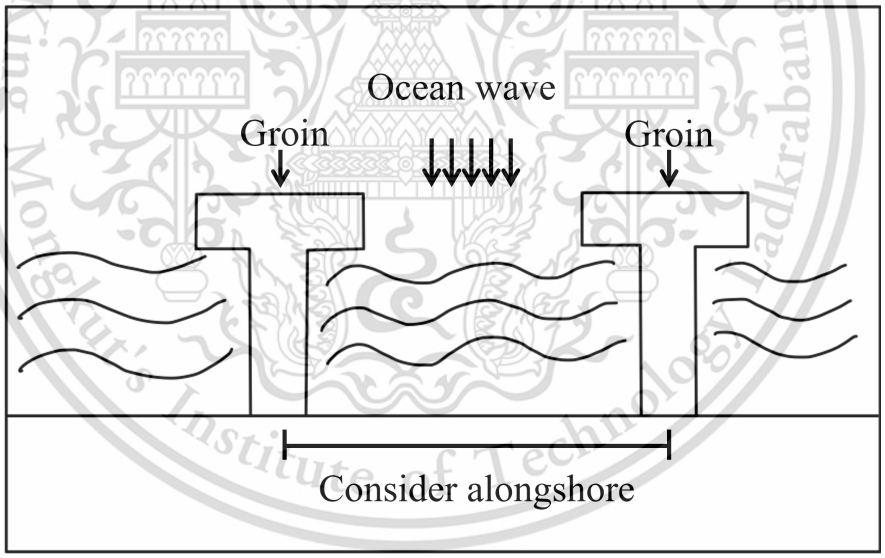

Figure 4.8*:* Initial and boundary conditions for T-head groin structure (2).

For eight lengths of the T-head groin that are being taken into consideration, the approximate wave crest impact model solution will be approximated using finite difference methods 2.37 are illustrated in Fig.4.9-4.16.

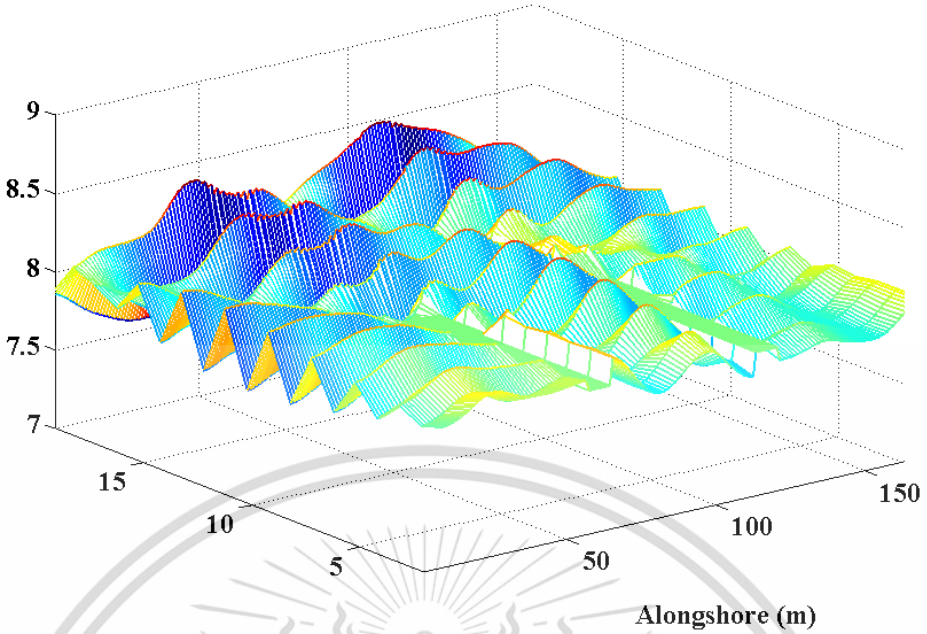

Figure 4.9*:* Wave crest impact in 9 years when T-head groin 16 m.

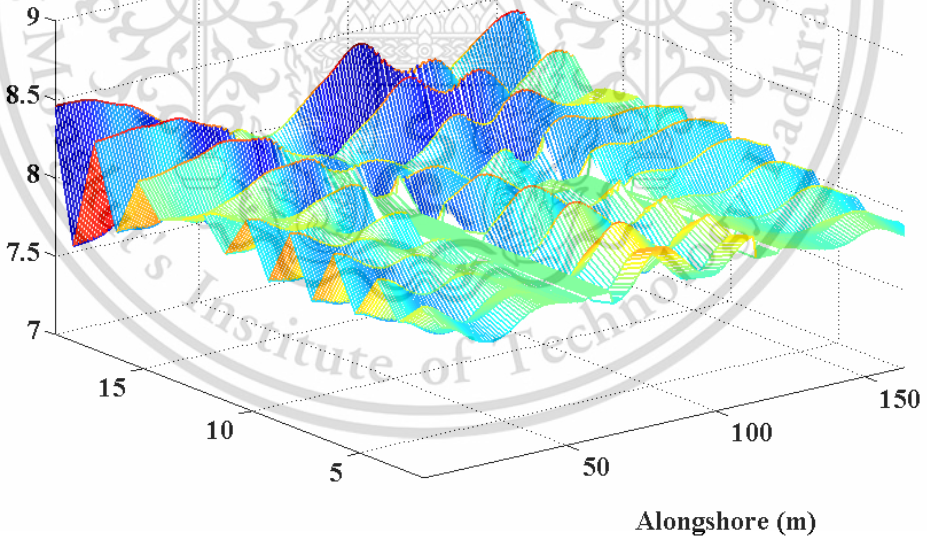

Figure 4.10*:* Wave crest impact in 11 years when T-head groin 18 m.

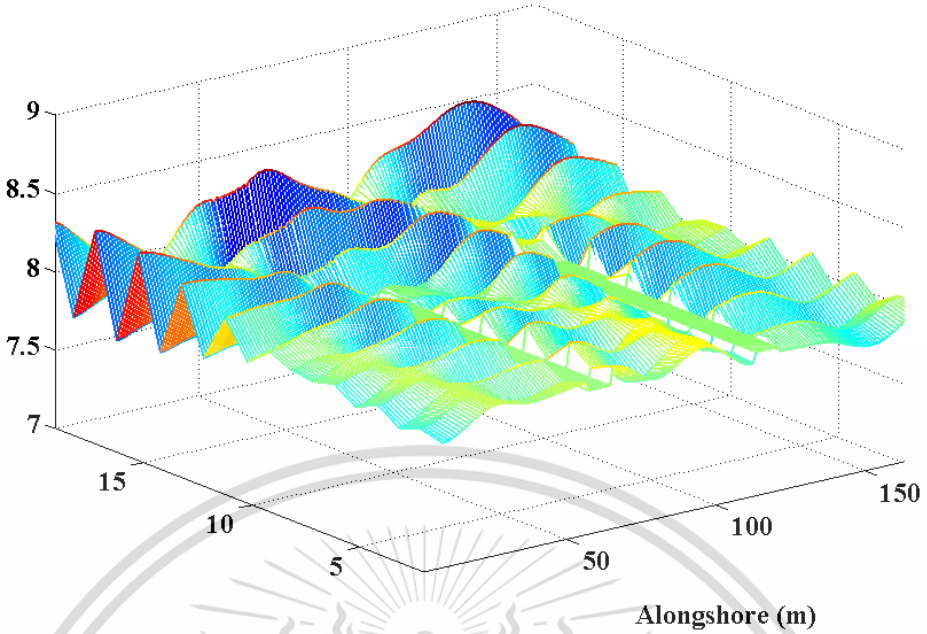

Figure 4.11: Wave crest impact in 15 years when T-head groin 20 m.

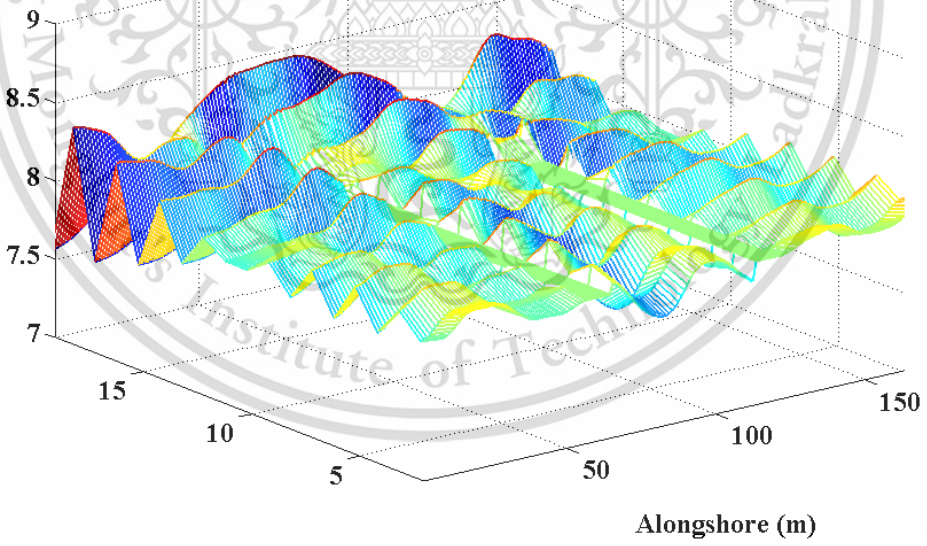

Figure 4.12: Wave crest impact in 13 years when T-head groin 22 m.

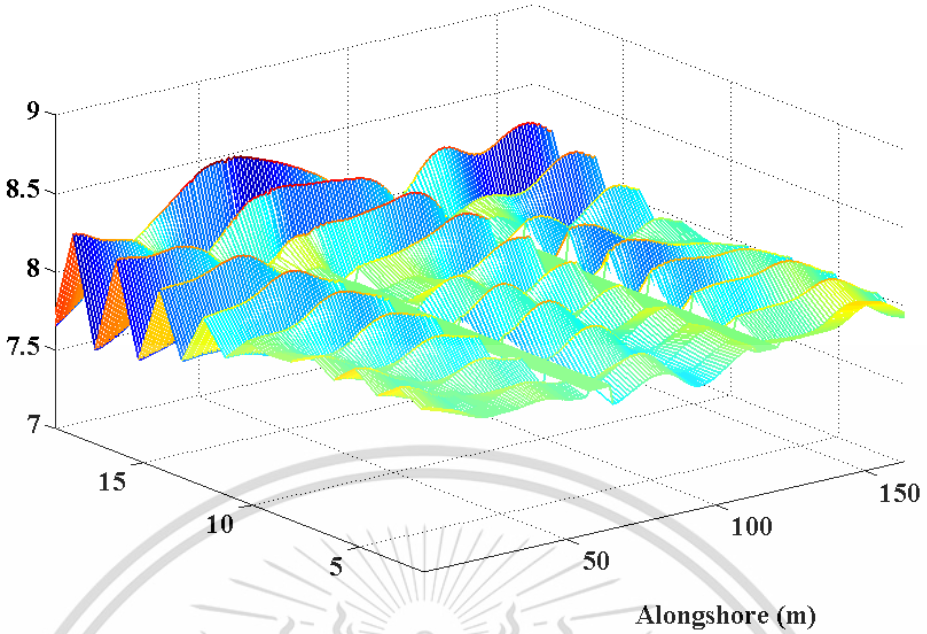

Figure 4.13: Wave crest impact in 20 years when T-head groin 24 m.

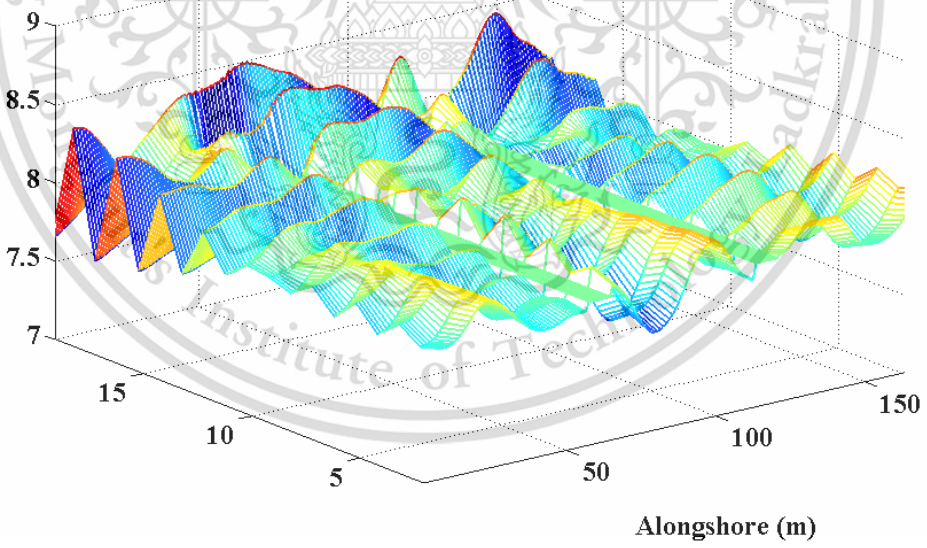

Figure 4.14: Wave crest impact in 20 years when T-head groin 26 m.

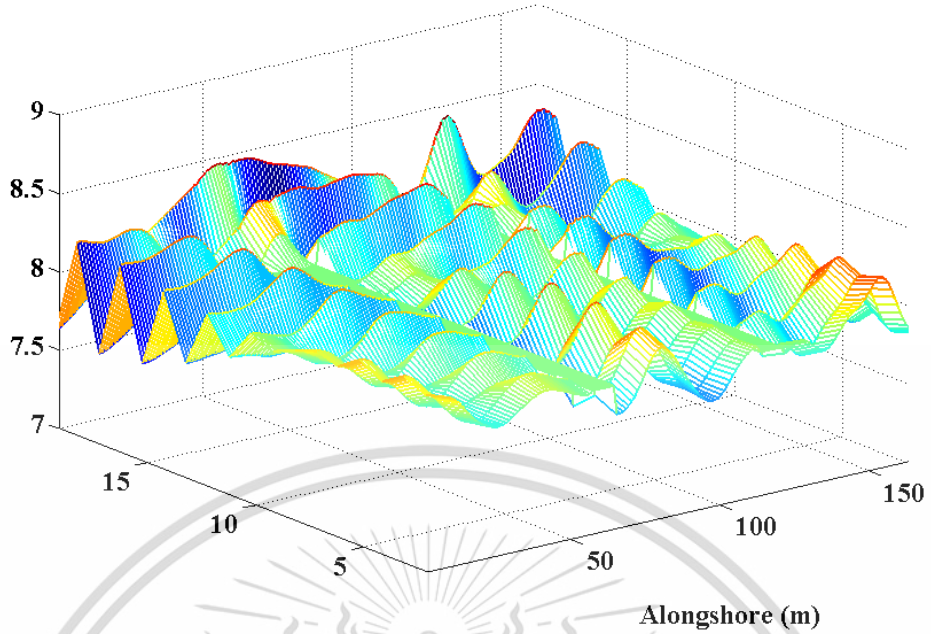

Figure 4.15*:* Wave crest impact in 20 years when T-head groin 28 m.

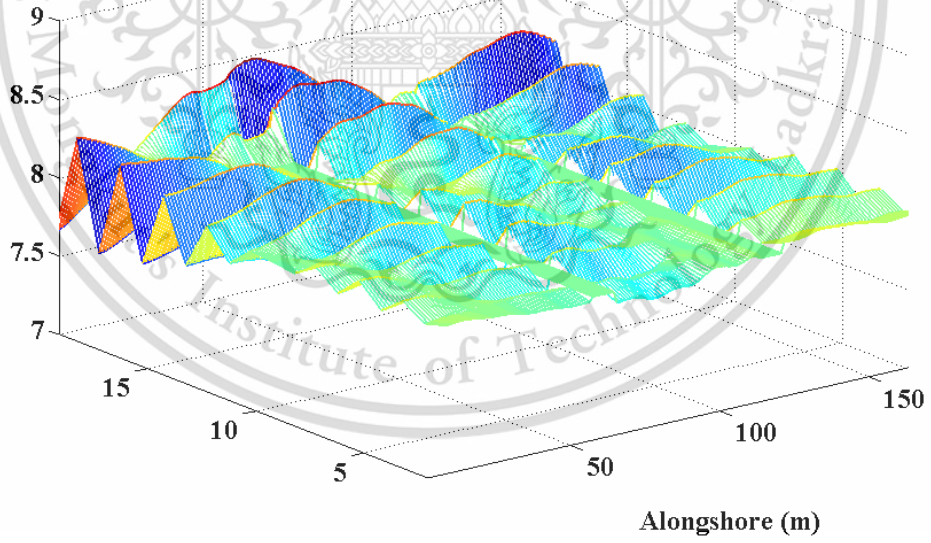

Figure 4.16*:* Wave crest impact in 20 years when T-head groin 30 m.

Table 4.1-4.8 shows the averaged wave crest impact α_0 obtained by 2.39 for eight lengths of the considered T-head groin.

Table 4.1*:* The averaged wave crest impact 9 years when T-head Groin Size 16 m.

Time	Minute					
(Years)	0-15	15-30	30-45	45-60	60-75	75-90
1	0.2635	0.2054	0.2100	0.2145	0.2189	0.2232
5	0.2645	0.2624	0.2604	0.2584	0.2564	0.2543
9	0.0264	0.0223	0.0181	0.0138	0.0093	0.0046
Time	Minute					
(Years)	...	1365-1380	1380-1395	1395-1410	1410-1425	1425-1440
1	...	-0.6192	-0.5621	-0.5047	-0.5098	-0.3890
5	...	0.0661	0.0633	0.0604	0.0575	0.0545
9	...	0.3304	0.3267	0.3859	0.3823	0.3786

Table 4.2*:* The averaged wave crest impact 11 years when T-head Groin Size 18 m.

Time	Minute					
(Years)	0-15	15-30	30-45	45-60	60-75	75-90
1	-0.0830	-0.0677	-0.0526	-0.1004	-0.0856	-0.0708
5	0.1572	0.1530	0.1488	0.1446	0.1404	0.1361
10	-0.1413	-0.1425	-0.2584	-0.0550	0.0099	0.1341
11	-0.0119	-0.0652	-0.0557	-0.0462	-0.0994	-0.0896
Time	Minute					
(Years)	...	1365-1380	1380-1395	1395-1410	1410-1425	1425-1440
1	...	-0.4803	-0.4885	-0.4339	-0.3791	-0.3242
5	...	0.0504	0.0493	0.0483	0.0472	0.0461
10	...	0.3557	0.3561	0.3564	0.3568	0.3572
11	...	-0.4077	-0.4091	-0.4107	-0.4123	-0.4769

Table 4.3: The averaged wave crest impact 15 years when T-head Groin Size 20 m.

Time	Minute					
(Years)	0-15	15-30	30-45	45-60	60-75	75-90
1	0.3146	0.3102	0.3052	0.2990	0.2906	0.3429
5	0.3369	0.3351	0.3333	0.3311	0.3284	0.3255
10	0.1009	0.1625	0.1610	0.1594	0.1577	0.1559
15	-0.4382	-0.3815	-0.3875	-0.3306	-0.2735	-0.2165
Time	Minute					
(Years)	...	1365-1380	1380-1395	1395-1410	1410-1425	1425-1440
1	...	-0.2437	-0.1238	-0.1295	-0.0096	-0.0154
5	...	0.1439	0.1422	0.1405	0.1388	0.1370
10	...	0.0145	0.0125	0.0104	0.0084	0.0062
15	...	0.2597	0.2581	0.2566	0.2551	0.2536

Table 4.4: The averaged wave crest impact 13 years when T-head Groin Size 22 m.

Time	Minute					
(Years)	0-15	15-30	30-45	45-60	60-75	75-90
1	-0.2305	-0.1621	-0.1569	-0.1521	-0.1476	-0.1436
5	0.1447	0.1365	0.1287	0.1844	0.1782	0.1736
10	-0.0869	0.0900	0.1422	0.2579	0.3114	0.3654
13	0.1755	0.1749	0.1741	0.1733	0.1723	0.2340
Time	Minute					
(Years)	...	1365-1380	1380-1395	1395-1410	1410-1425	1425-1440
1	...	-0.3895	-0.3405	-0.3536	-0.3033	-0.2524
5	...	0.0922	0.0925	0.0928	0.0931	0.0934
10	...	0.3630	0.3630	0.3631	0.3631	0.3632
13	...	0.4394	0.4358	0.4324	0.4291	0.4260

Table 4.5: The averaged wave crest impact 20 years when T-head Groin Size 24 m.

Time	Minute					
(Years)	0-15	15-30	30-45	45-60	60-75	75-90
1	0.2364	0.2312	0.2260	0.2837	0.2785	0.2734
5	0.6124	0.6008	0.5904	0.5802	0.5703	0.5607
10	-0.3096	-0.3150	-0.2575	-0.2628	-0.2680	-0.1474
15	0.3091	0.2975	0.3488	0.4002	0.3888	0.4403
20	-0.3199	-0.3810	-0.3794	-0.3778	-0.3763	-0.4377
Time	Minute					
(Years)	...	1365-1380	1380-1395	1395-1410	1410-1425	1425-1440
1	...	0.0385	0.0926	0.1468	0.1381	0.1293
5	...	0.2496	0.2483	0.2470	0.2458	0.2445
10	...	-0.3180	-0.3202	-0.3224	-0.3246	-0.3268
15	...	0.3869	0.3849	0.3829	0.3809	0.3790
20	...	-0.2951	-0.2964	-0.2977	-0.2991	-0.3004

Table 4.6: The averaged wave crest impact 20 years when T-head Groin Size 26 m.

Time	Minute					
(Years)	0-15	15-30	30-45	45-60	60-75	75-90
1	-0.2234	-0.1599	-0.2219	-0.2211	-0.2201	-0.2190
5	-0.1300	-0.1251	-0.1206	-0.1163	-0.1122	-0.0454
10	-0.2985	-0.2936	-0.2888	-0.2842	-0.2797	-0.2753
15	0.6864	0.7542	0.7602	0.7676	0.7130	0.5957
20	0.3344	0.3335	0.3324	0.3311	0.3926	0.3912
Time	Minute					
(Years)	...	1365-1380	1380-1395	1395-1410	1410-1425	1425-1440
1	...	0.3617	0.2390	0.2425	0.1210	0.1255
5	...	0.1702	0.1719	0.1736	0.1754	0.1771
10	...	-0.0298	-0.0289	-0.0280	-0.0272	-0.0263
15	...	0.1829	0.1846	0.1862	0.1879	0.1896
20	...	-0.1046	-0.1028	-0.1010	-0.0993	-0.0977

Table 4.7: The averaged wave crest impact 20 years when T-head Groin Size 28 m.

Time	Minute					
(Years)	0-15	15-30	30-45	45-60	60-75	75-90
1	0.2891	0.3499	0.3478	0.3457	0.3436	0.3415
5	0.3573	0.4161	0.4121	0.4080	0.4040	0.4000
10	-0.4099	-0.4122	-0.4145	-0.3541	-0.3567	-0.2965
15	0.2809	0.2764	0.2720	0.3304	0.3260	0.3216
20	-0.5731	-0.5733	-0.5735	-0.5738	-0.5742	-0.6375
Time	Minute					
(Years)	...	1365-1380	1380-1395	1395-1410	1410-1425	1425-1440
1	...	-0.0372	-0.0400	-0.0428	0.0173	0.0146
5	...	0.2837	0.2812	0.2788	0.2764	0.2740
10	...	-0.2584	-0.2628	-0.2672	-0.2716	-0.2760
15	...	0.4681	0.4643	0.4606	0.4570	0.4534
20	...	-0.1795	-0.1837	-0.1879	-0.1921	-0.1963

Table 4.8: The averaged wave crest impact 20 years when T-head Groin Size 30 m.

Time	Minute					
(Years)	0-15	15-30	30-45	45-60	60-75	75-90
1	0.0787	0.0682	0.1205	0.1100	0.0995	0.1519
5	0.4851	0.4890	0.4296	0.4322	0.4338	0.4341
10	-0.3801	-0.3713	-0.3625	-0.4168	-0.4086	-0.4013
15	0.4475	0.5016	0.4929	0.4842	0.5385	0.5928
20	-0.1901	-0.1795	-0.1690	-0.2213	-0.2110	-0.2007
Time	Minute					
(Years)	...	1365-1380	1380-1395	1395-1410	1410-1425	1425-1440
1	...	0.5101	0.4583	0.4694	0.4804	0.4283
5	...	0.4199	0.4210	0.4222	0.4235	0.4248
10	...	-0.4248	-0.4256	-0.4266	-0.4276	-0.4286
15	...	0.4115	0.4115	0.4114	0.4115	0.4116
20	...	-0.4275	-0.4266	-0.4258	-0.4251	-0.4244

4.6 Numerical Experiment

In this section, the numerical results of the various beach scenarios of T-head groin structure are considered, and the solution to the idealized problem is introduced. Assuming, during the experiments, that the length of the shoreline (L) under consideration is 100 m and the averaged wave crest impact α_0 for eight T-head groin

sizes. Table 4.2-4.10 shows the averaged wave crest impact of eight T-head groin structure sizes. Table 4.9 shows the long-shore transport rate D . The simulation setting is illustrated in Fig. 4.17.

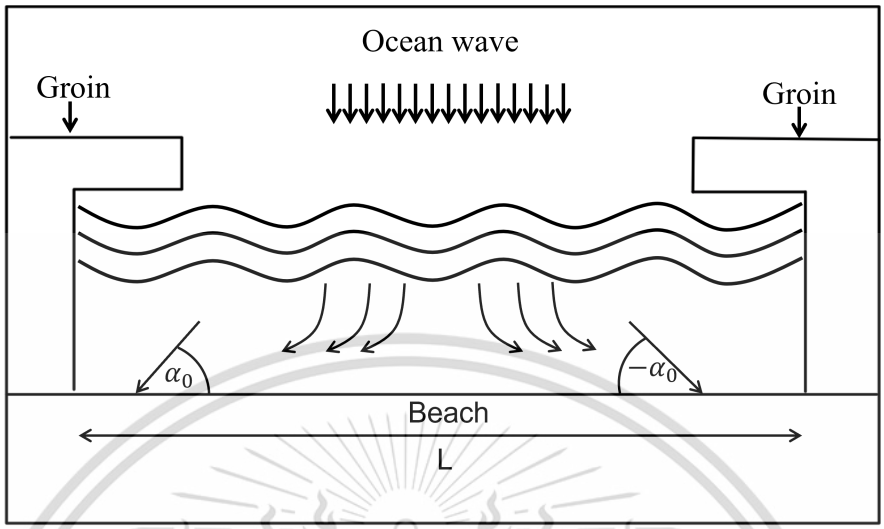

Figure 4.17*:* Initial shoreline.

Table 4.9*:* The long¬shore transport rates [37].

Month	$D\ (m/day)$
Jan	79.4659
Feb	62.1307
Mar	5.7869
Apr	61.4403
May	5.6420
Jun	5.4716
Jul	73.0227
Aug	83.071
Sep	121.7301
Oct	372.017
Nov	96.5710
Dec	101.1233

We are going to employ the traditional forward time centered space techniques (FTCS) 4.2, and the Saulyev finite difference techniques 4.4, to approximate the shoreline evolution model solution. The approximate solutions in each year are illustrated in Fig. 4.18-4.36. The approximate solutions in 5, 10, 15 and 20 years are illustrated in Fig. 4.37-4.44. Table 4.10-4.25 shows the calculated results.

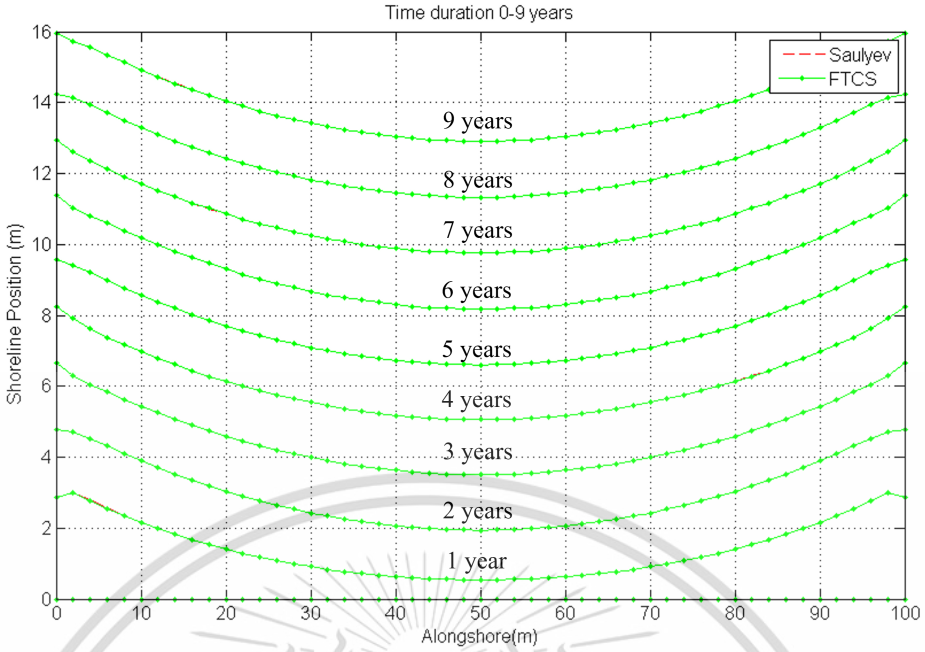

Figure 4.18*:* Shoreline evolution in 0-9 years when T-head Groin size 16 m.

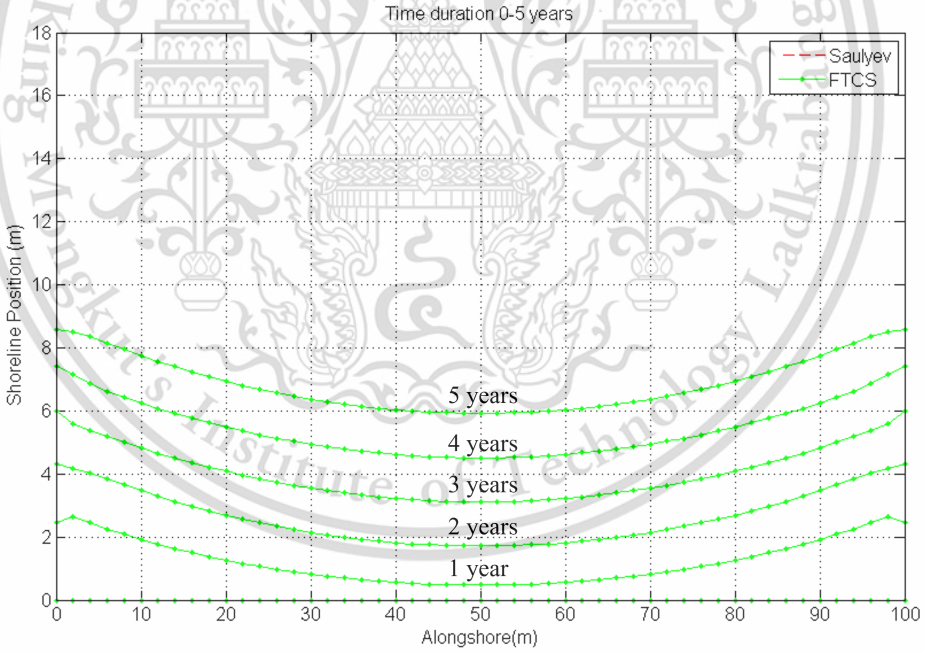

Figure 4.19*:* Shoreline evolution in 0-5 years when T-head Groin size 18 m.

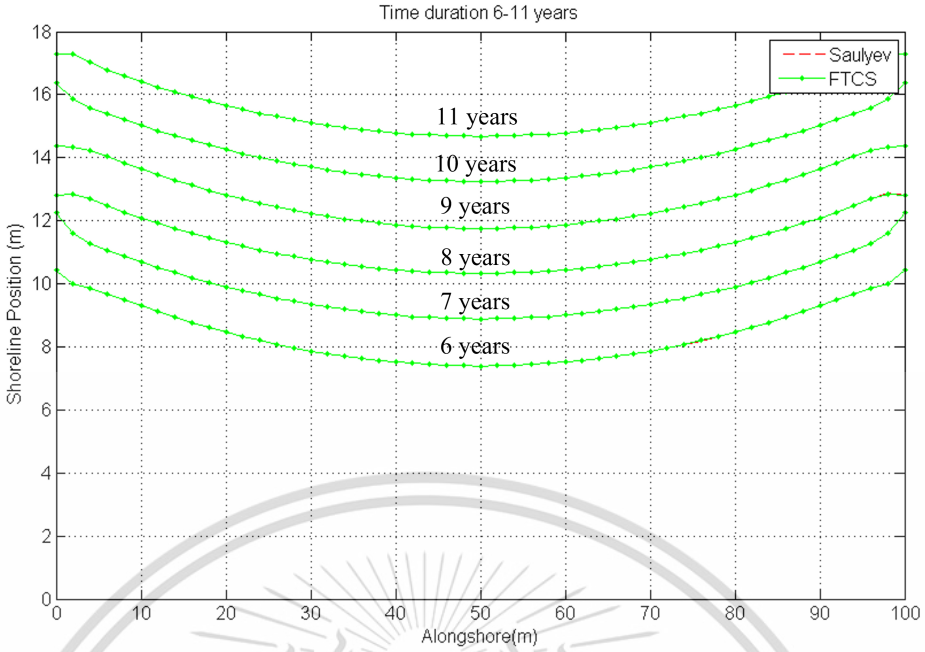

Figure 4.20*:* Shoreline evolution in 6-11 years when T-head Groin size 18 m.

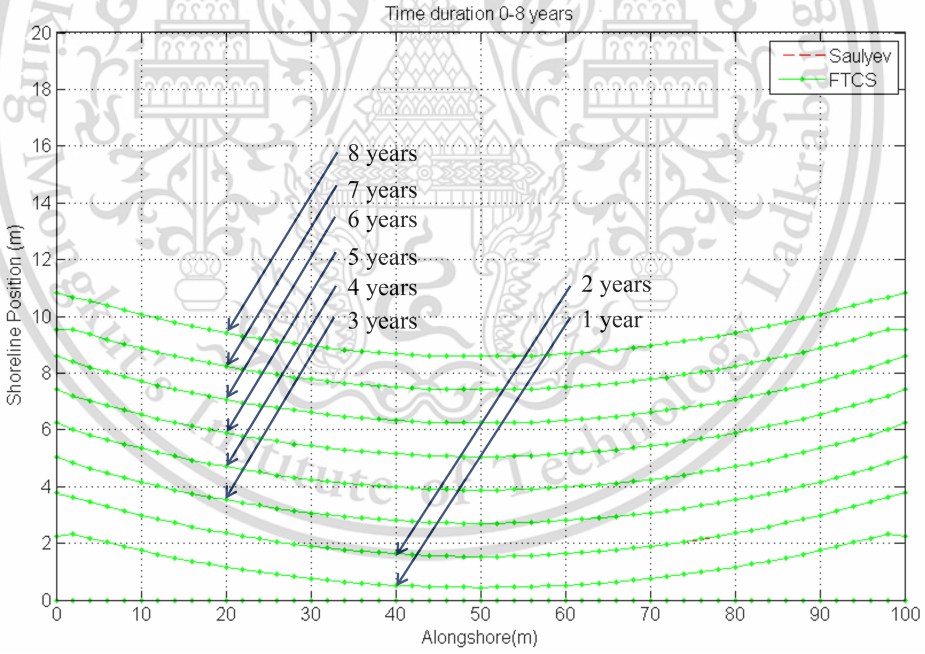

Figure 4.21*:* Shoreline evolution in 0-8 years when T-head Groin size 20 m.

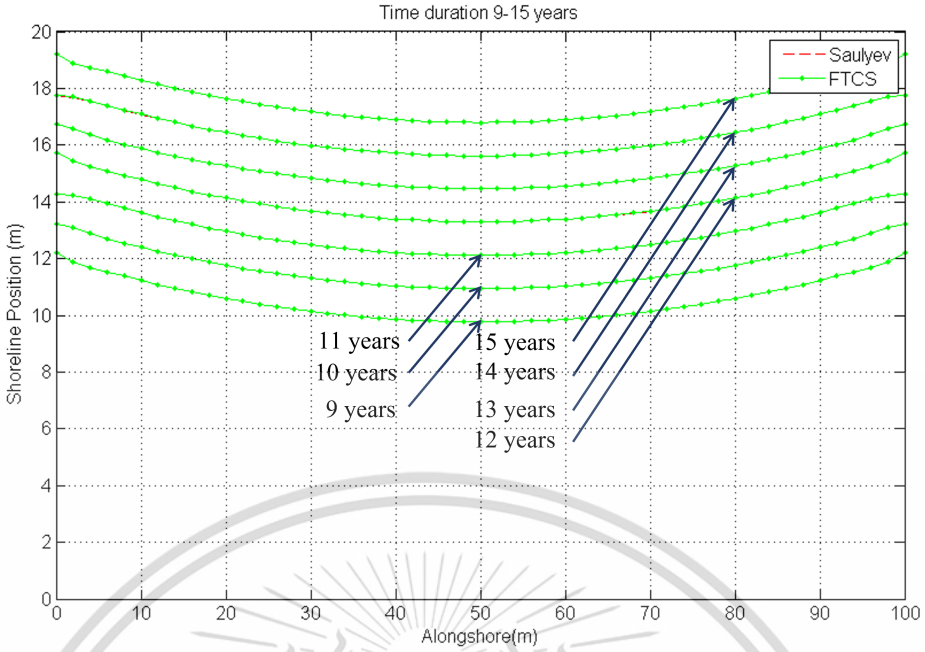

Figure 4.22*:* Shoreline evolution in 9-15 years when T-head Groin size 20 m.

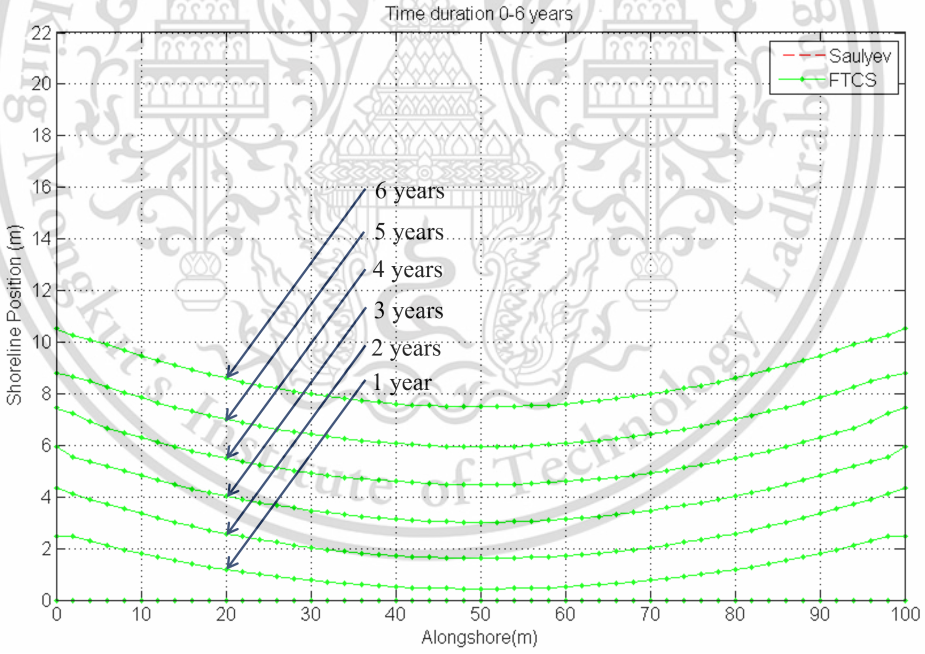

Figure 4.23*:* Shoreline evolution in 0-6 years when T-head Groin size 22 m.

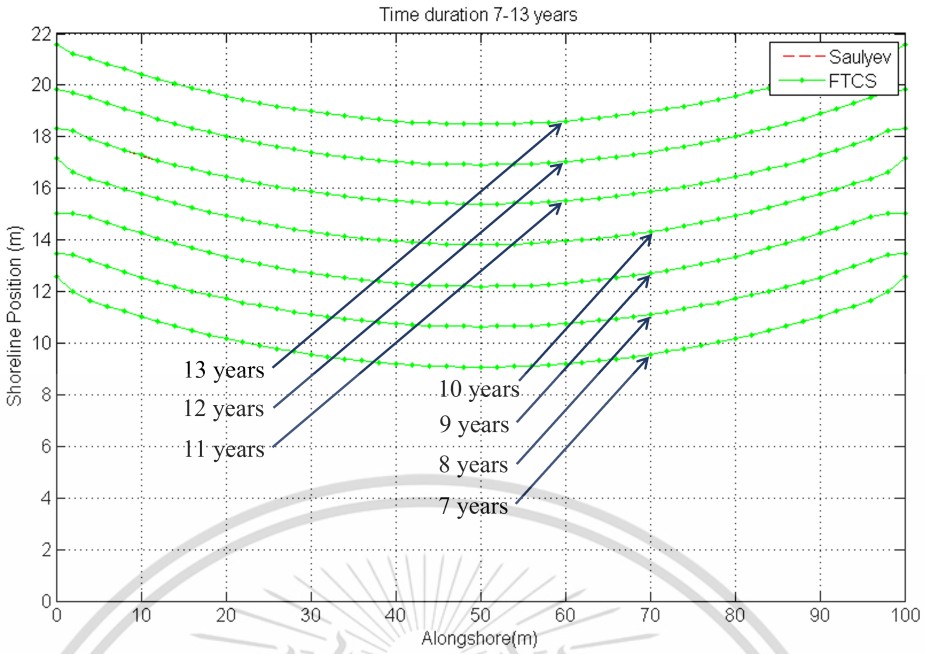

Figure 4.24*:* Shoreline evolution in 7-13 years when T-head Groin size 22 m.

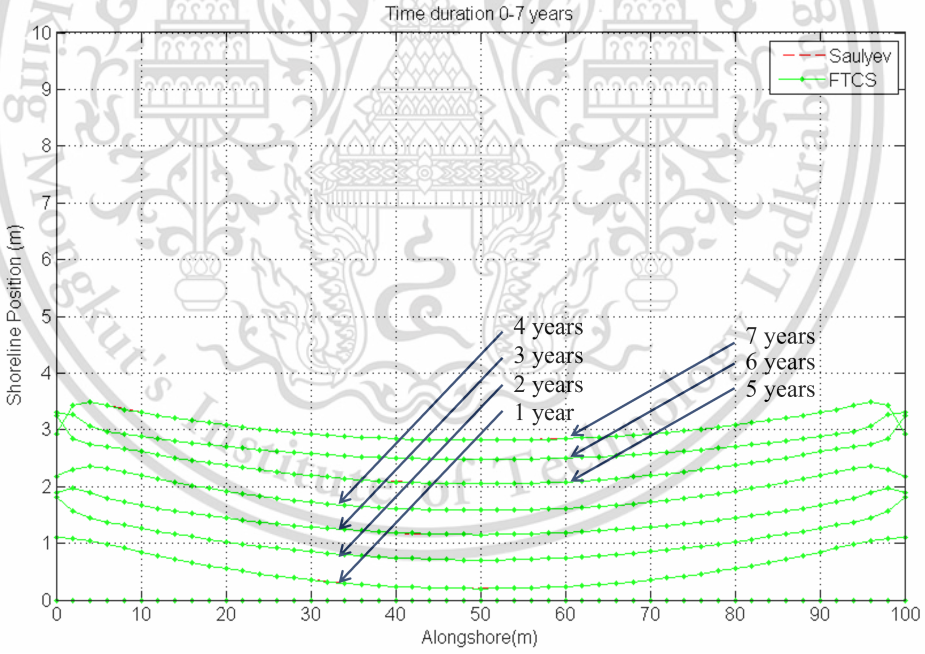

Figure 4.25*:* Shoreline evolution in 0-7 years when T-head Groin size 24 m.

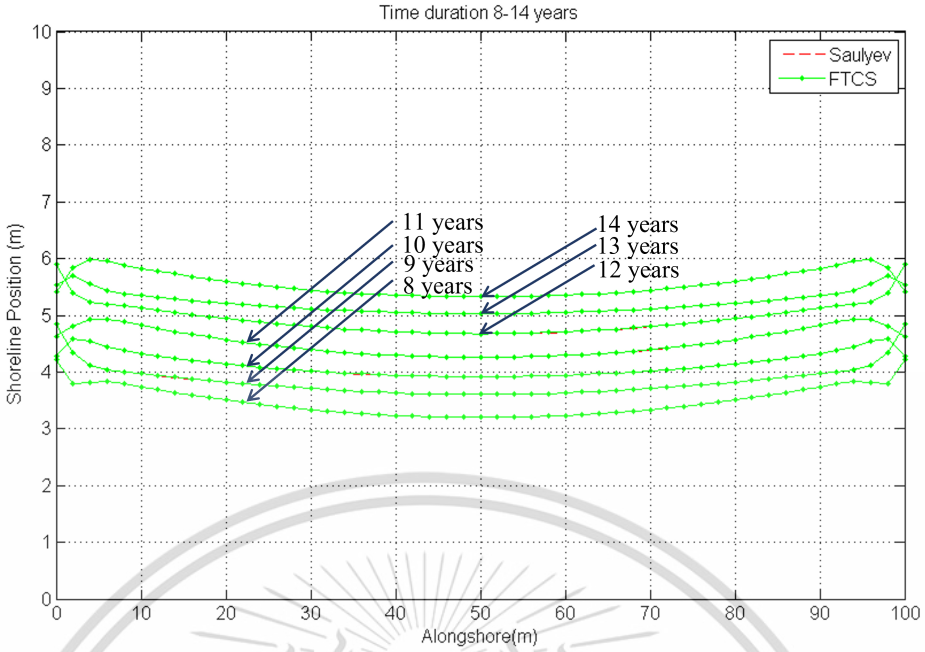

Figure 4.26*:* Shoreline evolution in 8-14 years when T-head Groin size 24 m.

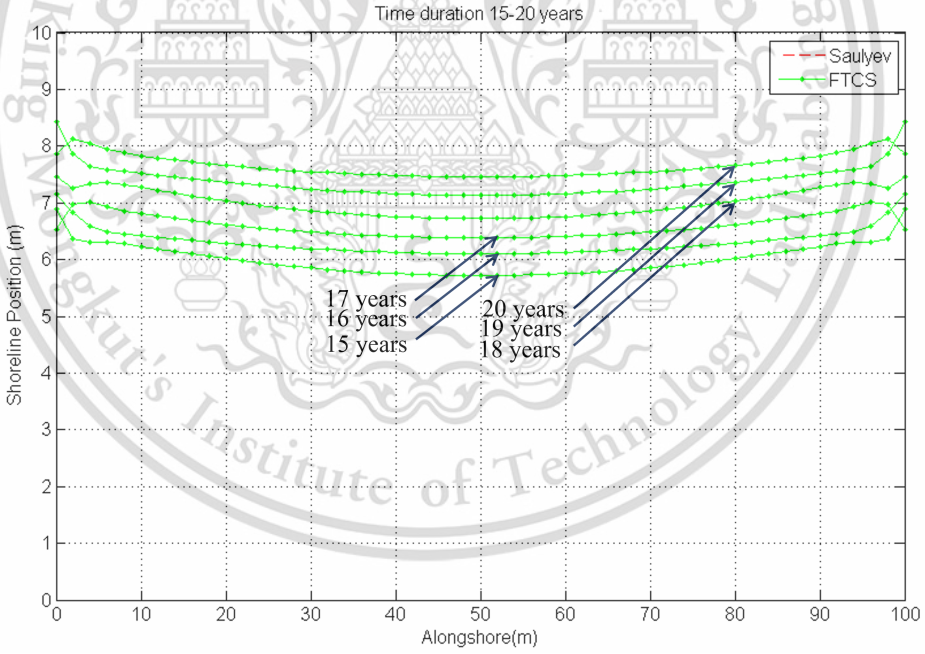

Figure 4.27*:* Shoreline evolution in 15-20 years when T-head Groin size 24 m.

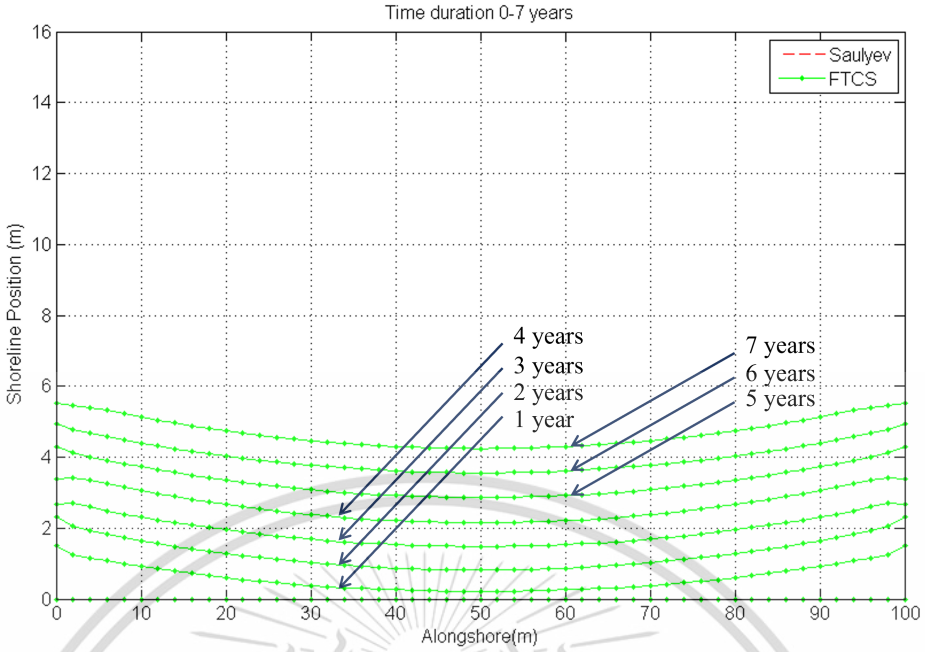

Figure 4.28*:* Shoreline evolution in 0-7 years when T-head Groin size 26 m.

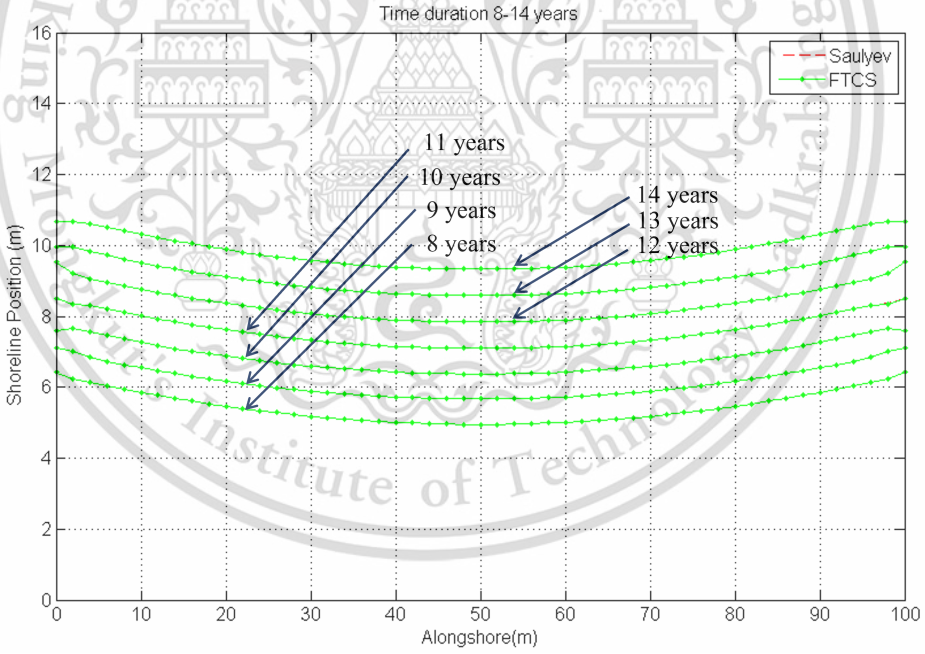

Figure 4.29*:* Shoreline evolution in 8-14 years when T-head Groin size 26 m.

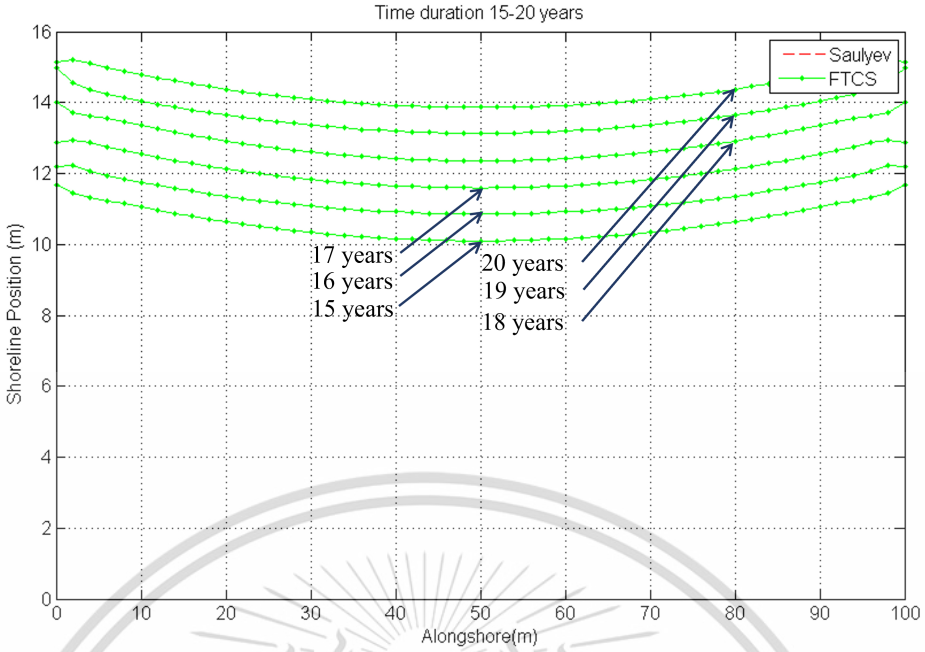

Figure 4.30*:* Shoreline evolution in 15-20 years when T-head Groin size 26 m.

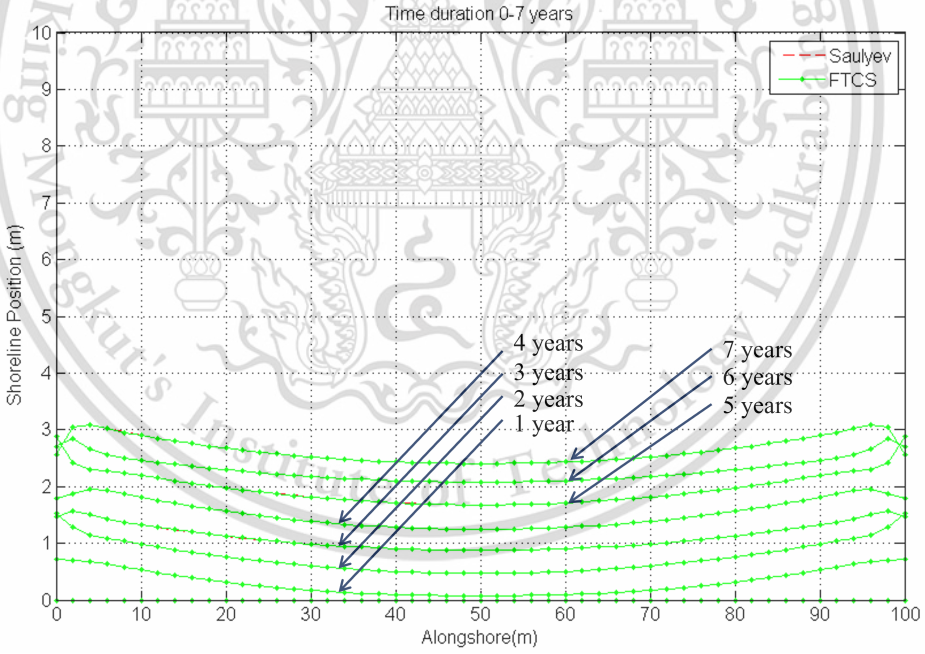

Figure 4.31*:* Shoreline evolution in 0-7 years when T-head Groin size 28 m.

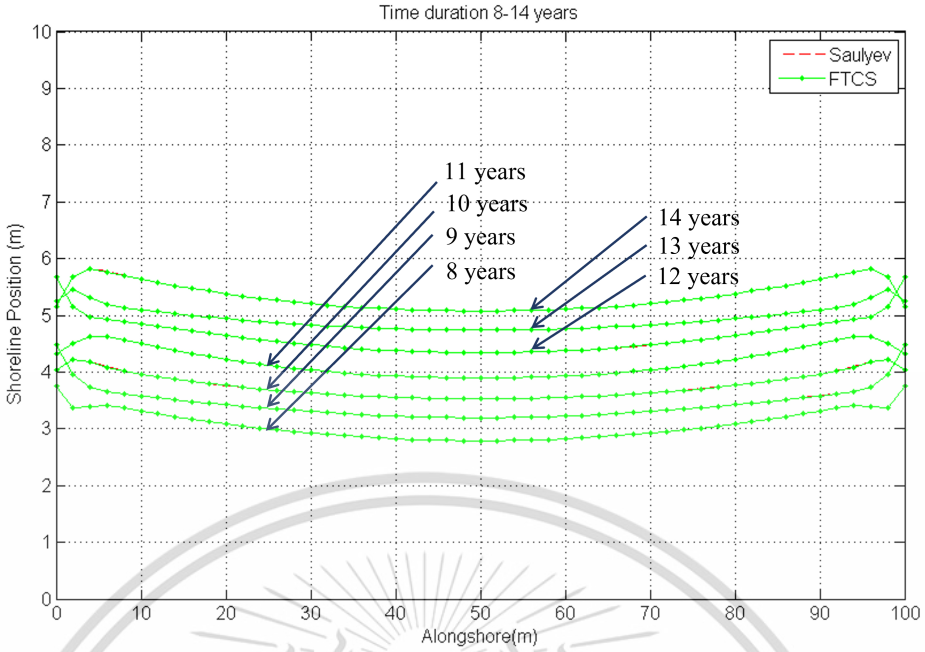

Figure 4.32*:* Shoreline evolution in 8-14 years when T-head Groin size 28 m.

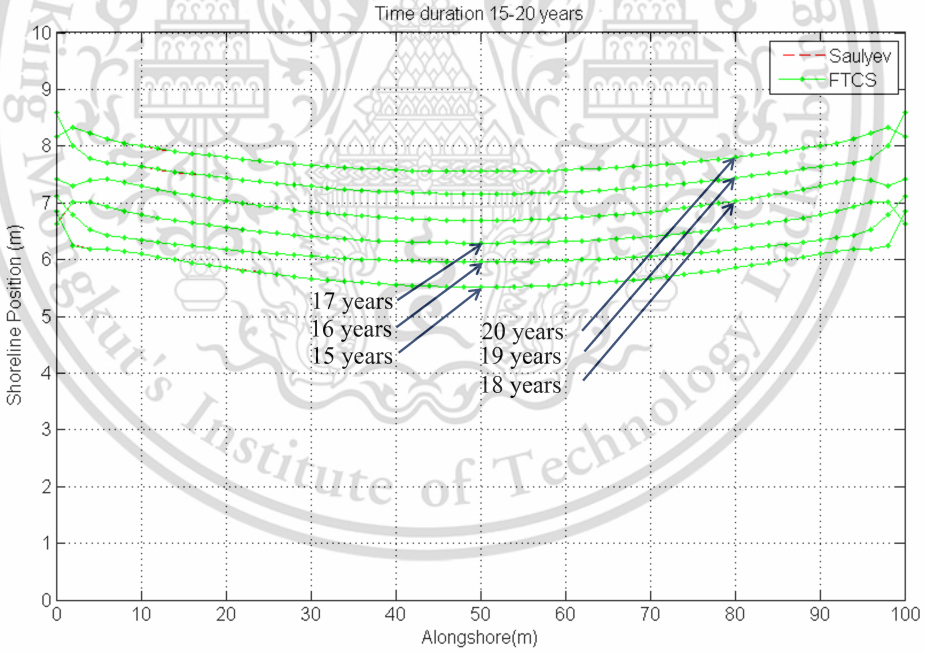

Figure 4.33*:* Shoreline evolution in 15-20 years when T-head Groin size 28 m.

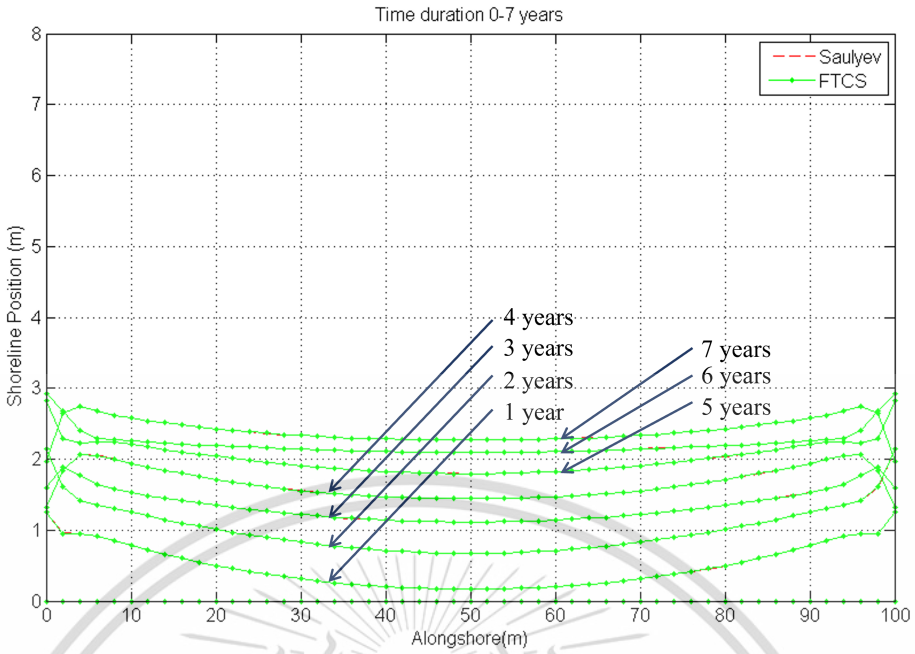

Figure 4.34*:* Shoreline evolution in 0-7 years when T-head Groin size 30 m.

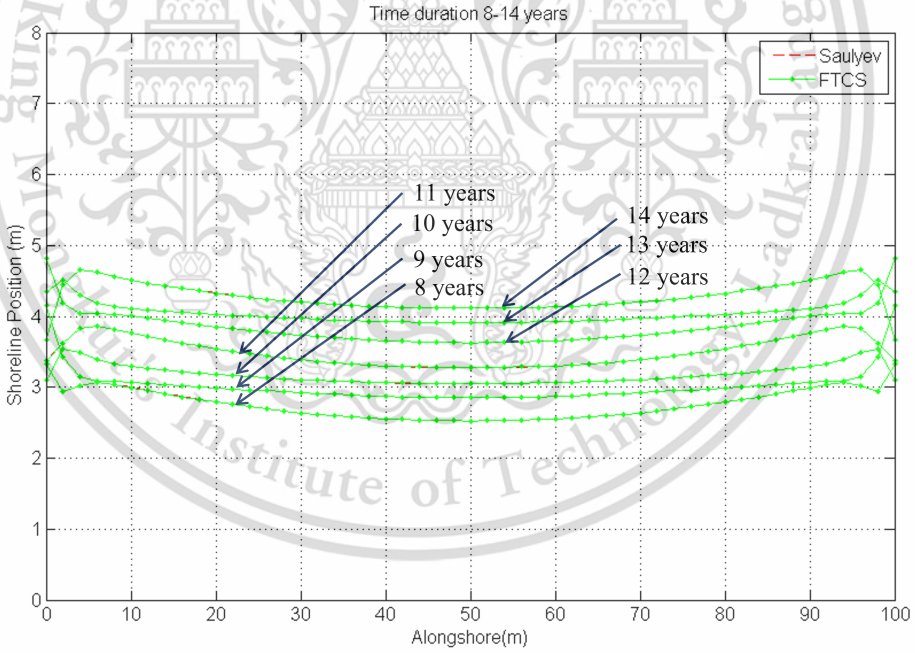

Figure 4.35*:* Shoreline evolution in 8-14 years when T-head Groin size 30 m.

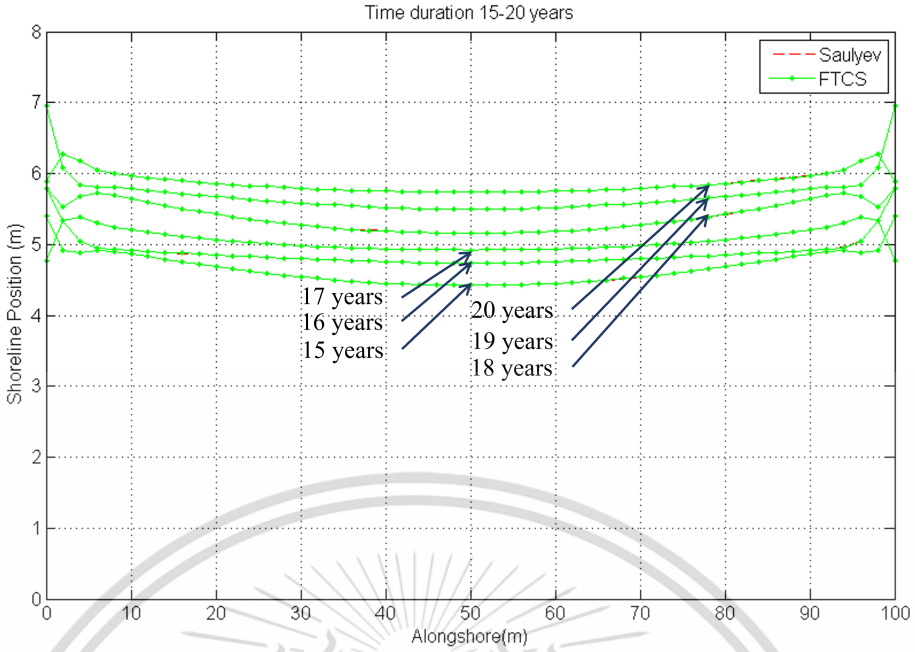

Figure 4.36*:* Shoreline evolution in 15-20 years when T-head Groin size 30 m.

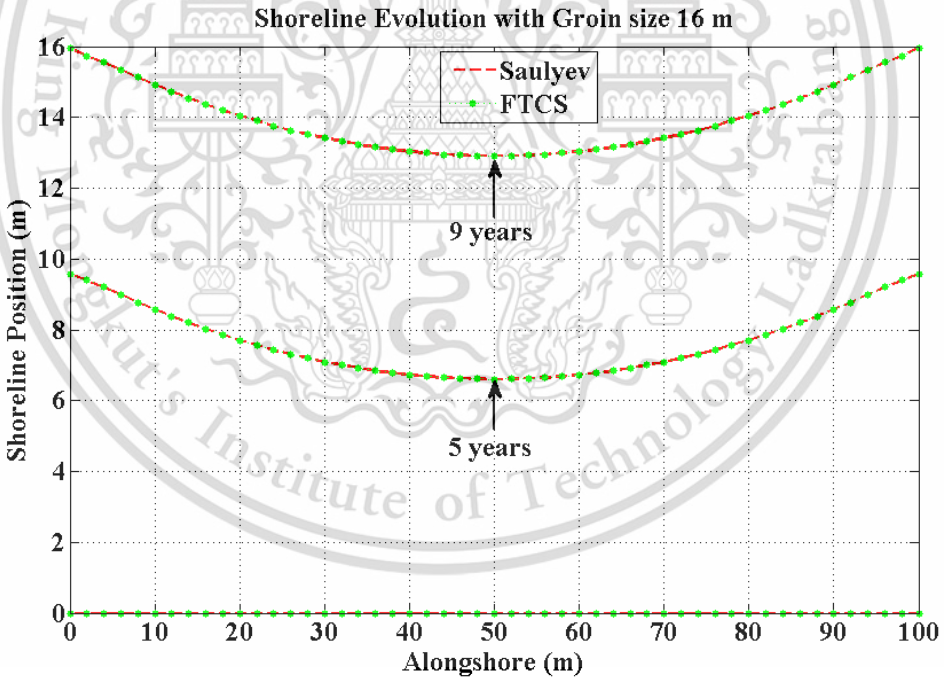

Figure 4.37*:* Shoreline evolution in 9 years when T-head Groin size 16 m.

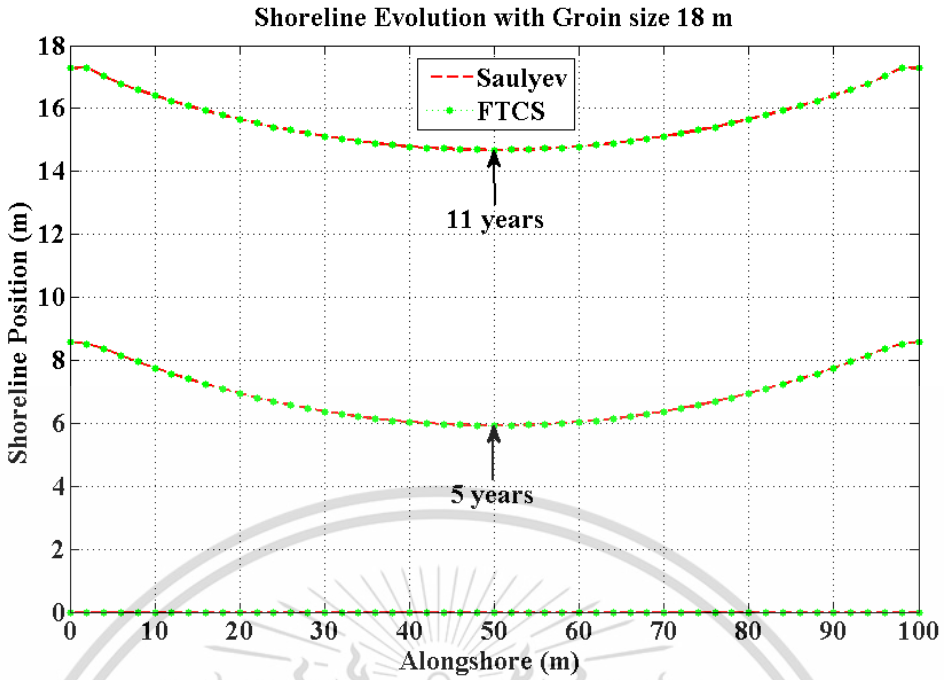

Figure 4.38: Shoreline evolution in 11 years when T-head Groin size 18 m.

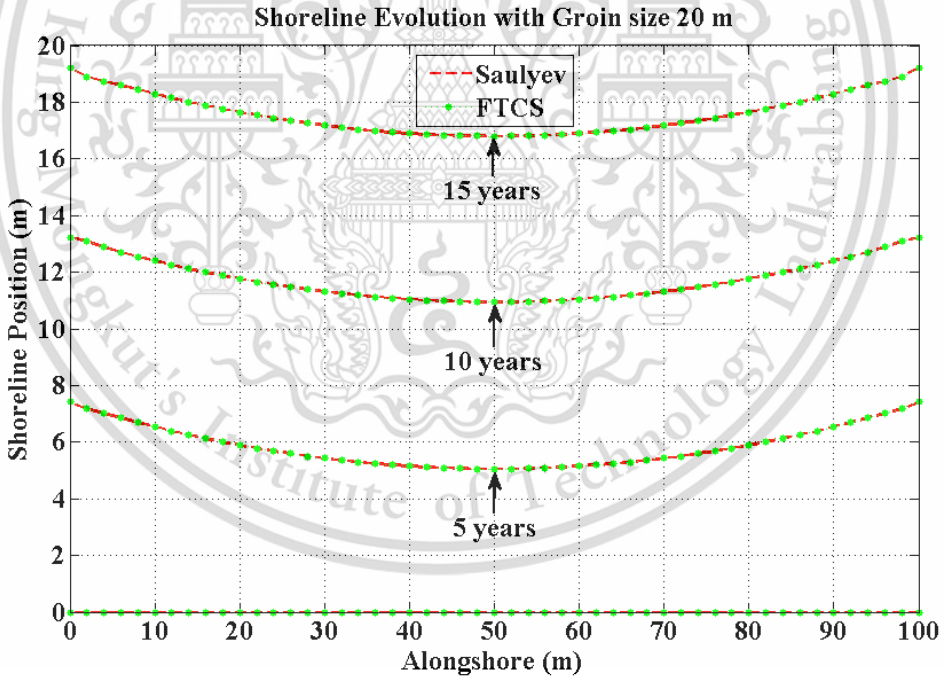

Figure 4.39: Shoreline evolution in 15 years when T-head Groin size 20 m.

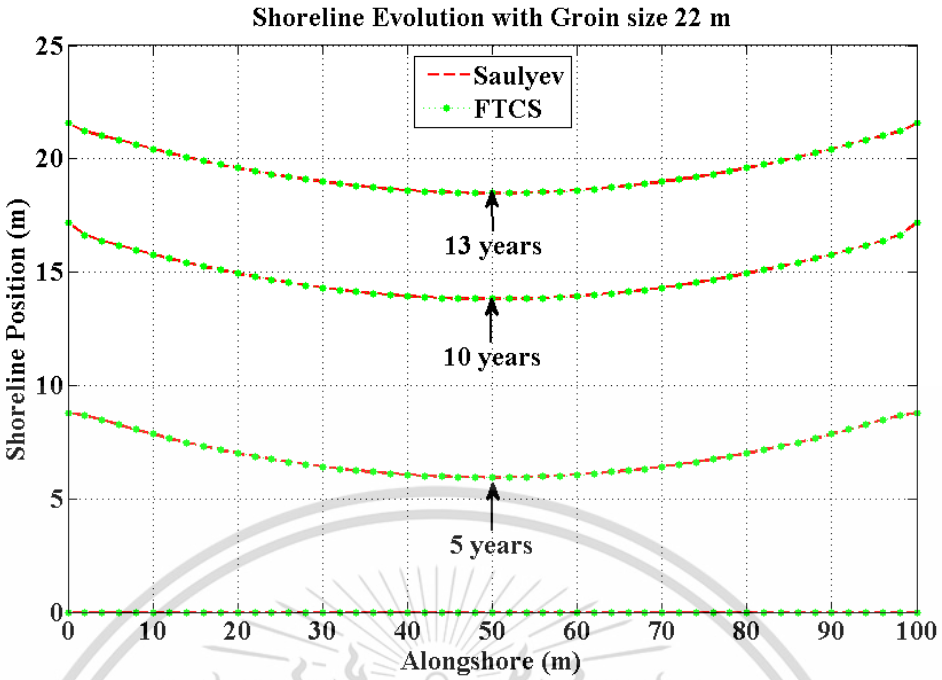

Figure 4.40: Shoreline evolution in 13 years when T-head Groin size 22 m.

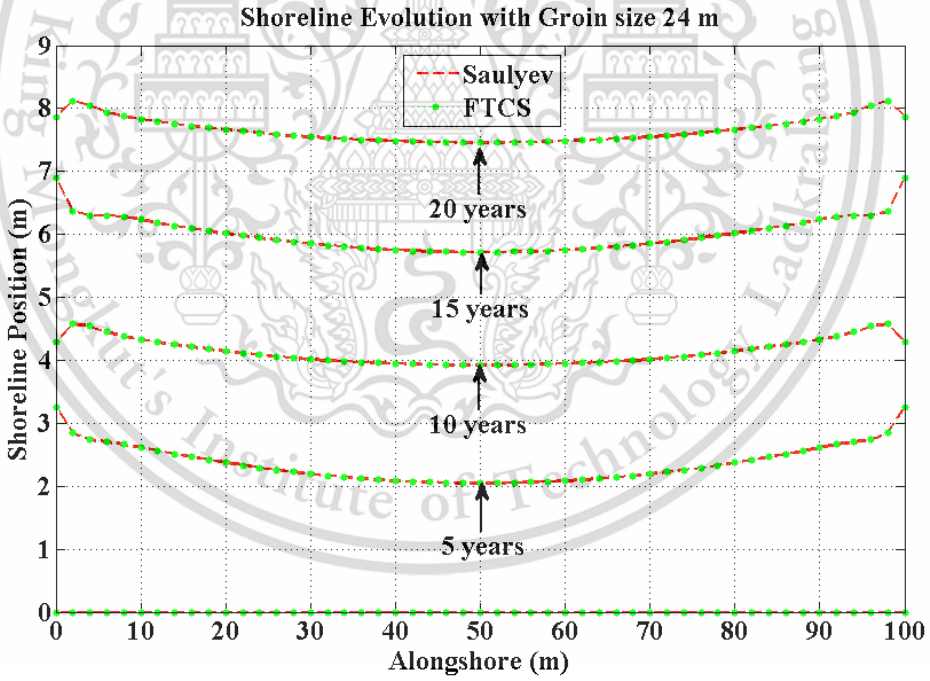

Figure 4.41: Shoreline evolution in 20 years when T-head Groin size 24 m.

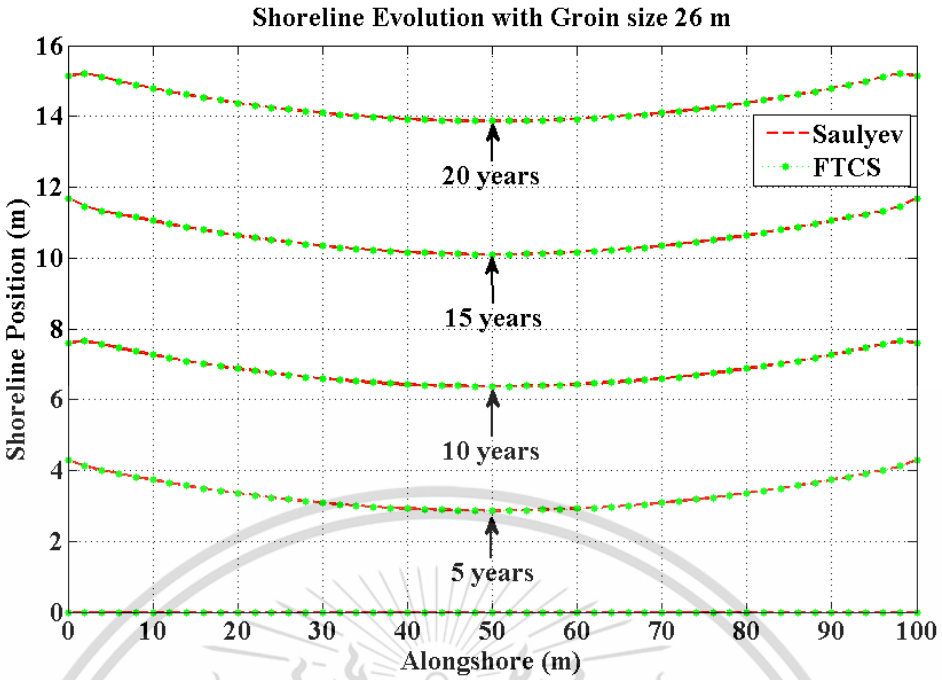

Figure 4.42: Shoreline evolution in 20 years when T-head Groin size 26 m.

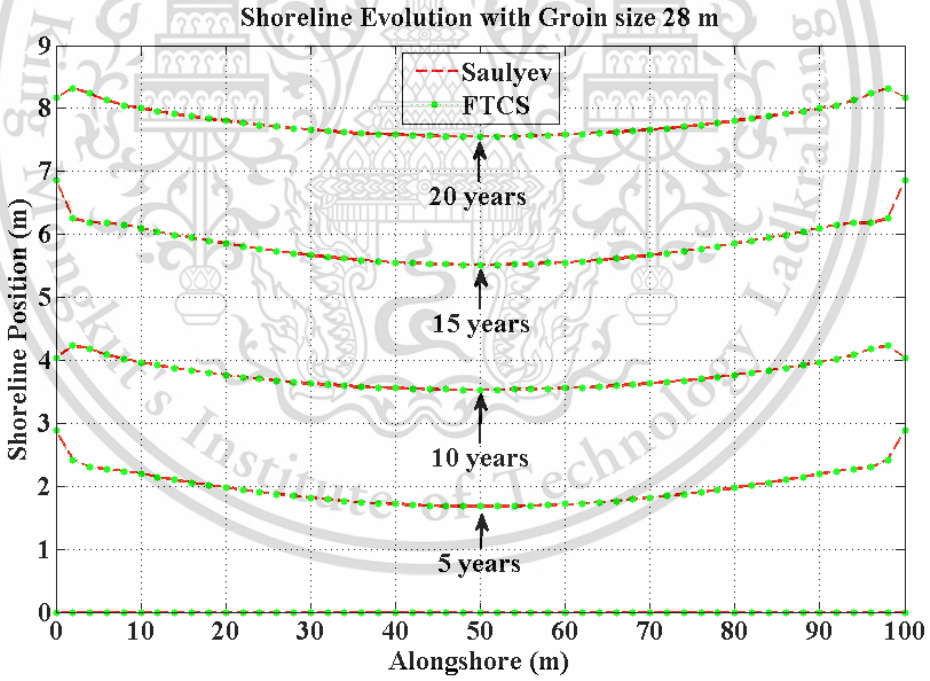

Figure 4.43: Shoreline evolution in 20 years when T-head Groin size 28 m.

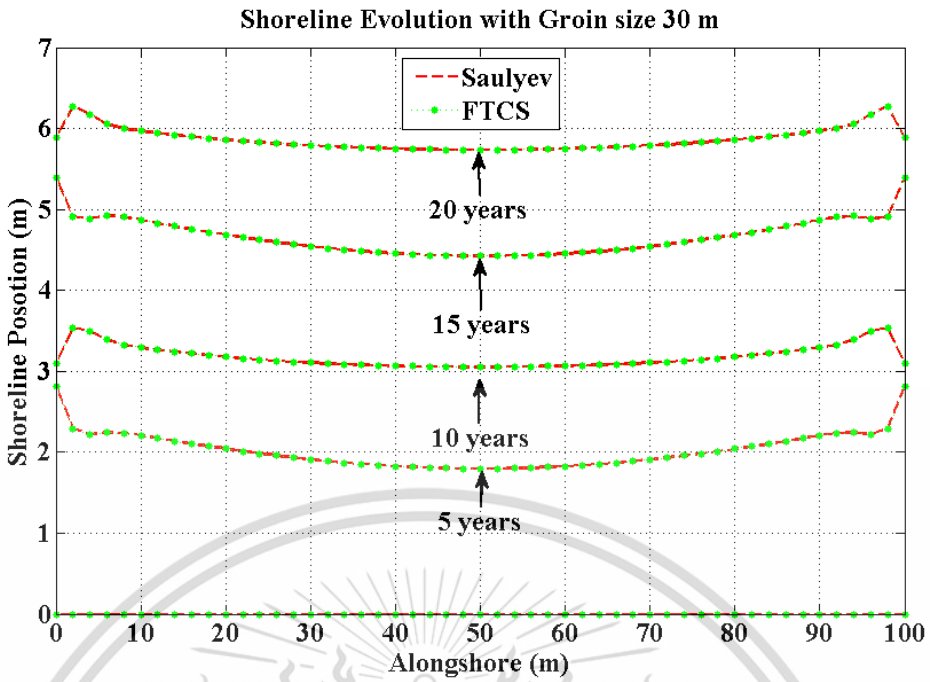

Figure 4.44: Shoreline evolution in 20 years when T-head Groin size 30 m.

Table 4.10: Approximated shoreline evolution along 9 years using the traditional forward time centered space techniques when T-head Groin Size 16 m.

Time	Distance (m)					
(Years)	0	20	40	60	80	100
1	2.8710	1.4100	0.6302	0.6302	1.4100	2.8710
5	9.5859	7.7058	6.7258	6.7258	7.7058	9.5859
9	15.9610	14.0431	13.0345	13.0345	14.0431	15.9610

Table 4.11: Approximated shoreline evolution along 9 years using the Saulyev finite difference techniques when T-head Groin Size 16 m.

Time	Distance (m)					
(Years)	0	20	40	60	80	100
1	2.8718	1.4107	0.6305	0.6300	1.4094	2.8701
5	9.5859	7.7059	6.7259	6.7260	7.7059	9.5860
9	15.9615	14.0435	13.0346	13.0345	14.0429	15.9609

Table 4.12*:* Approximated shoreline evolution along 11 years using the traditional forward time centered space techniques when T-head Groin Size 18 m.

Time	Distance (m)					
(Years)	0	20	40	60	80	100
1	2.4433	1.2654	0.5617	0.5617	1.2654	2.4433
5	8.5988	6.9462	6.0354	6.0354	6.9462	8.5988
10	16.3731	14.2624	13.3619	13.3619	14.2624	16.3731
11	17.2722	15.6527	14.7912	14.7912	15.6527	17.2722

Table 4.13*:* Approximated shoreline evolution along 11 years using the Saulyev finite difference techniques when T-head Groin Size 18 m.

Time	Distance (m)					
(Years)	0	20	40	60	80	100
1	2.4436	1.2659	0.5619	0.5615	1.2649	2.4427
5	8.5988	6.9463	6.0353	6.0355	6.9464	8.5989
10	16.3738	14.2626	13.3621	13.3618	14.2622	16.3731
11	17.2720	15.6525	14.7911	14.7912	15.6530	17.2724

Table 4.14*:* Approximated shoreline evolution along 15 years using the traditional forward time centered space techniques when T-head Groin Size 20 m.

Time	Distance (m)					
(Years)	0	20	40	60	80	100
1	2.2494	1.1606	0.5209	0.5209	1.1606	2.2494
5	7.4274	5.8894	5.1479	5.1479	5.8894	7.4274
10	13.2267	11.7631	11.0379	11.0379	11.7631	13.2267
15	19.2122	17.6409	16.8916	16.8916	17.6409	19.2122

Table 4.15*:* Approximated shoreline evolution along 15 years using the Saulyev finite difference techniques when T-head Groin Size 20 m.

Time	Distance (m)					
(Years)	0	20	40	60	80	100
1	2.2499	1.1610	0.5211	0.5207	1.1601	2.2488
5	7.4275	5.8894	5.1479	5.1479	5.8894	7.4273
10	13.2269	11.7631	11.0378	11.0379	11.7632	13.2268
15	19.2123	17.6410	16.8916	16.8915	17.6408	19.2122

Table 4.16*:* Approximated shoreline evolution along 13 years using the traditional forward time centered space techniques when T-head Groin Size 22 m.

Time	Distance (m)					
(Years)	0	20	40	60	80	100
1	2.4577	1.1767	0.5171	0.5171	1.1767	2.4577
5	8.7941	7.0079	6.0630	6.0630	7.0079	8.7941
10	17.1728	14.9308	13.9419	13.9419	14.9308	17.1728
13	21.5783	19.5870	18.6116	18.6116	19.5870	21.5783

Table 4.17*:* Approximated shoreline evolution along 13 years using the Saulyev finite difference techniques when T-head Groin Size 22 m.

Time	Distance (m)					
(Years)	0	20	40	60	80	100
1	2.4578	1.1770	0.5173	0.5169	1.1763	2.4574
5	8.7940	7.0079	6.0628	6.0629	7.0079	8.7940
10	17.1735	14.9311	13.9420	13.9417	14.9306	17.1728
13	21.5774	19.5868	18.6117	18.6116	19.5870	21.5786

Table 4.18*:* Approximated shoreline evolution along 20 years using the traditional forward time centered space techniques when T-head Groin Size 24 m.

Time	Distance (m)					
(Years)	0	20	40	60	80	100
1	1.0972	0.5544	0.2391	0.2391	0.5544	1.0972
5	3.2598	2.3726	2.0848	2.0848	2.3729	3.2598
10	4.2850	4.1421	3.9454	3.9454	4.1421	4.2850
15	6.8976	6.0140	5.7506	5.7506	6.0140	6.8976
20	7.8626	7.6623	7.4815	7.4815	7.6623	7.8626

Table 4.19*:* Approximated shoreline evolution along 20 years using the Saulyev finite difference techniques when T-head Groin Size 24 m.

Time	Distance (m)					
(Years)	0	20	40	60	80	100
1	1.0975	0.5547	0.2392	0.2389	0.5540	1.0968
5	3.2607	2.3731	2.0852	2.0848	2.3724	3.2596
10	4.2846	4.1417	3.9450	3.9455	4.1424	4.2851
15	6.8987	6.0147	5.7510	5.7506	6.0137	6.8975
20	7.8624	7.6618	7.4811	7.4815	7.6626	7.8627

Table 4.20*:* Approximated shoreline evolution along 20 years using the traditional forward time centered space techniques when T-head Groin Size 26 m.

Time	Distance (m)					
(Years)	0	20	40	60	80	100
1	1.4976	0.5985	0.2596	0.2596	0.5985	1.4976
5	4.3015	3.3562	2.9214	2.9214	3.3562	4.3015
10	7.6055	6.8702	6.4288	6.4288	6.8702	7.6055
15	11.6917	10.6384	10.1618	10.1618	10.6384	11.6917
20	15.1301	14.3789	13.9220	13.9220	14.3789	15.1301

Table 4.21*:* Approximated shoreline evolution along 20 years using the Saulyev finite difference techniques when T-head Groin Size 26 m.

Time	Distance (m)					
(Years)	0	20	40	60	80	100
1	1.4979	0.5988	0.2598	0.2595	0.5983	1.4974
5	4.3016	3.3563	2.9215	2.9213	3.3561	4.3014
10	7.6051	6.8701	6.4288	6.4289	6.8703	7.6056
15	11.6919	10.6386	10.1621	10.1619	10.6382	11.6916
20	15.1297	14.3787	13.9220	13.9222	14.3791	15.1303

Table 4.22*:* Approximated shoreline evolution along 20 years using the traditional forward time centered space techniques when T-head Groin Size 28 m.

Time	Distance (m)					
(Years)	0	20	40	60	80	100
1	0.7186	0.3100	0.0987	0.0987	0.3100	0.7186
5	2.8822	1.9768	1.7127	1.7127	1.9768	2.8822
10	4.0363	3.7656	3.5555	3.5555	3.7656	4.0363
15	6.8627	5.8516	5.5533	5.5533	5.8516	6.8627
20	8.1678	7.8000	7.5806	7.5806	7.8000	8.1678

Table 4.23*:* Approximated shoreline evolution along 20 years using the Saulyev finite difference techniques when T-head Groin Size 28 m.

Time	Distance (m)					
(Years)	0	20	40	60	80	100
1	0.7189	0.3103	0.0989	0.0986	0.3095	0.7180
5	2.8834	1.9772	1.7129	1.7125	1.9764	2.8819
10	4.0361	3.7650	3.5549	3.5555	3.7658	4.0364
15	6.8640	5.8523	5.5536	5.5532	5.8513	6.8625
20	8.1674	7.7994	7.5800	7.5805	7.8002	8.1679

Table 4.24*:* Approximated shoreline evolution along 20 years using the traditional forward time centered space techniques when T-head Groin Size 30 m.

Time	Distance (m)					
(Years)	0	20	40	60	80	100
1	1.2549	0.4986	0.2042	0.2042	0.4986	1.2549
5	2.8227	2.0405	1.8249	1.8249	2.0405	2.8227
10	3.0897	3.1776	3.0660	3.0660	3.1776	3.0897
15	5.4009	4.6835	4.4527	4.4527	4.6835	5.4009
20	5.8824	5.8600	5.7502	5.7502	5.8600	5.8824

Table 4.25*:* Approximated shoreline evolution along 20 years using the Saulyev finite difference techniques when T-head Groin Size 30 m.

Time	Distance (m)					
(Years)	0	20	40	60	80	100
1	1.2554	0.4992	0.2044	0.2041	0.4982	1.2546
5	2.8240	2.0415	1.8256	1.8249	2.0401	2.8224
10	3.0883	3.1765	3.0652	3.0660	3.1781	3.0900
15	5.4021	4.6844	4.4533	4.4527	4.6830	5.4006
20	5.8817	5.8593	5.7497	5.7502	5.8604	5.8824

Chapter 5

Discussion and Conclusion

5.1 Discussion

5.1.1 Discussion of A Shoreline Evolution Model With the Wavelength Effect of Breaking Waves on Groin Structures

We considered the averaged wave crest impact (α_0) as obtained by 2.39 for five case wavelengths as seen in Table 3.2-3.6. The long-shore transport rate for each month as seen in Table 3.7.

We used the numerical method, the traditional forward time centered space techniques, and the Saulyev finite difference techniques to predict the shoreline evolution for five case wavelengths with time duration of 5, 10, and 15 years.

The approximated shoreline evolution for wavelength $0.5\sin(t+0.01x)$ with a time duration of 15 years is seen in Table 3.8, 3.9 and Fig. 3.19, 3.20. The farthest distance from the shoreline evolution is 6.0537 m. The shortest distance from the shoreline evolution is 5.2833 m.

The approximated shoreline evolution for wavelength $0.5\sin(t+0.02x)$ with a time duration of 15 years is seen in Table 3.10, 3.11 and Fig. 3.21, 3.22. The farthest distance from the shoreline evolution is 9.7219 m. The shortest distance from the shoreline evolution is 8.3579 m.

The approximated shoreline evolution for wavelength $0.5\sin(t+0.03x)$ with a time duration of 15 years is seen in Table 3.12, 3.13 and Fig. 3.23, 3.24. The farthest distance from the shoreline evolution is 14.3339 m. The shortest distance from the shoreline evolution is 12.5092 m.

The approximated shoreline evolution for wavelength $0.5\sin(t+0.04x)$ with a time duration of 15 years is seen in Table 3.14, 3.15 and Fig. 3.25, 3.26. The farthest distance from the shoreline evolution is 6.4928 m. The shortest distance from the shoreline evolution is 5.8776 m.

The approximated shoreline evolution for wavelength $0.5\sin(t+0.05x)$ with a time duration of 15 years is seen in Table 3.16, 3.17 and Fig. 3.27, 3.28. The farthest distance from the shoreline evolution is 3.4704 m. The shortest distance from the shoreline evolution is 3.0672 m.

The approximated shoreline evolution for five case wavelengths with time durations of 5, 10, and 15 years is seen in Fig. 3.29, 3.30, 3.31, 3.32 and 3.33 respectively.

The approximate shoreline evolution of wavelengths $0.5\sin(t+0.01x)$, $0.5\sin(t+0.02x)$ and $0.5\sin(t+0.03x)$ shows that as the frequency of wavelength increases, the approximate shoreline area also increases. And in the approximate shoreline evolution

of wavelengths $0.5\sin(t+0.04x)$ and $0.5\sin(t+0.05x)$, the frequency of wavelength increases, but the approximate shoreline evolution has less area.

The approximated shoreline evolutions of both numerical approaches within five wavelengths of the considered shoreline are compatible.

5.1.2 Discussion of A Combination of A Shoreline Evolution Model and A Wave Crest Model on T-Head Groin Structures With the Breaking Wave Effect

We considered the averaged wave crest impact (α_0) as obtained by 2.39 for eight T-head groin sizes as seen in Table 4.2-4.10. The long-shore transport rate D for each month as seen in Table 4.10.

We used numerical techniques, the traditional forward time centered space techniques (FTCS), and the Saulyev finite difference techniques to approximate the shoreline evolution for eight T-head groin sizes.

The approximated shoreline evolution for T-head groin size 16 m with a time duration of 9 years is seen in Table 4.10, 4.11, and Fig. 4.18. As a result of shoreline evolution, the longest distance is 15.9615 meters, and the shortest distance is 12.9092 meters.

The approximated shoreline evolution for T-head groin size 18 m with a time duration of 11 years is seen in Table 4.12, 4.13, and Fig. 4.19, 4.20. As a result of shoreline evolution, the longest distance is 17.2724 meters, and the shortest distance is 14.6822 meters.

The approximated shoreline evolution for T-head groin size 20 m with a time duration of 15 years is seen in Table 4.14, 4.15, and Fig. 4.21, 4.22. As a result of shoreline evolution, the longest distance is 19.2123 meters, and the shortest distance is 16.7981 meters.

The approximated shoreline evolution for T-head groin size 22 m with a time duration of 13 years is seen in Table 4.16, 4.17, and Fig. 4.23, 4.24. As a result of shoreline evolution, the longest distance is 21.5786 meters, and the shortest distance is 18.4889 meters.

The approximated shoreline evolution for T-head groin size 24 m with a time duration of 20 years is seen in Table 4.18, 4.19, and Fig. 4.25, 4.26, 4.27. As a result of shoreline evolution, the longest distance is 8.1202 meters, and the shortest distance is 7.4590 meters.

The approximated shoreline evolution for T-head groin size 26 m with a time duration of 20 years is seen in Table 4.20, 4.21, and Fig. 4.28, 4.29, 4.30. As a result of shoreline evolution, the longest distance is 15.2122 meters, and the shortest distance is 13.8656 meters.

The approximated shoreline evolution for T-head groin size 28 m with a time

duration of 20 years is seen in Table 4.22, 4.23, and Fig. 4.31, 4.32, 4.33. As a result of shoreline evolution, the longest distance is 8.3230 meters, and the shortest distance is 7.5526 meters.

The approximated shoreline evolution for T-head groin size 30 m with a time duration of 20 years is seen in Table 4.24, 4.25, and Fig. 4.34, 4.35, 4.36. As a result of shoreline evolution, the longest distance is 6.2741 meters, and the shortest distance is 5.7362 meters.

Approximate shoreline evolutions of all numerical approaches in eight sizes of the considered T-head groin are compatible. The approximate shoreline evolution of T-head groin sizes of 16, 18, 20, and 22 m is used over time durations of 9, 11, 15, and 13 years, respectively, making the approximate shoreline comparable in size to the T-head groin. Other approximate T-head groin sizes are used over a time duration of 20 years. The approximate shoreline is still in the T-head groin area. The approximate shoreline tends to decrease with T-head groin sizes of 26, 28, and 30 m.

5.2 Conclusion

5.2.1 A Shoreline Evolution Model With the Wavelength Effect of Breaking Waves on Groin Structures

A more realistic shoreline evolution model was created in this research to adjust for the wavelength influence of breaking waves on groin construction. The initial condition setting approach and boundary conditions techniques, as well as various groin structural impacts, are discussed. Each year, the shoreline evolution is approximated using the conventional forward time centered space method and the unconditionally stable Saulyev finite differential methods. The estimated impacts of shoreline evolution were consistent with the wave crest impact model for five case wavelengths. As a result, the frequency of the wavelength influences the approximated shoreline evolution rate. In most cases, when the frequency of wavelength increases, the approximated shoreline evolution that obtains shoreline area also increases, but in some cases, when the frequency of wavelength increases, the approximated shoreline evolution has shoreline area obtained less. The approximated shoreline evolution is uncertain at different frequencies of wavelengths. The proposed modelling could be used to forecast the effectiveness of constructing a groin system on a nearby beach.

5.2.2 A Combination of A Shoreline Evolution Model and A Wave Crest Model on T-Head Groin Structures With the Breaking Wave Effect

We introduce a shoreline evolution model was created in this research to adjust for the T-head groin structure. The non-uniform breaking wave crest impact is estimated using the wave crest impact model. The average wave crest impact for eight

sizes of T-head groin structures is considered. The shoreline evolution in areas where T-head groins are installed on both sides. The initial condition setting approach and boundary conditions techniques, as well as the structural impacts of the T-head groin, are discussed. The traditional forward time centered space techniques (FTCS) and the unconditionally stable Saulyev finite differential techniques are used to approximate shoreline evolution each year. The estimated impacts of shoreline evolution were consistent with the wave crest impact model for eight different T-head groin sizes. As a result, the size of T-head groin influences the approximated shoreline evolution. The time duration of the approximate shoreline comparable in size to the T-head groin increases as the size of the T-head groin increases. But the size of the T-head groin is too large, the approximate shoreline evolution rate is lower, and the approximate shoreline evolution has resulted in a smaller shoreline area.

5.3 Summarize

In this research, we study the wavelength effect of breaking waves and the T-head groin construction effect on the shoreline evolution model. We introduce a shoreline evolution model, the initial condition setting approach, boundary condition techniques, and the wave crest impact model to adjust for two cases of study. The shoreline evolution is approximated using the traditional forward time centered space techniques (FTCS) and the unconditionally stable Saulyev finite differential techniques. In the first case, the wavelength effect of breaking waves, we study the influence of the breaking waves from the wave crest impact model in five cases of wavelength. The first case study provides, the frequency of the wavelength influences the approximate shoreline evolution rate. In most cases, when the frequency of the wavelength increases, the approximated shoreline evolution that obtains shoreline area also increases, but in some cases, when the frequency of the wavelength increases, the approximated shoreline evolution obtains less shoreline area. In the second case, The T-head groin construction effect, we study the influence of the size of T-head groin construction in eight cases of different sizes of T-head groin. The second case study shows that the size of the T-head groin influences the approximated shoreline evolution. The duration of the approximate shoreline comparable in size to the T-head groin increases as the size of the T-head groin increases. But the size of the T-head groin is too large, the approximate shoreline evolution rate is lower, and the approximate shoreline evolution has resulted in a smaller shoreline area.

5.4 Further work

1) We will simulate 2D, 3D shoreline evolution model.
2) We will change groin design.

References

[1] Knkx. 2018. **New hope to stop—or greatly slow—seemingly unstoppable shoreline erosion.** May 23, 2018, form https://www.knkx.org/post/new-hope-stop-or-greatly-slow-seemingly-unstoppable-shoreline-erosion.

[2] Civil Beat. 2022. **North Shore Group Confronts Growing Threats Of Erosion, Sea Level Rise.** 2020, form https://www.civilbeat.org/2022/10/north-shore-group-confronts-growing-threats-of-erosion-sea-level-rise/

[3] Thaiger. 2019. **Reconstructed Pattaya Beach officially opened.**June 14, 2019, from https:// thethaiger.com/ hot-news/ environment/ reconstructed-pattaya-beach-officially-opened

[4] Thaiger. 2019. **Reconstructed Pattaya Beach officially opened.**June 14, 2019, from https:// thethaiger.com/ hot-news/ environment/ reconstructed-pattaya-beach-officially-opened

[5] Surfertoday. 2018. **What are the differences between breakwaters, groins, jetties and seawalls.** November 28, 2018, form https://www.surfertoday.com/ environment/ what-are-the-differences-between-breakwaters-groins-jetties-and-seawalls.

[6] ACE Geosynthetics. 2020. **Marine and Coastal Structures Construction.** 2020, form https://www.geoace.com/app/Marine-and-Coastal-Structures-Construction/ lists

[7] CapeMay. 2009. **Rebuilding a Beach.** 2009, form https://www.capemay.com/ blog/2009/01/rebuilding-a-beach/

[8] G. Alexandrakis, C. Manasakis, and N. A. Kampanis. 2015. **Valuating the effects of beach erosion to tourism revenue. A management perspective.** Ocean & Coastal Management. vol. 111. pp. 1-11.

[9] N. Pucino, D. M. Kennedy, R. C. Carvalho, B. Allan and D. Ierodiaconou. 2021. **Citizen science for monitoring seasonal□scale beach erosion and behaviour with aerial drones.** Scientific Reports 11. 3935 (2021). 17 pages.

[10] A.H. Mohamed Rashidi, M. H. Jamal, M. Z. Hassan, S. S. Mohd Sendek, S. I. Mohd Sopie, and M. R. Abd Hamid. 2021. **Coastal Structures as Beach Erosion Control and Sea Level Rise Adaptation in Malaysia: A Review.** Water. Vol. 13. pp. 34 pages.

[11] T. Beuzen, I. L. Turner, C. E. Blenkinsopp, A. Atkinson, F. Flocard, and T. E. Baldock. 2018. **Physical model study of beach profile evolution by sea level rise in the presence of seawalls.** Coastal Engineering. vol. 136. pp. 172-182.

[12] A. Fitri. R. Hashim, S. Abolfathi, and Khairul Nizam Abdul Maulud. 2019. **Dynamics of Sediment Transport and Erosion-Deposition Patterns in the Locality of a Detached Low-Crested Breakwater on a Cohesive Coast.** Water, Vol. 11, 28 pages.

[13] L. P. Stein, and E. Siegle. 2020. **Overtopping events on seawall-backed beaches: Santos Bay, SP, Brazil.** Regional Studies in Marine Science. vol. 40. 101492.

[14] W. T. Bakker. 1969. **The dynamics of coast with a groin system.** Proceeding of 11th Coastal Engineering Conference 1969. pp. 492-517.

[15] W. T. Bakker, and T. Edelman. 1965. **The coastline of river deltas.** Proceeding of 9th Coastal Engineering Conference 1965. pp. 199-218.

[16] W. Grijimr. 1961 **Theoretical form of shoreline.** Proceeding of 7^{th} Coastal Engineering Conference 1961. pp. 197-202.

[17] W. Grijimr. 1965. **Theoretical form of shoreline.** Proceeding of 9^{th} Coastal Engineering Conference 1965. pp. 219-235.

[18] B. Le Mahute, and M. Soldate. 1977. **Mathematical Modeling of Shoreline Evolution.** US Army Corps of Engineer Waterways Experiment Station. CERC.

[19] H. Hanson, M. Larson, and N. C. Kraus. 1987 **Analytical Solution of the One-line Model for Shoreline Changel.** US Army Corps of Engineer Waterways Experiment Station. CERC.

[20] T. Waltonand, and T. Chiu. 1979. **A review of analytical technique to solve the sand transport equation and some simplified solution.** Coastal Structure. pp. 809-837.

[21] US Army Corp of Engineers. 1984. **Shore Protection Manual.** Coastal Engineering Research Centre. Washington.

[22] L. X. Hoan. 2006. **Some result of comparison between numerical and analytical solutions of the one-line model for shoreline change.** Vietnam Journal of Mechanics. pp. 94-102.

[23] M. Mamat Subiyanto, M. F. Ahmad, and M. L. Husain. 2013. **Comparison of numerical method for forward and backward time centered space for long – term simulation of shoreline evolution.** Applied Mathematical Sciences. Vol. 7. pp. 5165-5173.

[24] N. Pochai. 2017. **Unconditional stable numerical techniques for a water-quality model in a non-uniform flow stream.** Advances in Difference Equations, vol. 2017. Article ID 286. 13 pages.

[25] P. Samalerk, and N. Pochai. 2018. **Numerical simulation of a one-dimensional water-quality model in a stream using a Saulyev technique with quadratic interpolated initial-boundary conditions.** Abstract and Applied Analysis. vol. 2018. Article ID 1926519. 7 pages.

[26] US Army Corp of Engineers. 1984. **Shore protection manual.** Coastal Engineering Research Center. Washington.

[27] R. Tenzer and V. Gladkikh. 2014. **Assessment of density variations of marine sediments with ocean and sediment depths.** The Scientific World Journal. vol. 2014. Article ID 823296. 9 pages.

[28] Wikipedia. 2018 **Seawater.** [Online]. Avalable : https://en.wikipedia.org/wiki/Sea-water.

[29] J. Román-Sierra, J. J. Muñoz-Perez, and M. Navarro-Pons. 2014. **Beach nourishment effects on sand porosity variability.** Coastal Engineering. pp. 221-232.

[30] J. Dronkers and Janrik van den Berg. **Coastal and marine sediments.** [Online]. Avalable : http://www.coastalwiki.org/wiki/Coastal_and_marine_sediments?fbclid=IwAR2UkENgXUxyEJIj5tIaau2yPrDOCuRniHu3FqSCrLwVD_KpKMtqXob1iZc.

[31] Geo-Informatics and Space Technology Development Agency (Public Organization) (GISTDA). **Announce.** [Online]. Avalable : http://coastalradar.gistda.or.th/wp/?page=announce-small.

[32] W. Kraychang, and N. Pochai. 2015 **Numerical Treatment to a Water-Quality Measurement Model in an Opened-Closed Reservoir.** Thai Journal of Mathematics. vol. 13. pp. 775-788.

[33] Chung-Yau LAM. **Applied numerical methods for partial differential equations.** JPrentice h4Hall. New York. 1994.

[34] A. R. Mitchell. **Computational methods in partial differential equations.** John Wiley & Sons Ltd. London. 1969.

[35] N. Pochai. 2017. **Unconditional stable numerical techniques for a water-quality model in a non-uniform flow stream.** Advances in Difference Equations, vol. 2017. Article ID 286. 13 pages.

[36] P. Unyapoti and N. Pochai. 2020. **A One-Dimensional Mathematical Model of Long-Term Shoreline Evolution with Groin System using an Unconditionally**

Stable Explicit Finite Difference Method. International Journal of Simulation: Systems, Science and Technology. vol. 21. no.3. pp. 2.1-2.6.

[37] P. Unyapoti and N. Pochai. 2021. **A Shoreline Evolution Model with a Twin Groins Structure using Unconditionally Stable Explicit Finite Difference Techniques.** Engineering Letters, vol. 29, no. 1, pp. 288-296.

Appendix

Appendix A

computation

MDPI

Article

A Shoreline Evolution Model with a Groin Structure under Non-Uniform Breaking Wave Crest Impact

Pidok Unyapoti [1,2,†] and Nopparat Pochai [1,2,*,†]

[1] Department of Mathematics, Faculty of Science, King Mongkut's Institute of Technology Ladkrabang, Bangkok 10520, Thailand; pidokunyapoti@gmail.com
[2] Centre of Excellence in Mathematics, CHE, Si Ayutthaya Road, Bangkok 10400, Thailand
* Correspondence: nopparat.po@kmitl.ac.th
† These authors contributed equally to this work.

Abstract: Beach erosion is a natural phenomenon that is not compensated by depositing fresh material on the shoreline while transporting sand away from the shoreline. There are three phenomena that have a serious influence on the coastal structure, such as increases in flooding, accretion, and water levels. In addition, the prediction of coastal evolution is used to investigate the topography of the beach. In this research, we present a one-dimensional mathematical model of shoreline evolution, and the parameters that influence this model are described on a monthly basis over a period of one year. Consideration is given to the wave crest impact model for evaluating the impact of the wave crest at that stage. It focuses on the evolution of the shoreline in environments where groins are installed on both sides. The initial and boundary condition setting techniques are proposed by the groins and their environmental parameters. The non-uniform influence of the crest of the breaking wave is so often considered. We then used the traditional forward time centered space technique and the Saulyev finite difference technique to estimate the monthly evolution of the shoreline for each year.

Keywords: shoreline evolution; groin system; explicit finite difference methods; wave crest impact; mathematical model

Citation: Unyapoti, P.; Pochai, N. A Shoreline Evolution Model with a Groin Structure under Non-Uniform Breaking Wave Crest Impact. *Computation* **2021**, *9*, 42. https://doi.org/10.3390/computation9040042

Academic Editors: Yongwimon Lenbury, Ravi P. Agarwal, Philip Broadbridge and Dongwoo Sheen

Received: 4 March 2021
Accepted: 20 March 2021
Published: 26 March 2021

1. Introduction

Beach erosion is a natural process which occurs whenever the transport of material away from the shoreline is not balanced by new material being deposited onto the shoreline. This is a problem that causes a decrease in beach areas. In order to prevent beach erosion and beach deposition which may devise a sea wall and groin, in [1], the design of the functional groin and a simulation of the action of single and multiple groins using GENESIS was proposed. Predictions of shoreline changes have been tested at 15 groins in Westhampton, Long Island, and New York. In [2], changes in the beach profile due to the construction of a single zigzag type of porous groin, named GROPOZAG, were reported.

Qualitative awareness of the idealized reaction of the shoreline to the governance process is required to examine beach erosion and beach deposition. The only instrument which can consider this is an analytical solution based on a mathematical model that explains fundamental physics. Many authors have developed an analytical solution to the evolution of the shoreline using a basic mathematical formula. Many authors have developed a one-line theory, and several contributors have included [3–8] in the analytical solution of the evolution of the shoreline. It cannot be assumed that the analytical solution would have quantitatively precise solutions to the problems containing complex boundary conditions and wave inputs. In the actual case, a numerical model of the evolution of the shoreline will be more fitting. In [9,10], the authors used conditionally stable explicit finite difference methods to approximate their model solutions.

In [11], the authors proposed a numerical model developed for the site conditions, which was used to measure the impact of lengthening the groin to a depth of 5 m to position it across the zone of bar migration. The model accurately represents observed processes, predicting less scour and more deposition at the coastal tip of the extended groin, as well as an increased probability of a rip current near the structure at Marina di Ronchi, Italy. In [12], a new numerical scheme for simulating flows around buildings with sharp-cornered structures was proposed. The proposed numerical model was tested against a well-known present experiment involving a wave group entering a shoreline and the presence of a T-head groin design. In [13], the effect of a groin application to erosion at the shoreline was proposed. The method utilized the bathymetry and topography data of the north beach of Balongan, West Java. In [14], probabilistic changes to the shoreline were calculated by using two simulations. The first simulation was the GenCade simulation, which was used to predict the long-term evolution of the shoreline induced by natural offshore waves. The second was the Monte Carlo simulation, which was used to simulate the evolution of the shoreline in response to changes in sea level. In [15], the ONELINE modeling method was presented, and its capabilities were demonstrated by model testing of two case studies. The first one has a groin area at Sea Isle City, New Jersey along the East Coast of the United States. The second is along the Nile Delta Coast in Egypt. In [16], a comparison between the analytic and numerical solutions in the idealized wave condition for four different shoreline configurations was proposed.

In this research, we introduce a governing equation of a one-dimensional shoreline evolution model when a couple of groins is added. We introduce a non-uniform impact effect of the breaking wave crest. We introduce the initial condition and the boundary conditions setting. Finite difference techniques will be used to approximate the model solution. A numerical model is being developed to predict the efficiency of the groin effect on shoreline evolution. We focus on predicting the efficiency of a straight, impermeable groin.

2. Governing Equation

2.1. Shoreline Evolution Model

In a one-dimensional shoreline evolution model, while maintaining the same shape, the beach shape is supposed to move towards land and towards the sea, meaning that all the bottom outlines become parallel. As a result, under this presumption, it is necessary to define the horizontal position of the shape relative to the baseline, and one outline could be used to explain changes in the form and volume of the beach plane as the beach erodes and accretes. The model's main assumption is that the sand is transported alongshore on the profile between two well-defined limiting elevations. If there is a disparity in the long-shore sand transport rate on the side of the segment and the related s and consistency, one contribution would be to obtain volume adjustment results. The principles of conservation of mass must be applied to the system at all times. The corresponding differential equation for the evolution of the shoreline is generated by considering the definitions above.

$$\frac{\partial y}{\partial t} = \frac{1}{D_B + D_C}\left(-\frac{\partial Q}{\partial x}\right), \tag{1}$$

where x is the co-ordinate on the shores (m), y is the location of the shoreline (m) and is perpendicular to the x-axis, t is time (day), Q is the long-shore sand transport rate (m^3/day), D_B is the average height of the berm (m), and D_C is the average depth of closure (m). To solve Equation (1), it was necessary to define a term for the long-shore sand transport rate (Q). This quantity is assumed to have been obtained by the oblique wave occurring at the shoreline. The US Army Corp developed a generalized term for the long-shore sand transport rate [17]:

$$Q = Q_0 \sin(2\alpha_b), \tag{2}$$

where Q_0 is the long-shore sand transport rate amplitude, and α_b is the angle between the breaking wave crest impact angle and local shoreline. The general formula for the long-shore sand transport rate amplitude is as follows [18]:

$$Q_0 = \frac{\rho}{16}(H_b^2 c_{gb}) \frac{K}{(\rho_s - \rho)(1-n)}, \tag{3}$$

where the b subscription signifies the value at the breaking point, c_g is the velocity of the wave group, H is the wave height, ρ_s is the sediment density (kg/m^3), ρ is the sea water's density, n is the porosity, and K is the non-dimensional coefficient of the particle size function, and α_b can be written as:

$$\alpha_b = \alpha_0 - \tan^{-1}\left(\frac{\partial y}{\partial x}\right), \tag{4}$$

where α_0 is the angle between breaking wave crests' impact angle and x-axis. It can be assumed for beaches with a mild slope that the angle of the wave breaking to the shoreline is minimal. Assuming that

$$\sin(2\alpha_b) \approx 2\alpha_b, \tag{5}$$

and

$$\tan^{-1}\left(\frac{\partial y}{\partial x}\right) \approx \frac{\partial y}{\partial x}, \tag{6}$$

replacing the Equation (2) with the Equation (4), and assuming that the beach has a mild slope:

$$Q = Q_0\left(2\alpha_b - 2\frac{\partial y}{\partial x}\right), \tag{7}$$

replacing the Equation (1) with the Equation (7) and ignoring the sources or sinks along the shoreline provides the following:

$$\frac{\partial y}{\partial x} = D\frac{\partial^2 y}{\partial x^2}, \tag{8}$$

for all $(x, t) \in (L, T)$, where

$$D = \frac{2Q_0}{D_B + D_C}. \tag{9}$$

Equation (8) is similar to a one-dimensional heat diffusion equation, which can be solved analytically under varying initial and boundary conditions.

2.2. *Physical Parameters*

The physical parameter of the model can be illustrated as shown in Figures 1 and 2 that are listed below.

α_0 is the angle between breaking wave crests' impact angle and x-axis.
Q_0 is the long-shore sand transport rate amplitude.
D_B is the average height of the berm.
D_C is the average depth of closure.
L is alongshore.
T is the time of simulation.

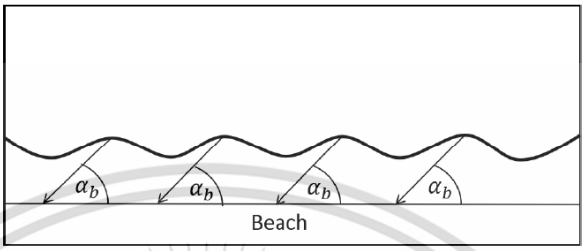

Figure 1. Breaking wave crests' impact angle.

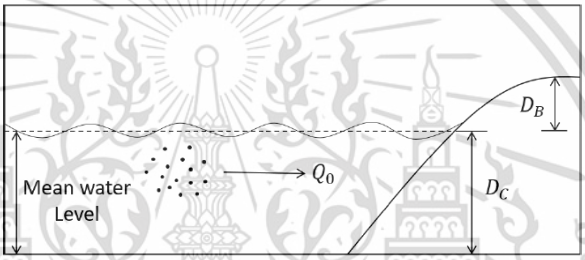

Figure 2. Shoreline's physical parameters.

2.3. The Initial and Boundary Conditions

Straight, impermeable groin system. The initial shoreline is assumed to be parallel to the x-axis. Assuming that, the sand transport rate along the shoreline is uniform. The groin is instantaneously added at $x = 0$, as shown in Figure 3. This means that the initial condition becomes,

$$y(x,0) = 0, \tag{10}$$

the wave crest impact effect to the boundary condition setting. This means that the boundary condition becomes,

$$\frac{\partial y(0,t)}{\partial x} = -\tan(\alpha_0) \quad \text{at } x = 0, \tag{11}$$

and

$$\frac{\partial y(L,t)}{\partial x} = -\tan(-\alpha_0) \quad \text{at } x = L. \tag{12}$$

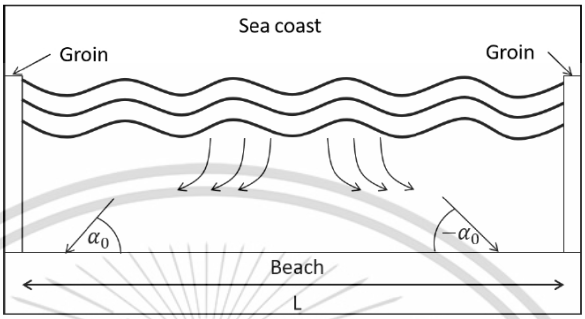

Figure 3. Initial shoreline.

2.4. Wave Crest Impact Model

The hydrodynamic model is introduced to obtain the wave crest impact in the shoreline evolution model [19].

The two-dimensional unstable water flow into and out of the seashore may be calculated by the use of a system of shallow water equations, taking into consideration the mass conservation and the momentum conservation. The equations of this method should be derived from the vertical direction of the depth-averaging of the Navier-Stokes equations, neglecting the diffusion of momentum due to vibration and discarding the terms representing the effects of friction, surface wind, Coriolis factor, and shear stress. The equation of continuity is then expressed as follows:

$$\frac{\partial h}{\partial t} + \frac{\partial (uh)}{\partial x} + \frac{\partial (vh)}{\partial y} = 0, \tag{13}$$

and the momentum equations are expressed as below:

$$\frac{\partial (uh)}{\partial t} + \frac{\partial \left(u^2 h + \frac{1}{2} g h^2\right)}{\partial x} + \frac{\partial (uvh)}{\partial y} = 0, \tag{14}$$

$$\frac{\partial (vh)}{\partial t} + \frac{\partial (uvh)}{\partial x} + \frac{\partial \left(v^2 h + \frac{1}{2} g h^2\right)}{\partial y} = 0, \tag{15}$$

where

$h(x, y, t)$ is the depth estimated from the average water surface to the seashore bed $h = H + \zeta$(m),
$\zeta(x, y, t)$ is the elevation of water surface from the average water level at seashore (m),
$H(x, y)$ is the interpolated bottom topography function of the seashore (m),
$u(x, y, t)$ is velocity in the direction of x (m/s),
$v(x, y, t)$ is velocity in the direction of y (m/s),
g is a constant in gravity (9.8 m/s^2).

Such time (t), and two space coordinates, x and y are the independent variables. Likewise, the conserved quantities are mass, which is proportional to h, and momentum, which is proportional to (uh) and (vh). As taken with respect to the same term, the partial

derivatives are grouped into vectors $(\partial x, \partial y, \partial t)$ and then rewritten as a partial differential hyperbolic equation, as follows:

$$U = \begin{pmatrix} h \\ uh \\ vh \end{pmatrix}, F(U) = \begin{pmatrix} uh \\ u^2h + \frac{1}{2}gh^2 \\ uvh \end{pmatrix}, G(U) = \begin{pmatrix} vh \\ uvh \\ v^2h + \frac{1}{2}gh^2 \end{pmatrix}. \tag{16}$$

The hyperbolic PDE:

$$\frac{\partial U}{\partial t} + \frac{\partial F(U)}{\partial x} + \frac{\partial G(U)}{\partial y} = 0. \tag{17}$$

2.5. The Initial and Boundary Condition for Wave Crest Impact Model

The initial conditions of the reservoir were as follows: The x- and y-velocity components were zero, as well as the water elevation of $u = 0, v = 0$, and $\zeta = 0$.

Assuming that the break-water is not a perfect barrier to water as it is made of an aggregate of rocks with large gaps, the boundary conditions were as follows: $(i) u = 0, \frac{\partial v}{\partial y} = 0, \xi = f(x, y, t)$ for waves coming into the beach, $(ii) \frac{\partial u}{\partial x} = 0, v = 0, \frac{\partial \xi}{\partial x} = 0$ for left and right groin structures, and $(iii) u = 0, \frac{\partial v}{\partial y} = 0, \frac{\partial \xi}{\partial y} = 0$ for along the beach, as shown in Figure 4.

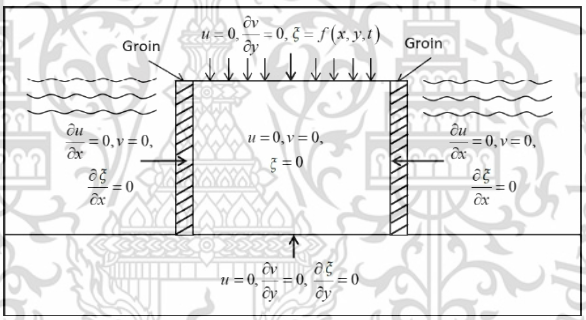

Figure 4. Initial and boundary conditions.

3. Numerical Techniques

3.1. Grid Spacing

We now discretize Equation (8) by dividing the interval $[0, L]$ into M sub-intervals, such that $M\Delta x = L$, and the interval $[0, T]$ into N sub-intervals, such that $N\Delta t = T$. We then approximate $y(x_n, t_n)$ by y_i^n, at the point $x_i = i\Delta x$ and $t_n = n\Delta t$, where $0 \leq i \leq M$ and $0 \leq n \leq N$ in which there are positive integers of M and N.

3.2. Traditional Forward Time-Centered Space Technique

The forward time-centered space schemes is employed. Consequently, the finite difference approximation becomes [20]

$$y \cong y_i^n, \tag{18}$$

$$\frac{\partial y}{\partial t} \cong \frac{y_i^{n+1} - y_i^n}{\Delta t}, \tag{19}$$

$$\frac{\partial y}{\partial x} \cong \frac{y_{i+1}^n - y_{i-1}^n}{2\Delta x}, \tag{20}$$

$$\frac{\partial^2 y}{\partial x^2} \cong \frac{y_{i+1}^n - 2y_i^n + y_{i-1}^n}{(\Delta x)^2}, \tag{21}$$

where $A = \frac{D\Delta t}{(\Delta x)^2}$.

Replacing the Equation (8) with the Equations (18)–(21), we obtain

$$\frac{y_i^{n+1} - y_i^n}{\Delta t} = D\left(\frac{y_{i+1}^n - 2y_i^n + y_{i-1}^n}{(\Delta x)^2}\right), \tag{22}$$

for $1 \leq i \leq M-1$ and $0 \leq n \leq N-1$. Equation (22) can be written in an explicit form of finite difference as follows,

$$y_i^{n+1} = Ay_{i+1}^n + (1-2A)y_i^n + Ay_{i-1}^n, \tag{23}$$

for $1 \leq i \leq M-1$ and $0 \leq n \leq N-1$.

3.3. Unconditionally Saulyev Finite Difference Techniques

The Saulyev scheme is employed. Consequently, the finite difference approximation becomes [9]

$$y \cong y_i^n, \tag{24}$$

$$\frac{\partial y}{\partial t} \cong \frac{y_i^{n+1} - y_i^n}{\Delta t}, \tag{25}$$

$$\frac{\partial^2 y}{\partial x^2} \cong \frac{y_{i+1}^n - y_i^n - y_i^{n+1} + y_{i-1}^{n+1}}{(\Delta x)^2}, \tag{26}$$

where $A = \frac{D\Delta t}{(\Delta x)^2}$.

Replacing the Equation (8) with the Equations (24)–(26), we obtain

$$\frac{y_i^{n+1} - y_i^n}{\Delta t} = D\left(\frac{y_{i+1}^n - y_i^n - y_i^{n+1} + y_{i-1}^{n+1}}{(\Delta x)^2}\right), \tag{27}$$

for $1 \leq i \leq M-1$ and $0 \leq n \leq N-1$. Equation (27) can be written in an explicit form of finite difference as follows,

$$y_i^{n+1} = \frac{1}{1+A}(Ay_{i+1}^n + (1-A)y_i^n + Ay_{i-1}^{n+1}), \tag{28}$$

for $1 \leq i \leq M-1$ and $0 \leq n \leq N-1$.

3.4. Numerical Techniques for the Wave Crest Impact Model

The finite difference technique [19]:

$$U_{i,j}^{n+1} = U_{i,j}^n - \frac{\Delta t}{\Delta x}\left(F_{i+\frac{1}{2},j}^{n+\frac{1}{2}} - F_{i-\frac{1}{2},j}^{n+\frac{1}{2}}\right) - \frac{\Delta t}{\Delta y}\left(G_{i,j+\frac{1}{2}}^{n+\frac{1}{2}} - G_{i,j-\frac{1}{2}}^{n+\frac{1}{2}}\right). \tag{29}$$

3.5. The Wave Crest Impact

The wave crest impact becomes

$$\alpha(x_i, y_j, t) = tan^{-1}\left(\frac{v(x_i, y_j, t)}{u(x_i, y_j, t)}\right), \tag{30}$$

and the averaged wave crest impact is assumed by

$$\alpha_0(t) = \frac{\sum_{i=1}^{N_p} \alpha(x_i, 0, t)}{N_p}, \tag{31}$$

where N_p is a number of wave crest impact sample points along the shoreline.

3.6. The Employment of Traditional Forward Time-Centered Space Technique to the Left and the Right Boundary Conditions

The forward time-centered space method is employed. Consequently, the finite difference approximation becomes

$$y \cong y_i^n, \tag{32}$$

$$\frac{\partial y}{\partial t} \cong \frac{y_i^{n+1} - y_i^n}{\Delta t}, \tag{33}$$

$$\frac{\partial y}{\partial x} \cong \frac{y_{i+1}^n - y_{i-1}^n}{2\Delta x}, \tag{34}$$

$$\frac{\partial^2 y}{\partial x^2} \cong \frac{y_{i+1}^n - 2y_i^n + y_{i-1}^n}{(\Delta x)^2}, \tag{35}$$

where $A = \frac{D\Delta t}{(\Delta x)^2}$.

Replacing the Equation (8) with the Equations (32)–(35), we obtain

$$\frac{y_i^{n+1} - y_i^n}{\Delta t} = D\left(\frac{y_{i+1}^n - 2y_i^n + y_{i-1}^n}{(\Delta x)^2}\right), \tag{36}$$

for $i = 0$, where replacing the uncertain value of the left boundary is approximated by the method of center difference with the specified left boundary condition

$$y_{-1}^n = y_1^n - 2(\Delta x)(-\tan(\alpha_0)), \tag{37}$$

replacing the Equation (36) with the Equation (37), we obtain

$$y_i^{n+1} = (1 - 2A)y_i^n + 2Ay_{i+1}^n - 2A(\Delta x)(-\tan(\alpha_0)), \tag{38}$$

for $i = M$, replacing the uncertain value of the right boundary is approximated by the method of center difference with the specified right boundary condition

$$y_{M+1}^n = y_{M-1}^n + 2(\Delta x)(-\tan(-\alpha_0)), \tag{39}$$

replacing the Equation (36) with the Equation (39), we obtain

$$y_i^{n+1} = 2Ay_{i-1}^n + (1 - 2A)y_i^n + 2A(\Delta x)(-\tan(-\alpha_0)). \tag{40}$$

The Equations (38) and (40) could be used to approximate the y_i^n values on the solution's domain grid points.

4. Physical Parameters' Setting Techniques

Assuming that the sediment density (ρ_s) [21], the sea water's density (ρ) [22], the porosity (n) [23], the non-dimensional coefficient of the particle size function (K) [24], the average height of the berm (D_B), and the average depth of closure (D_C) are listed below.

The wave group velocity (c_g) and the wave height (H) in each month along a year measured by field data on the gulf of Thailand are collected by the GeoInformatics and Space Technology Development Agency (Public Organization) (GISTDA) [25], as listed below.

The long-shore sand transport rate amplitude (Q_0) is obtained by Equation (3) and the long-shore transport rates (D) are obtained by Equation (9), as listed below.

5. Numerical Experiment

To analyze the evolution of the shoreline on a long-term scale, the numerical results of the beach scenario are considered and the solution to the idealized problem is introduced.

Assuming, during the simulation, that the length of the shoreline considered is $L = 100$ m, we set the physical parameter in Tables 1–3. The simulation setting is illustrated in Figure 3.

We will employ the finite difference techniques Equation (29) to approximate the wave crest impact model solution, as shown in Figure 5.

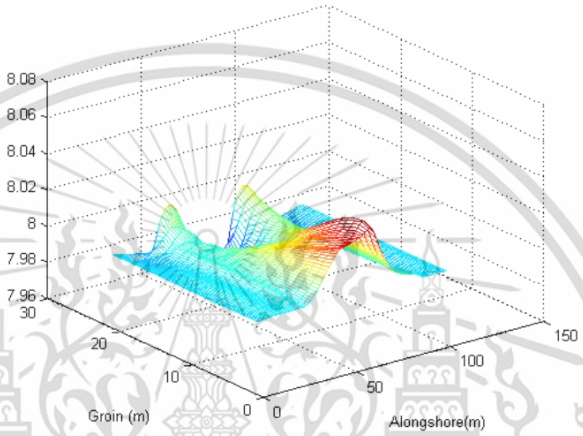

Figure 5. Wave crest impact in one year (360 days).

Table 1. Parameters of sand transport rate.

The sediment density (ρ_s (kg/m^3))	1700
The sea water's density (ρ (kg/m^3))	1020
The porosity (n)	0.406
The non-dimensional coefficient of the particle size function (K)	0.375
The average height of the berm. (D_B (m))	2
The average depth of closure. (D_C (m))	8

Table 2. The wave group velocity and the wave height.

Month	c_g (m/day)	H (m)
January 2019	8951.04	1.5
February 2019	6998.4	1.5
March 2019	5866.56	0.5
April 2019	6920.64	1.5
May 2019	5719.68	0.5
June 2019	5546.88	0.5
July 2018	8225.28	1.5
August 2018	9357.12	1.5
September 2018	13,711.68	1.5
October 2018	15,085.44	2.5
November 2018	10,877.76	1.5
December 2018	11,396.16	1.5

Table 3. The amplitude of the longshore transport rates and the longshore transport rates.

Month	Q_0 (m/day)	D (m/day)
January 2019	1191.99	238.3977
February 2019	931.96	186.3921
March 2019	86.80	17.3607
April 2019	921.61	184.3209
May 2019	84.63	16.9260
June 2019	82.07	16.4148
July 2018	1095.34	219.0681
August 2018	1246.07	249.2130
September 2018	1825.95	365.1903
October 2018	5580.26	1116.0520
November 2018	1448.57	289.7130
December 2018	1517.60	303.3699

The averaged wave crest impact (α_0) is obtained by Equation (31), as shown in Table 4.

Table 4. The averaged wave crest impact in one year (360 days).

Time				**min**			
day	**0–90**	**90–180**	**180–270**	**270–360**	**360–450**	**450–540**	**540–630**
30	−0.0186	−0.0185	−0.0184	−0.0182	−0.0181	−0.0180	−0.0179
60	0.0052	0.0052	0.0051	0.0051	0.0051	0.0051	0.0050
90	0.0623	0.0621	0.0619	0.0617	0.0615	0.0614	0.0612
.	.	.	.	.	.	.	.
.	.	.	.	.	.	.	.
.	.	.	.	.	.	.	.
360	0.1306	0.1306	0.1306	0.1306	0.1306	0.1306	0.1306
Time				**min**			
day	**630–720**	**720–810**	**810–900**	**900–990**	**990–1080**	**1080–1170**	**1170–1260**
30	−0.0178	−0.0178	−0.0177	−0.0176	−0.0175	−0.0175	−0.0174
60	0.0049	0.0048	0.0047	0.0046	0.0046	0.0046	0.0046
90	0.0610	0.0608	0.0606	0.0604	0.0602	0.0600	0.0598
.	.	.	.	.	.	.	.
.	.	.	.	.	.	.	.
.	.	.	.	.	.	.	.
360	0.1307	0.1618	0.1618	0.1618	0.1618	0.1618	0.1619
Time		**min**					
day	**1260–1350**	**1350–1440**					
30	−0.0173	−0.0172					
60	0.0046	0.0046					
90	0.0597	0.0595					
.	.	.					
.	.	.					
.	.	.					
360	0.1619	0.1619					

We will employ the traditional forward time-centered space technique (23), and the Saulyev finite difference techniques (28), to approximate the model solution. The calculated results $L = 100$ m are as shown in Figure 6.

The approximated solutions of the traditional forward time-centered space technique and Saulyev finite difference techniques give approximated solutions in Tables 5 and 6.

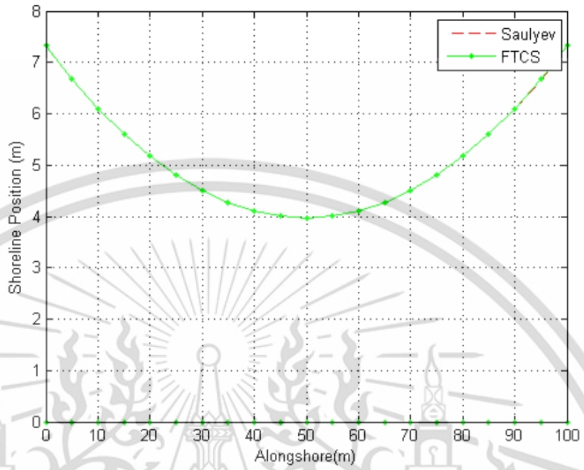

Figure 6. Shoreline evolution in one year.

Table 5. Approximated shoreline evolution along one year by a traditional forward time-centered space technique.

Time (years)	Distance (m)					
	0	**20**	**40**	**60**	**80**	**100**
1	7.3252	5.1761	4.1060	4.1060	5.1761	7.3252

Table 6. Approximated shoreline evolution along one year by Saulyev finite difference techniques.

Time (years)	Distance (m)					
	0	**20**	**40**	**60**	**80**	**100**
1	7.3260	5.1764	4.1053	4.1060	5.1756	7.3238

6. Discussion

The effect of the wave crest from Equation (31) as shown in Table 4. The long-shore transport rates (D) are also measured on a monthly basis during the year. The long-shore transport rates (D) were obtained by using Equation (9). The amplitude of the long-shore transport rates (Q_0) was obtained by Equation (3), the density of the sediment (ρ_s), the density of seawater (ρ), the porosity (n), the non-dimensional coefficient of the particle size function (K), the averaged berm height (D_B) and the closure depth (D_C), as shown in Table 1. The wave group velocity (c_g) and the wave height (H) for each month are seen in Table 2.The amplitude of the long-distance transport rate (Q_0) and the long-distance transport rate (D) for each month are simulated as shown in Table 3.

The evolution of the coastline in each year is predicted by the use of a traditional forward time-centered space technique and Saulyev finite difference techniques, as seen in Tables 5 and 6 and Figure 3. The distance from the most distant shoreline evolution is 7.32 m. The shortest distance from the shoreline evolution is 3.96 m. The calculated shoreline evolution of the two numerical techniques is closed.

7. Conclusions

In this research, we presented a one-dimensional mathematical model of shoreline evolution, and the parameters that affect this model are presented monthly over one year. The wave crest impact model was used to estimate the nonuniform breaking wave crest impact at the time it was considered. The evolution of the shoreline in areas where groins are installed on both sides was focused on. The initial and boundary conditions were defined by the groins on both sides. We then used the traditional forward time-centered space technique and Saulyev finite difference techniques to estimate the monthly evolution of the shoreline for each year. The traditional forward time-centered space technique provides a more accurate measurement than the Saulyev finite difference techniques. However, if any time increment cases are chosen, the traditional forward time-centered space technique is not capable of estimating the solution—see also [26]. Fortunately, the solution can always be estimated by the Saulyev finite difference techniques. The approximate effects of the shoreline evolution where consistent with the nonuniform breaking wave crest impact by the wave crest impact model and the installation properties of the beach groins.

Author Contributions: Conceptualization, N.P.; investigation, N.P. and P.U.; project administration, N.P.; supervision, N.P.; writing—original draft, N.P. and P.U.; writing— review and editing, N.P. All authors have read and agreed to the published version of the manuscript.

Funding: The Centre of Excellence in Mathematics, the Commission on Higher Education, Thailand.

Institutional Review Board Statement: Not applicable.

Informed Consent Statement: Not applicable.

Data Availability Statement: All data generated or analysed during this study are included in this published article.

Acknowledgments: This paper is supported by the Centre of Excellence in Mathematics, the Commission on Higher Education, Thailand.

Conflicts of Interest: The authors declare no conflict of interest.

References

1. Hanson, H.; Kraus, N.C.; Blomgren, S.H. Modern functional design of groin systems. *Coast. Eng.* **1994**, *96*, 1327–1342.
2. Fatimah, E.; Ariff, A.; Aulia, T.B. The influence of single zigzag type porous groin in the change of beach profile. *Procedia Eng.* **2015**, *125*, 257–262. [CrossRef]
3. Bakker, W.T.; Breteler, E.K.; Roos, A. The dynamics of coast with a groin system. *Coast. Eng. Proc.* **1970**, *1*, 492–517. doi:10.9753/icce.v12.64. [CrossRef]
4. Bakker, W.T.; Edelman, T. The coastline of river deltas. *Coast. Eng. Proc.* **1964**, *1*, 199–218. doi:10.9753/icce.v9.13. [CrossRef]
5. Grijimr, W. Theoretical form of shoreline. Available online: https://ascelibrary.org/doi/abs/10.1061/9780872620056.014 (accessed on 25 March 2021).
6. Mahute, B.L.; Soldate, M. Mathematical Modeling of Shoreline Evolution. In *US Army Corps of Engineer Waterways Experiment Station*; CERC: Rockville, MD, USA, 1977.
7. Hanson, H.; Larson, M.; Kraus, N.C. Analytical Solution of the One-line Model for Shoreline Changel. In *US Army Corps of Engineer Waterways Experiment Station*; CERC: Rockville, MD, USA, 1987.
8. Walton, T.; Chiu, T. A review of analytical technique to solve the sand transport equation and some simplified solution. *Coast. Struct.* **1979**, 809–837.
9. Pochai, P. Unconditional stable numerical techniques for a water-quality model in a non-uniform flow stream. *Adv. Differ. Eq.* **2017**, *2017*, 13. [CrossRef]
10. Samalerk, P.; Pochai, N. Numerical Simulation of a One-Dimensional Water-Quality Model in a Stream Using a Saulyev Technique with Quadratic Interpolated Initial-Boundary Conditions. *Abstr. Appl. Anal.* **2018**, *2018*, 1926519. [CrossRef]
11. Aminti, P.; Cammelli, C.; Cappietti, L.; Jackson, N.L.; Nordstrom, K.F.; Pranzini, E. Evaluation of Beach Response to Submerged Groin Construction at Marina di Ronchi, Italy, Using Field Data and a Numerical Simulation Model. *J. Coast. Res.* **2004**, *33*, 99–120.
12. Cannata, G.; Tamburrino, M.; Gallerano, F. 3D Numerical Simulation of the Interaction between Waves and a T-Head Groin Structure. *J. Mar. Sci. Eng.* **2020**, *8*, 227. [CrossRef]
13. Setyandito, O.; Purnama, A.C.; Yuwono, N.J.; Wijayanti, Y. Shoreline Change with Groin Coastal Protection Structure at North Java Beach. *ComTech Comput. Math. Eng. Appl.* **2020**, *11*, 19–28. [CrossRef]

14. Ding, Y.; Kim, S.; Frey, A.E. Probabilistic Shoreline Evolution Modeling in Response to Sea Level Changes. *World Environ. Water Resour. Congr.* **2018**. [CrossRef]
15. Dabees, M.; Kamphuis, J.W. Oneline, A Numerical Model for Shoreline Change. In Proceeding of the 26th Coastal Engineering Conference 1998, Copenhagen, Denmark, 22–26 June 1998; pp. 2668–2681.
16. Subiyanto, M.M.; Ahmad, M.F.; Husain, M.L. Comparison of numerical method for forward and backward time centered space for long—Term simulation of shoreline evolution. *Appl. Math. Sci.* **2013**, *7*, 5165–5173. [CrossRef]
17. US Army Corp of Engineers. *Shore Protection Manual*; Coastal Engineering Research Centre: Washington, DC, USA, 1984.
18. Hoan, L.X. Some result of comparison between numerical and analytical solutions of the one-line model for shoreline change. *Vietnam. J. Mech.* **2006**, *28*, 94–102. [CrossRef]
19. Kraychang, W.; Pochai, N. Numerical Treatment to a Water-Quality Measurement Model in an Opened-Closed Reservoir. *Thai J. Math.* **2015**, *13*, 775–788.
20. Mitchell, A.R. *Computational Methods in Partial Differential Equations*; John Wiley & Sons Ltd.: London, UK, 1969.
21. Tenzer, R.; Gladkikh, V. Assessment of density variations of marine sediments with ocean and sediment depths. *Sci. World J.* **2014**, *2014*, 823296. [CrossRef] [PubMed]
22. Wikipedia. Available online: https://en.wikipedia.org/wiki/Seawater (accessed on 25 March 2021).
23. Román-Sierra, J.; Muñoz-Perez, J.J.; Navarro-Pons, M. Beach nourishment effects on sand porosity variability. *Coast. Eng.* **2014**, *83*, 221–232. [CrossRef]
24. Dronkers, J.; van den Berg, J. Available online: http://www.coastalwiki.org/wiki/Coastal_and_marine_sediments?fbclid=IwAR2UkENgXUxyEJIj5tIaau2yPrDOCuRniHu3FqSCrLwVD_KpKMtqXob1iZc (accessed on 25 March 2021).
25. GeoInformatics and Space Technology Development Agency (Public Organization) (GISTDA). Available online: http://http://coastalradar.gistda.or.th/wp/?page=announce-small (accessed on 25 March 2021).
26. Unyapoti, P.; Pochai, N. A One-Dimensional Mathematical Model of Long-Term Shoreline Evolution with Groin System using an Unconditionally Stable Explicit Finite Difference Method. *Int. J. Simul. Syst. Sci. Technol.* **2020**, *21*.,2.1–2.6. [CrossRef]

IAENG International Journal of Computer Science, 49:3, IJCS_49_3_07

A Shoreline Evolution Model With the Wavelength Effect of Breaking Waves on Groin Structures

Pidok Unyapoti, Nopparat Pochai

Abstract— **Local sea level rise, strong wave action, and tidal currents all wear down or carry away rocks, soil, and sand along the beaches. The quantity of beach areas has decreased as a result of this issue. Analyzing the progression of the shoreline can help us better understand how the beach will look in the future. A groin structure was built to stop beach erosion and repair the beach. Beach erosion and beach deposition research requires a qualitative analysis of the model shoreline behavior in connection to the governing process. Models for shoreline evolution are the subject of some research. However, they focus on the shoreline evolution in an area between a couple of groin structures. The investigated area of shoreline evolution with a pair of groin structures is enlarged in this research to include the groin system and surrounding area. A more realistic shoreline evolution model has been presented, which takes into account the wavelength influence of breaking waves on groin constructions. The initial condition setting approach and boundary conditions techniques, as well as various groin structural impacts, are discussed. A wave crest impact model and five wavelength effects of breaking waves are introduced. Each year, the coastline evolution is approximated using the classical forward-time centered-space method and the unconditionally stable Saulyev finite differential methods. The estimated impacts of shoreline evolution were consistent with the wave crest impact model for five case wavelengths. For assessing long coastline evolution, the numerical models presented enable a reasonable simulation. The efficiency of building a groin system on a nearby beach might be predicted using the proposed modeling.**

Index Terms—**shoreline evolution, groin system, explicit finite method, wave crest impact, mathematical model**

I. Introduction

Beach erosion is a natural process by which local sea-level rise, strong wave action, and coastal flooding wear down or carry away rocks, soils, and sands along the beach. In many countries, beach erosion is responsible for coastal property loss, including damage to structures and loss of land. This is a problem that causes a decrease in beach areas. A groin structure was invented to prevent beach erosion and thus restore the beach. In [1], they proposed a new method to practical groin modeling, which is explained through the use of the GENESIS shoreline response model to examine the effect of single and multiple groins. The study's predictions are put to test in the replication of the shoreline modification observed in the groin area of Westhampton, Long Island, New York. In [2], They presented groynes-constructed coir geotextiles in the shape of cocologs, as well as the effects of positioning groynes at various angles to determine the most capable setting for minimizing erosion. The results show that a groyne angle of 1350 provides the best protection.

Many authors have developed one-line theory, and several contributors to the analytical solution of the evolution of the shoreline include [3], [4], [5], [6], [7], [8], and [9]. Analytical solutions are usually useful for providing qualitative insight and comprehending the characteristics of long-term shoreline modification. However, analytical solutions have limitations. A numerical method of shoreline evolution may be more relevant for the actual scenario than an analytical solution because an analytical solution cannot be anticipated to tackle problems with complicated boundary conditions and wave inputs.

In [12], they presented a comparison of analytical solutions and two numerical techniques of shoreline evolution under idealized wave conditions for two case shoreline scenarios. The two numerical methods are Forward Time Centered Space techniques and Backward Time Centered Space techniques. The results show that Backward Time Centered Space techniques are more appropriate than Forward Time Centered Space techniques for simulating long-term shoreline change. In [13], [14], [15], [16], [17], and [32], they approximated their model solutions using conditionally stable explicit finite difference methods. In [18], [19], [20], [21], [33], and [34], they approximated their model solution using numerical approaches. In [30], they introduced shoreline evolution when a couple of groins were added. They use two numerical methods to develop shoreline evolution. The first numerical method is the classic forward time-centered space method. The second numerical method is the unconditionally stable Saulyev finite difference methods.

In [22], the purpose of this research is to generate a practical, universal, and replicable chain approach that can aid in comprehensively understanding the dynamics of a coastal system, identifying typical and recurring erosion-accretion processes, and prediction likely future trends relevant to coastal activity planning. In [23], they proposed a

Manuscript received February 25, 2022; revised June 23, 2022.

This paper is supported by Centre of Excellence in Mathematics, Ministry of Higher Education, Science, Research and Innovation, Bangkok, Thailand.

N. Pochai is an Assistant Professor of Department of Mathematics, Faculty of Science, King Mongkut's Institute of Technology Ladkrabang, Bangkok, 10520, Thailand (corresponding author to provide phone: 662-329-8400; fax: 662-329-8400; e-mail: nop_math@yahoo.com).

P. Unyapoti is a PhD. candidate of Mathematics Department, Faculty of Science, King Mongkut's Institute of Technology Ladkrabang, Bangkok, 10520, Thailand (e-mail: pidokunyapoti@gmail.com).

one-line model idea, which has been used to achieve long-term shoreline modeling as well as to aid and generate stronger coastal engineering techniques for managing erosion. The model was tested on Portugal's two northwest coasts, Aveiro and Figueira da Foz. In [24], they proposed using a long-term morphological dataset to morphometrically characterize the evolution of the shoreline along the Holland coast, from Den Helder to Hoek van Holland, and to relate this to the evolution of the complete littoral profile (1964-1992). In [25], they proposed that the research results, in addition to assessing the effects of groins on shoreline modification, serve as a precursor for initiating appropriate mitigation measures to prevent future erosion and instability of the coastline while maintaining the safety and economic design of offshore, coastal, and port structures. In [26], they proposed that the evolution of a beach restoration project in Long Branch, NJ be examined using the empirical orthogonal functions method (EOF). The majority of EOF applications on beach fill projects have been on classic linear fills on generally long, straight, uninterrupted coastlines. The Long Branch project was unusual in that it was conceived as a feeder beach and built within a groin field. In [27], they proposed the comparison of analytical and numerical solutions in the idealized wave condition for four different shoreline situations.

In this research, a shoreline evolution model that takes into consideration the wavelength effect of breaking waves on groin structures is focused. We introduce a governing equation for a one-dimensional shoreline evolution model, initial conditions, and boundary conditions when a couple of groins are added, a wave crest impact model, and five case wavelength effects of breaking waves. Finite difference techniques will be used to approximate the model solution.

II. Governing Equation

A. Shoreline evolution model

In a one-dimensional shoreline evolution model, while maintaining the same shape, the beach shape is supposed to move towards land and towards the sea, meaning that all the bottom outlines become parallel.

As a result of this assumption, the horizontal direction of the baseline profile must be defined, and one contour line should be used to specify changes to the design and volume of the beach plane as the beach erodes and accumulates. The model's main assumption is that sand is transported along the coast on a profile between two well-defined limit elevations. A contribution to the adjustment in volume occurs where there is a discrepancy in the rate of longshore sand transfer on the side of the segment and the related sand consistency. The principles of conservation of mass must be always adapted to the system. The following differential equation for the evolution of the shoreline is generated by considering the above concepts,

$$\frac{\partial y}{\partial t} = \frac{1}{D_B + D_C}\left(-\frac{\partial Q}{\partial x}\right), \tag{1}$$

where x is the co-ordinate on the shores (m), y is the location of the shoreline (m) and perpendicular to the x-axis, t is time (day), Q is the long-shore sand transport rate (m^3/day), D_B is the average height of the berm (m) and D_C is the average depth of closure (m).

To solve (1), it was necessary to define a term for the longshore sand transport rate (Q). This quantity is assumed to have been obtained by the oblique wave occurring to the shoreline. The US Army Corp has created a generalized term for long-shore sand transport rate [10],

$$Q = Q_0 \sin(2\alpha_b), \tag{2}$$

where Q_0 is the long-shore sand transport rate amplitude. The general formula for the long-shore sand transport rate amplitude is as follows [11],

$$Q_0 = \frac{\rho}{16}\left(H_b^2 c_{gb}\right)\frac{K}{(\rho_s - \rho)(1-n)}, \tag{3}$$

The angle between breaking wave crest impact angle and local shoreline (α_b) can be written as,

$$\alpha_b = \alpha_0 - \tan^{-1}\left(\frac{\partial y}{\partial x}\right), \tag{4}$$

where α_0 is the angle between breaking wave crests impact angle and x-axis. In the case of shoreline with a slight slope, it can be concluded that the angle of the wave breaking to the shoreline is minimal.

Assuming that, $\sin(2\alpha_b) \approx 2\alpha_b$ and $\tan^{-1}\left(\frac{\partial y}{\partial x}\right) \approx \left(\frac{\partial y}{\partial x}\right)$.

By substituting (4), in (2), and assuming a shoreline with a slight slope, we obtain,

$$Q = Q_0\left(2\alpha_b - 2\frac{\partial y}{\partial x}\right), \tag{5}$$

by substituting (5), in (1), and ignoring the sources or sinks along the shoreline provides the following:

$$\frac{\partial y}{\partial t} = D\frac{\partial^2 y}{\partial x^2}, \tag{6}$$

for all $(x,t) \in (L,T)$, where $D = \frac{2Q_0}{D_B + D_C}$.

B. Physical parameters

The physical parameters of the model are illustrated in Fig. 1-2. which are listed below.

α_0 is the angle between breaking wave crests impact angle and x-axis.

Q_0 is the long-shore sand transport rate amplitude.

D_B is the averaged berm height.

D_C is the averaged closure depth.

L is Alongshore.

T is the Time of simulation.

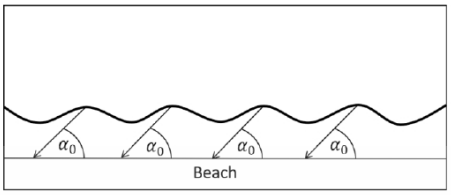

Fig. 1. Breaking wave crests impact angle

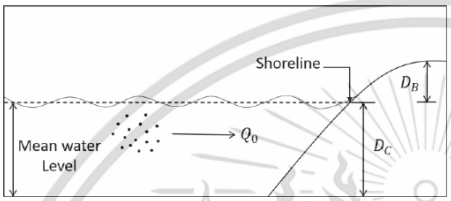

Fig. 2. Shoreline physical parameters

C. The initial and boundary conditions

Straight Impermeable groin system.

The initial shoreline is assumed to be parallel to the x-axis. Assuming that, the angle between breaking wave crests impact angle to the shoreline is α_0 as shown in Fig. 3. It follows that the sand transport rate along the shoreline is uniform. The groin is added instantly at $x=0$ are illustrated in Fig. 3. These means that the initial condition becomes,

$$y(x,0)=0, \tag{7}$$

boundary conditions are also assumed by,

$$\frac{\partial y(0,t)}{\partial x}=-\tan(\alpha_0) \quad \text{at} \quad x=0, \tag{8}$$

and

$$\frac{\partial y(L,t)}{\partial x}=-\tan(-\alpha_0) \quad \text{at} \quad x=L, \tag{9}$$

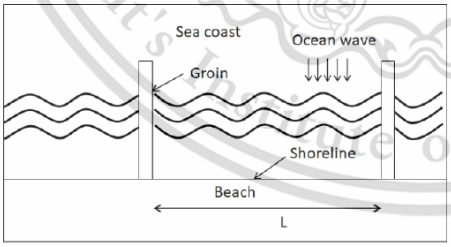

Fig. 3. Initial shoreline with configuration straight impermeable groins.

D. Wave crest impact model

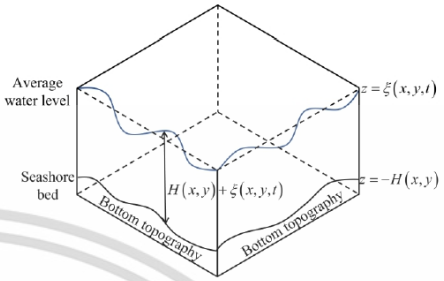

Fig. 4. Water elevation and bottom topography.

The hydrodynamic model is introduced to obtain the wave crest impact in the shoreline evolution model [28].

The two-dimensional unstable water flows into and out of the seashore can be predicted using a system of shallow water equations that account for mass and momentum conservation. The equations of this method should be derived from the vertical direction of the depth-averaging of the Navier-Stokes equations, ignoring momentum diffusion owing to vibration and excluding terms indicating the effects of friction, surface wind, Coriolis factor, and shear stress. The equation of continuity is then expressed as follows:

$$\frac{\partial h}{\partial t}+\frac{\partial(uh)}{\partial x}+\frac{\partial(vh)}{\partial y}=0, \tag{10}$$

and the momentum equations are expressed as below:

$$\frac{\partial(uh)}{\partial t}+\frac{\partial\left(u^2h+\frac{1}{2}gh^2\right)}{\partial x}+\frac{\partial(uvh)}{\partial y}=0, \tag{11}$$

$$\frac{\partial(uh)}{\partial t}+\frac{\partial(uvh)}{\partial x}+\frac{\partial\left(v^2h+\frac{1}{2}gh^2\right)}{\partial y}=0, \tag{12}$$

where

$h(x,y,t)$ is the depth estimated from the average water surface to the seashore bed (m) $h=H+\xi$,

$\xi(x,y,t)$ is the elevation of the water surface from the average water level in the seashore (m),

$H(x,y)$ is the interpolated bottom topography function of the seashore (m),

$u(x,y,t)$ is the velocity in the direction of x (m/s),

$v(x,y,t)$ is the velocity in the direction of y (m/s),

g is a constant of gravity $(9.8\ m/s^2)$.

Such time (t), and two space coordinates, x and y are the independent variables. Likewise, the conserved quantities are mass, which is proportional to h, and momentum, which is proportional to (uh) and (vh). The partial derivatives are grouped into vectors $(\partial x,\partial y,\partial t)$ and

then rewritten as a partial differential hyperbolic equation concerning the same term as follows:

$$U = \begin{pmatrix} h \\ uh \\ vh \end{pmatrix}, F(U) = \begin{pmatrix} uh \\ u^2 h + \frac{1}{2} g h^2 \\ uvh \end{pmatrix}, \quad (13)$$

$$G(U) = \begin{pmatrix} vh \\ uvh \\ v^2 h + \frac{1}{2} g h^2 \end{pmatrix}, \quad (14)$$

the hyperbolic PDE:

$$\frac{\partial U}{\partial t} + \frac{\partial F(U)}{\partial x} + \frac{\partial G(U)}{\partial y} = 0. \quad (15)$$

E. The initial and boundary condition for wave crest impact model

The initial condition of the reservoir was as follows: the x and y velocity components were zero as well as the water elevation: $u = 0, v = 0$ and $\xi = 0$.

Assuming that the breakwater is not a perfect barrier to water as it is made of an aggregate of rocks with large gaps.

The boundary condition was as follows:

$(i)\ u = 0, \frac{\partial v}{\partial y} = 0, \xi = f(x, y, t)$ for wave coming,

$(ii)\ \frac{\partial u}{\partial x} = 0, \mathrm{v} = 0, \frac{\partial \xi}{\partial x} = 0$ for left and right boundary,

$(iii)\ u = 0, \frac{\partial v}{\partial y} = 0, \frac{\partial \xi}{\partial y} = 0$ for along the beach,

$(iv)\ u = 0, \frac{\partial v}{\partial y} = 0, \frac{\partial \xi}{\partial y} = 0$ for top groin structure, and

$(v)\ \frac{\partial u}{\partial x} = 0, \mathrm{v} = 0, \frac{\partial \xi}{\partial x} = 0$ for left and right groin structure.

The boundary conditions are illustrated in Fig. 5-6.

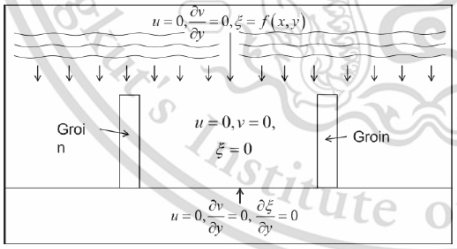

Fig. 5. Initial and boundary conditions.

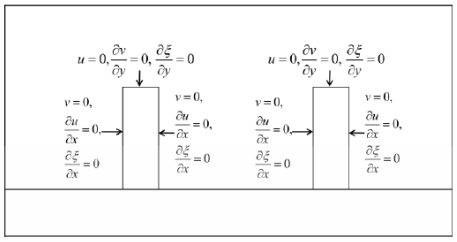

Fig. 6. Initial and boundary conditions for groin structure.

III. Numerical Techniques

A. Grid Spacing

We are discretizing (6) by splitting the interval $[0, L]$ into M subintervals such as $M\Delta x = L$ and the interval $[0, T]$ into N subintervals such as $N\Delta t = T$. We then approximate $y(x_i, t_n)$ by y_i^n, at the point $x_i = i\Delta x$ and $t_n = n\Delta t$, where $0 \le i \le M$ and $0 \le n \le N$ in which there are positive integers of M and N.

B. Traditional forward time centered space techniques

The forward time centered space techniques will also be used. Consequently, the finite difference approximation becomes [29],

$$y \cong y_i^n, \quad (16)$$

$$\frac{\partial y}{\partial t} \cong \frac{y_i^{n+1} - y_i^n}{\Delta t}, \quad (17)$$

$$\frac{\partial y}{\partial x} \cong \frac{y_{i+1}^n - y_{i-1}^n}{2\Delta x}, \quad (18)$$

$$\frac{\partial^2 y}{\partial x^2} \cong \frac{y_{i+1}^n - 2y_i^n + y_{i-1}^n}{(\Delta x)^2}, \quad (19)$$

where $A = \frac{D\Delta t}{(\Delta x)^2}$.

By substituting (16) – (19), in (6), we obtain,

$$\frac{y_i^{n+1} - y_i^n}{\Delta t} = D\left(\frac{y_{i+1}^n - 2y_i^n + y_{i-1}^n}{(\Delta x)^2}\right), \quad (20)$$

for $1 \le i \le M-1$ and $0 \le n \le N-1$. From (20), we get an explicit form of finite difference as follows:

$$y_i^{n+1} = Ay_{i+1}^n + (1-2A)y_i^n + Ay_{i-1}^n, \quad (21)$$

for $1 \le i \le M-1$ and $0 \le n \le N-1$.

C. An unconditionally Saulyev finite difference techniques

The Saulyev finite difference techniques will also be used. We can obtain that the finite difference approximation is

$$y \cong y_i^n, \quad (22)$$

$$\frac{\partial y}{\partial t} \cong \frac{y_i^{n+1} - y_i^n}{\Delta t}, \tag{23}$$

$$\frac{\partial^2 y}{\partial x^2} \cong \frac{y_{i+1}^n - y_i^n - y_i^{n+1} + y_{i-1}^{n+1}}{(\Delta x)^2}, \tag{24}$$

where $A = \frac{D\Delta t}{(\Delta x)^2}$.

By substituting (22) – (24), in (6), we obtain,

$$\frac{y_i^{n+1} - y_i^n}{\Delta t} = D\left(\frac{y_{i+1}^n - y_i^n - y_i^{n+1} + y_{i-1}^{n+1}}{(\Delta x)^2}\right), \tag{25}$$

for $1 \le i \le M-1$ and $0 \le n \le N-1$. From (25), we get an explicit form of finite difference as follows:

$$y_i^{n+1} = \frac{1}{(1+A)}\left(Ay_{i+1}^n + (1-A)y_i^n + Ay_{i-1}^{n+1}\right), \tag{26}$$

for $1 \le i \le M-1$ and $0 \le n \le N-1$.

D. Numerical techniques for the wave crest impact model

The finite difference technique:

$$U_{i,j}^{n+1} = U_{i,j}^n - \frac{\Delta t}{\Delta x}\left(F_{i+\frac{1}{2},j}^{n+\frac{1}{2}} - F_{i-\frac{1}{2},j}^{n+\frac{1}{2}}\right) - \frac{\Delta t}{\Delta y}\left(G_{i,j+\frac{1}{2}}^{n+\frac{1}{2}} - G_{i,j-\frac{1}{2}}^{n+\frac{1}{2}}\right), \tag{27}$$

E. The wave crest impact

The wave crest impact becomes

$$\alpha(x_i, y_j, t) = \tan^{-1}\left(\frac{v(x_i, y_j, t)}{u(x_i, y_j, t)}\right), \tag{28}$$

the averaged wave crest impact is assumed by

$$\alpha_0(t) = \frac{\sum_{i=1}^{N_P} \alpha(x_i, 0, t)}{N_P}, \tag{29}$$

where N_P is several wave crest impact sample points along the shoreline.

F. The employment of traditional forward time centered space techniques to the left and the right boundary conditions

The forward time centered space techniques will also be used. Consequently, the finite difference approximation becomes,

$$y \cong y_i^n, \tag{30}$$

$$\frac{\partial y}{\partial t} \cong \frac{y_i^{n+1} - y_i^n}{\Delta t}, \tag{31}$$

$$\frac{\partial y}{\partial x} \cong \frac{y_{i+1}^n - y_{i-1}^n}{2\Delta x}, \tag{32}$$

where $A = \frac{D\Delta t}{(\Delta x)^2}$.

By substituting (30) - (32), in (6), we obtain,

$$\frac{y_i^{n+1} - y_i^n}{\Delta t} = D\left(\frac{y_{i+1}^n - 2y_i^n + y_{i-1}^n}{(\Delta x)^2}\right), \tag{33}$$

For i = 0, the substitution of the uncertain value of the left boundary is approximated by the method of center difference with the specified left boundary condition. We obtain,

$$y_{-1}^n = y_1^n - 2(\Delta x)(-\tan(\alpha_0)), \tag{34}$$

by substituting (34), in (33), we obtain,

$$y_i^{n+1} = (1-2A)y_i^n + 2Ay_{i+1}^n - 2A(\Delta x)(-\tan(\alpha_0)), \tag{35}$$

For i = M, the substitution of the uncertain value of the right boundary is approximated by the method of center difference with the specified right boundary condition. We obtain,

$$y_{M+1}^n = y_{M-1}^n + 2(\Delta x)(-\tan(-\alpha_0)), \tag{36}$$

by substituting (36), in (33), we obtain,

$$y_i^{n+1} = 2Ay_{i-1}^n + (1-2A)y_i^n + 2A(\Delta x)(-\tan(-\alpha_0)), \tag{37}$$

(35), and (37), could be used to approximate the values y_i^n of the solution domain grid points.

IV. Wavelength Setting Techniques

The simulation considers alongshore between groin are illustrated in Fig. 7. Table 1 shows the consideration of wavelengths. We assumed waves came in a function of wavelength $0.5\sin(t + \Lambda x)$.

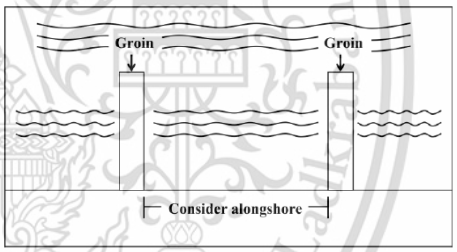

Fig. 7. Consider alongshore.

TABLE I
WAVELENGTH SETTING

Simulation	Λ	Wavelength
1	0.01	$0.5\sin(t+0.01x)$
2	0.02	$0.5\sin(t+0.02x)$
3	0.03	$0.5\sin(t+0.03x)$
4	0.04	$0.5\sin(t+0.04x)$
5	0.05	$0.5\sin(t+0.05x)$

We will employ the finite difference techniques to approximate the wave crest impact model solution for wavelengths $0.5\sin(t+0.01x)$, $0.5\sin(t+0.02x)$, $0.5\sin(t+0.03x)$, $0.5\sin(t+0.04x)$ and $0.5\sin(t+0.05x)$. The approximated wave crest impact model solutions for five case wavelengths are illustrated in Fig.8-12. The approximated vector fields of velocities for five case wavelengths are illustrated in Fig. 13-17.

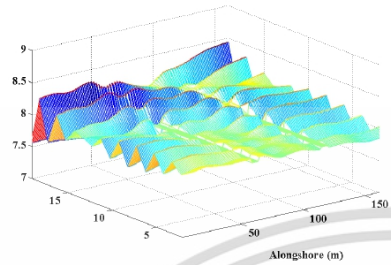

Fig. 8. Wave crest impact in 15 years when wavelength $0.5\sin(t+0.01x)$.

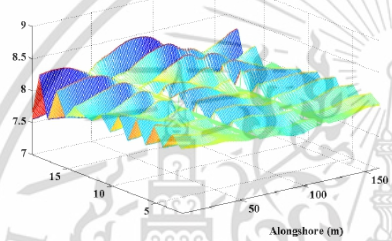

Fig. 9. Wave crest impact in 15 years when wavelength $0.5\sin(t+0.02x)$.

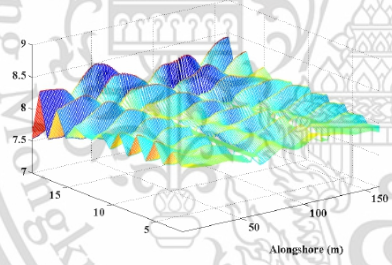

Fig. 10. Wave crest impact in 15 years when wavelength $0.5\sin(t+0.03x)$.

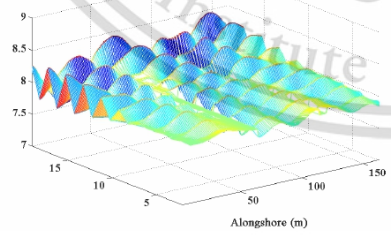

Fig. 11. Wave crest impact in 15 years when wavelength $0.5\sin(t+0.04x)$.

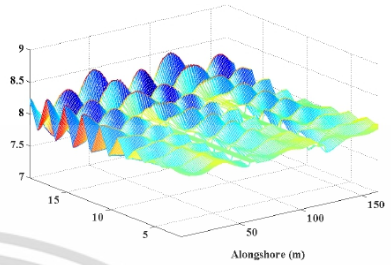

Fig. 12. Wave crest impact in 15 years when wavelength $0.5\sin(t+0.05x)$.

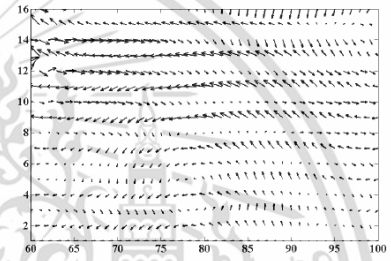

Fig. 13. vector field of velocities between groin when wavelength $0.5\sin(t+0.01x)$.

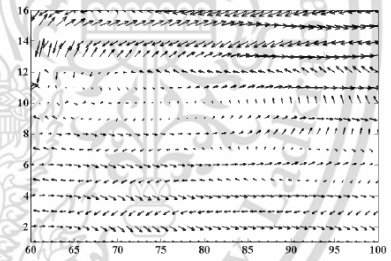

Fig. 14. vector field of velocities between groin when wavelength $0.5\sin(t+0.02x)$.

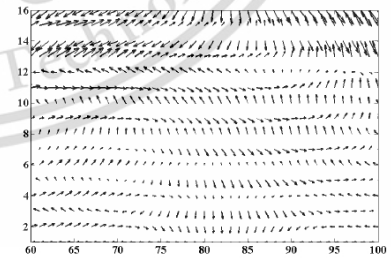

Fig. 15. vector field of velocities between groin when wavelength $0.5\sin(t+0.03x)$.

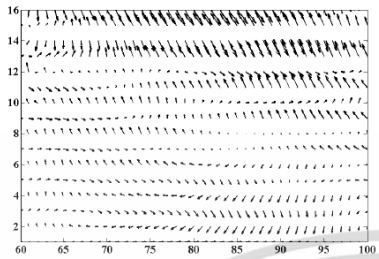

Fig. 16. vector field of velocities between groin when wavelength $0.5\sin(t+0.04x)$.

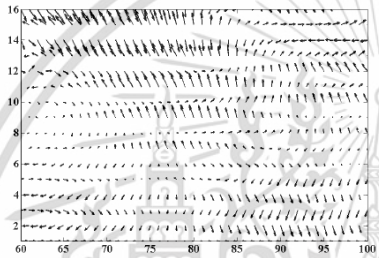

Fig. 17. vector field of velocities between groin when wavelength $0.5\sin(t+0.05x)$.

Table 2-6 shows the averaged wave crest impact (α_0) as obtained by (29).

TABLE II
THE AVERAGED WAVE CREST IMPACT 15 YEARS WHEN WAVELENGTH 1

Time (Years)	Min					
	0-15	15-30	30-45	45-60	60-75	75-90
1	0.0455	0.0448	0.0440	0.0433	0.0426	0.0419
5	-0.0400	-0.0419	-0.0439	-0.0459	-0.0480	-0.0501
10	-0.0705	-0.0721	-0.0737	-0.0754	-0.0770	-0.0786
15	0.0293	0.0284	0.0274	0.0264	0.0254	0.0244
Time (Years)	Distance(m)					
	…	1365-1380	1380-1395	1395-1410	1410-1425	1425-1440
1	…	-0.0379	-0.0394	-0.0410	-0.0426	-0.0442
5	…	-0.0496	-0.1140	-0.1158	-0.1178	-0.1830
10	…	0.1472	0.1363	0.1881	0.1770	0.1658
15	…	0.1930	0.1961	0.1985	0.2003	0.2018

TABLE III
THE AVERAGED WAVE CREST IMPACT 15 YEARS WHEN WAVELENGTH 2

Time (Years)	Min					
	0-15	15-30	30-45	45-60	60-75	75-90
1	0.1817	0.2377	0.2309	0.2241	0.2802	0.2734
5	0.3973	0.4493	0.3794	0.4342	0.4231	0.4109
10	-0.2747	-0.2215	-0.2315	-0.2418	-0.1899	-0.1385
15	-0.0364	-0.0478	0.0037	-0.0077	-0.0191	0.0323
Time (Years)	Distance(m)					
	…	1365-1380	1380-1395	1395-1410	1410-1425	1425-1440
1	…	-0.0275	-0.0380	-0.0485	0.0037	0.0559
5	…	0.1168	0.1154	0.1139	0.1124	0.1109
10	…	-0.1047	-0.1069	-0.1091	-0.1114	-0.1136
15	…	0.2057	0.2040	0.2024	0.2009	0.1993

TABLE IV
THE AVERAGED WAVE CREST IMPACT 15 YEARS WHEN WAVELENGTH 3

Time (Years)	Min					
	0-15	15-30	30-45	45-60	60-75	75-90
1	0.3715	0.3653	0.3595	0.3541	0.3489	0.3440
5	0.1662	0.1767	0.1243	0.1347	0.1449	0.1550
10	0.0148	0.0093	0.0039	-0.0015	-0.0070	-0.0123
15	0.1732	0.1821	0.1910	0.2000	0.2091	0.2182
Time (Years)	Distance(m)					
	…	1365-1380	1380-1395	1395-1410	1410-1425	1425-1440
1	…	0.1182	0.0881	0.1162	0.0782	0.0951
5	…	-0.1423	-0.1392	-0.1361	-0.1330	-0.1300
10	…	0.1488	0.1398	0.1276	0.1550	0.1307
15	…	-0.0660	-0.0623	-0.0586	-0.0550	-0.0514

TABLE V
THE AVERAGED WAVE CREST IMPACT 15 YEARS WHEN WAVELENGTH 4

Time (Years)	Min					
	0-15	15-30	30-45	45-60	60-75	75-90
1	-0.0060	-0.0017	0.0026	0.0068	0.0110	0.0151
5	-0.4238	-0.4291	-0.4346	-0.4403	-0.3833	-0.3894
10	0.3286	0.3249	0.3213	0.3177	0.3142	0.3108
15	-0.4203	-0.4178	-0.4781	-0.4754	-0.4728	-0.4701
Time (Years)	Distance(m)					
	…	1365-1380	1380-1395	1395-1410	1410-1425	1425-1440
1	…	-0.2516	-0.2551	-0.2586	-0.2621	-0.2656
5	…	-0.0892	-0.0940	-0.0360	-0.0408	-0.0454
10	…	0.2663	0.2698	0.2104	0.2139	0.2175
15	…	-0.3283	-0.2725	-0.2801	-0.2880	-0.2960

TABLE VI
THE AVERAGED WAVE CREST IMPACT 15 YEARS WHEN WAVELENGTH 5

Time (Years)	Min					
	0-15	15-30	30-45	45-60	60-75	75-90
1	-0.1214	-0.1405	-0.1557	-0.1691	-0.1188	-0.1310
5	0.1536	0.1497	0.2085	0.2046	0.2006	0.1966
10	-0.0695	-0.0659	-0.0623	-0.0586	-0.0550	-0.0514
15	0.0316	0.0913	0.0882	0.0850	0.0818	0.0786
Time (Years)	Distance(m)					
	…	1365-1380	1380-1395	1395-1410	1410-1425	1425-1440
1	…	0.2402	0.2359	0.2315	0.2271	0.2856
5	…	0.3529	0.3504	0.3479	0.4084	0.4060
10	…	-0.3659	-0.3637	-0.3616	-0.3595	-0.3574
15	…	0.3791	0.3757	0.3723	0.3690	0.3657

V. Numerical Experiment

In this section, the numerical results of the various beach scenarios are considered and the solution to the idealized problem is introduced. Assuming, during the experiments, that the length of the shoreline considered is L = 100 m and the averaged wave crest impact (α_0) of five case wavelengths. Table 2-6 shows the average wave crest impact of five case wavelengths. Table 7 shows the long-shore transport rate (D) [30]. The simulation setting is illustrated in Fig. 18.

We are going to employ the traditional forward time centered space techniques (15), and the Saulyev finite difference techniques (20), to approximate the shoreline evolution model solution. The approximated solutions are

illustrated in Fig. 19-23. Table 8-17 shows the approximated solutions.

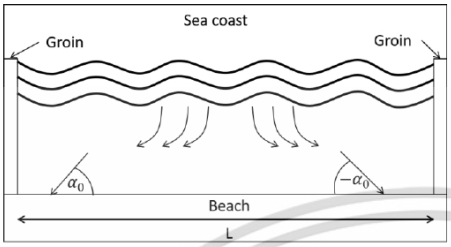

Fig. 18. Initial shoreline.

TABLE VII
THE LONG-SHORE TRANSPORT RATE

Month	$D\ (m/day)$
Jan	79.4659
Feb	62.1307
Mar	5.7869
Apr	61.4403
May	5.6420
Jun	5.4716
Jul	73.0227
Aug	83.071
Sep	121.7301
Oct	372.017
Nov	96.5710
Dec	101.1233

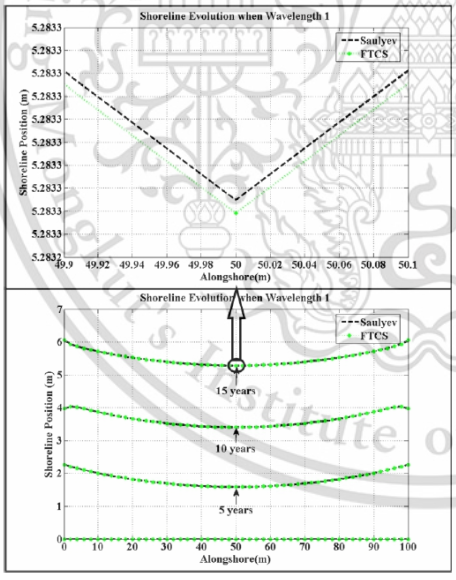

Fig. 19. Shoreline evolution in 15 years when wavelength $0.5\sin(t+0.01x)$.

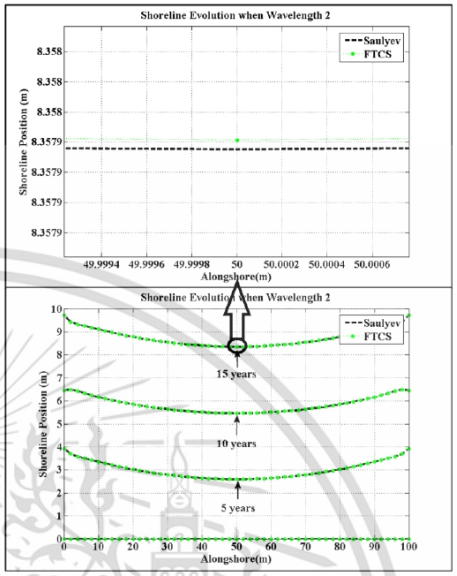

Fig. 20. Shoreline evolution in 15 years when wavelength $0.5\sin(t+0.02x)$.

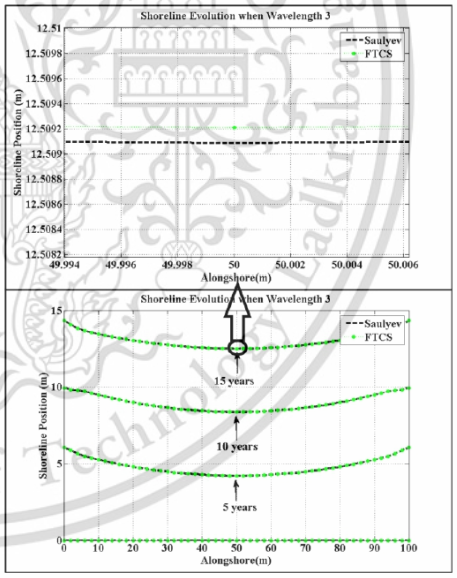

Fig. 21. Shoreline evolution in 15 years when wavelength $0.5\sin(t+0.03x)$.

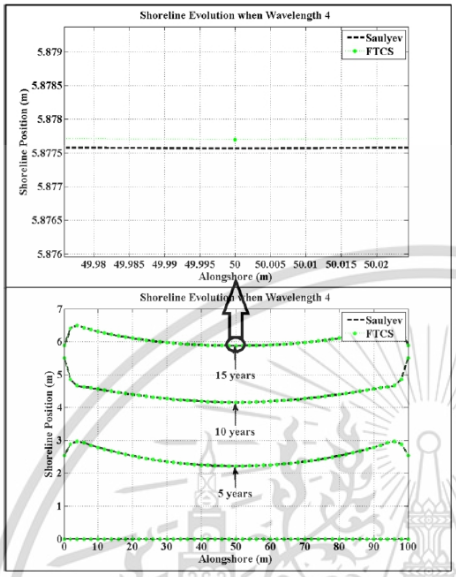

Fig. 22. Shoreline evolution in 15 years when wavelength $0.5\sin(t+0.04x)$.

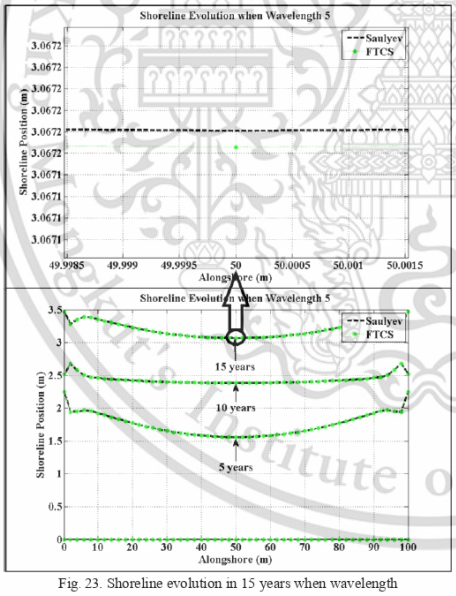

Fig. 23. Shoreline evolution in 15 years when wavelength $0.5\sin(t+0.05x)$.

TABLE VIII
APPROXIMATED SHORELINE EVOLUTION ALONG 15 YEARS USING THE TRADITIONAL FORWARD TIME CENTERED SPACE TECHNIQUES WHEN WAVELENGTH 1

Time (Years)	Distance(m)					
	0	20	40	60	80	100
1	0.8609	0.3967	0.1801	0.1801	0.3967	0.8609
5	2.2665	1.8264	1.6152	1.6152	1.8264	2.2665
10	3.9788	3.6680	3.4335	3.4335	3.6680	3.9788
15	6.0537	5.5284	5.3113	5.3113	5.5284	6.0537

TABLE IX
APPROXIMATED SHORELINE EVOLUTION ALONG 15 YEARS USING THE SAULYEV FINITE DIFFERENCE TECHNIQUES WHEN WAVELENGTH 1

Time (Years)	Distance (m)					
	0	20	40	60	80	100
1	0.8613	0.3969	0.1802	0.1800	0.3965	0.8606
5	2.2662	1.8588	1.6152	1.6152	1.8266	2.2667
10	3.9783	3.6679	3.4334	3.4334	3.6679	3.9788
15	6.0529	5.5280	5.3113	5.3113	5.5285	6.0538

TABLE X
APPROXIMATED SHORELINE EVOLUTION ALONG 15 YEARS USING THE TRADITIONAL FORWARD TIME CENTERED SPACE TECHNIQUES WHEN WAVELENGTH 2

Time (Years)	Distance(m)					
	0	20	40	60	80	100
1	1.2300	0.6412	0.2861	0.2861	0.6412	1.2300
5	3.9256	3.0263	2.6466	2.6466	3.0263	3.9256
10	6.4567	5.8539	5.5070	5.5070	5.8539	6.4567
15	9.7213	8.7855	8.4059	8.4059	8.7855	9.7213

TABLE XI
APPROXIMATED SHORELINE EVOLUTION ALONG 15 YEARS USING THE SAULYEV FINITE DIFFERENCE TECHNIQUES WHEN WAVELENGTH 2

Time (Years)	Distance (m)					
	0	20	40	60	80	100
1	1.2304	0.6416	0.2863	0.2860	0.6409	1.2296
5	3.9260	3.0264	2.6295	2.6466	3.0262	3.9255
10	6.4566	5.8537	5.5068	5.5071	5.8540	6.4568
15	9.7219	8.7857	8.4060	8.4058	8.7853	9.7212

TABLE XII
APPROXIMATED SHORELINE EVOLUTION ALONG 15 YEARS USING THE TRADITIONAL FORWARD TIME CENTERED SPACE TECHNIQUES WHEN WAVELENGTH 3

Time (Years)	Distance(m)					
	0	20	40	60	80	100
1	2.4426	1.0204	0.4643	0.4643	1.0204	2.4426
5	6.0495	4.8087	4.2833	4.2833	4.8087	6.0495
10	9.9512	9.0056	8.4521	8.4521	9.0056	9.9512
15	14.3340	13.0512	12.5716	12.5716	13.0512	14.3340

TABLE XIII
APPROXIMATED SHORELINE EVOLUTION ALONG 15 YEARS USING THE SAULYEV FINITE DIFFERENCE TECHNIQUES WHEN WAVELENGTH 3

Time (Years)	Distance(m)					
	0	20	40	60	80	100
1	2.4427	1.0205	0.4644	0.4641	1.0201	2.4423
5	6.0495	4.8082	4.2831	4.2833	4.8088	6.0495
10	9.9518	9.0062	8.4522	8.4521	9.0054	9.9509
15	14.3339	13.0507	12.5714	12.5715	13.0513	14.3341

TABLE XIV
APPROXIMATED SHORELINE EVOLUTION ALONG 15 YEARS USING THE TRADITIONAL FORWARD TIME CENTERED SPACE TECHNIQUES WHEN WAVELENGTH 4

Time (Years)	Distance(m)					
	0	20	40	60	80	100
1	1.2192	0.6492	0.2962	0.2962	0.6492	1.2192
5	2.5437	2.5297	2.2522	2.2522	2.5297	2.5437
10	5.5018	4.3970	4.1878	4.1878	4.3970	5.5018
15	5.8860	6.1114	5.9015	5.9015	6.1114	5.8860

TABLE XV
APPROXIMATED SHORELINE EVOLUTION ALONG 15 YEARS USING THE SAULYEV FINITE DIFFERENCE TECHNIQUES WHEN WAVELENGTH 4

Time (Years)	Distance (m)					
	0	20	40	60	80	100
1	1.2190	0.6492	0.2962	0.2961	0.6490	1.2189
5	2.5443	2.5302	2.2521	2.2522	2.5295	2.5434
10	5.5016	4.3967	4.1881	4.1879	4.3972	5.5022
15	5.8859	6.1116	5.9013	5.9015	6.1115	5.8859

TABLE XVI
APPROXIMATED SHORELINE EVOLUTION ALONG 15 YEARS USING THE TRADITIONAL FORWARD TIME CENTERED SPACE TECHNIQUES WHEN WAVELENGTH 5

Time (Years)	Distance(m)					
	0	20	40	60	80	100
1	1.1699	0.6231	0.2817	0.2817	0.6231	1.1699
5	2.2472	1.7718	1.5839	1.5839	1.7718	2.2472
10	2.5173	2.4222	2.3866	2.3866	2.4222	2.5173
15	3.4696	3.2305	3.0839	3.0839	3.2305	3.4696

TABLE XVII
APPROXIMATED SHORELINE EVOLUTION ALONG 15 YEARS USING THE SAULYEV FINITE DIFFERENCE TECHNIQUES WHEN WAVELENGTH 5

Time (Years)	Distance(m)					
	0	20	40	60	80	100
1	1.1701	0.6235	0.2819	0.2816	0.6226	1.1696
5	2.2477	1.7722	1.5840	1.5837	1.7713	2.2466
10	2.5165	2.4214	2.3861	2.3865	2.4226	2.5175
15	3.4704	3.2312	3.0841	3.0837	3.2299	3.4691

We will compare the five wavelengths with time durations of 5, 10, and 15 years, as illustrated in Fig. 24-27.

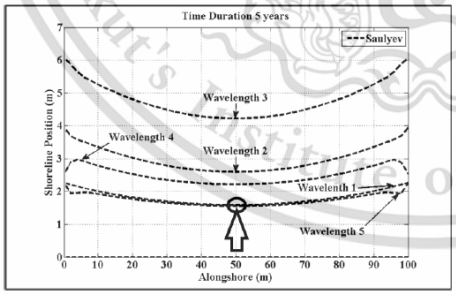

Fig. 24. Wavelength Comparisons in 5 years.

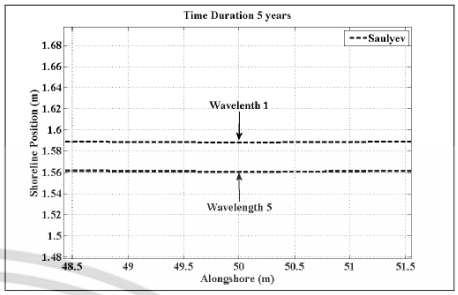

Fig. 25. Enlarge Between Wavelength 1 and Wavelength 5 at 50 m.

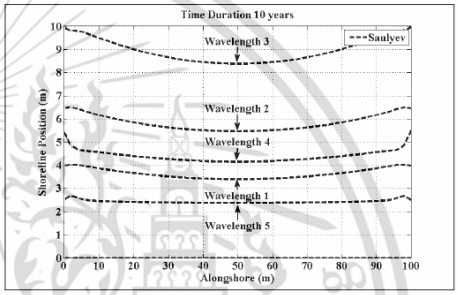

Fig. 26. Wavelength Comparisons in 10 years.

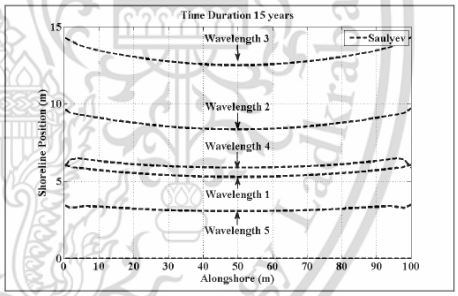

Fig. 27. Wavelength Comparisons in 15 years.

VI. Discussion

In this paper, we considered the averaged wave crest impact (α_0) as obtained by (29) for five case wavelengths as seen in Table 2-6. The long-shore transport rate (D) for each month as seen in Table 7.

We used the numerical method, the traditional forward time centered space techniques, and the Saulyev finite difference techniques to predict the shoreline evolution for five case wavelengths with time duration of 5, 10, and 15 years.

The approximated shoreline evolution for wavelength $0.5\sin(t+0.01x)$ with a time duration of 15 years is seen in Table 8, 9, and Fig. 19. The farthest distance from the shoreline evolution is 6.0537 m. The shortest distance from the shoreline evolution is 5.2833 m.

The approximated shoreline evolution for wavelength $0.5\sin(t+0.02x)$ with a time duration of 15 years is seen in Table 10, 11, and Fig. 20. The farthest distance from the shoreline evolution is 9.7219 m. The shortest distance from the shoreline evolution is 8.3579 m.

The approximated shoreline evolution for wavelength $0.5\sin(t+0.03x)$ with a time duration of 15 years is seen in Table 12, 13, and Fig. 21. The farthest distance from the shoreline evolution is 14.3339 m. The shortest distance from the shoreline evolution is 12.5092 m.

The approximated shoreline evolution for wavelength $0.5\sin(t+0.04x)$ with a time duration of 15 years is seen in Table 14, 15, and Fig. 22. The farthest distance from the shoreline evolution is 6.4928 m. The shortest distance from the shoreline evolution is 5.8776 m.

The approximated shoreline evolution for wavelength $0.5\sin(t+0.05x)$ with a time duration of 15 years is seen in Table 16, 17, and Fig. 23. The farthest distance from the shoreline evolution is 3.4704 m. The shortest distance from the shoreline evolution is 3.0672 m.

The approximated shoreline evolution for five case wavelengths with time durations of 5, 10, and 15 years is seen in Fig 24, 25, 26, and 27 respectively.

The approximated shoreline evolutions of both numerical approaches within five wavelengths of the considered shoreline are compatible.

VII. Conclusion

A more realistic shoreline evolution model was created in this research to adjust for the wavelength influence of breaking waves on groin construction. The initial condition setting approach and boundary conditions techniques, as well as various groin structural impacts, are discussed. Each year, the shoreline evolution is approximated using the conventional forward time centered space method and the unconditionally stable Saulyev finite differential methods. The estimated impacts of shoreline evolution were consistent with the wave crest impact model for five case wavelengths. As a result, the frequency of the wavelength influences the approximated shoreline evolution rate. In most cases, when the frequency of wavelength increases, the approximated shoreline evolution that obtains shoreline area also increases, but in some cases, when the frequency of wavelength increases, the approximated shoreline evolution has shoreline area obtained less. The approximated shoreline evolution is uncertain at different frequencies of wavelengths. The proposed modeling could be used to forecast the effectiveness of constructing a groin system on a nearby beach.

References

[1] H. Hanson, N. C. Kraus, and S. H. Blomgren, "Modern functional design of groin systems," Coastal Engineering, pp. 1327–1342, 1994.

[2] S. Krishna Prasad, K. P. Indulekha, and K. Balan, "Analysis of groyne placement on minimising river bank erosion," Procedia Technology, vol. 24, pp. 47–53, 2016.

[3] W. T. Bakker, "The dynamics of coast with a groin system," Proceeding of 11th Coastal Engineering Conference 1969, pp. 492–517.

[4] W. T. Bakker, and T. Edelman, "The coastline of river deltas," Proceeding of 9th Coastal Engineering Conference 1965, pp. 199–218.

[5] W. Grijimr, "Theoretical form of shoreline," Proceeding of 7th Coastal Engineering Conference 1961, pp. 197–202.

[6] W. Grijimr, "Theoretical form of shoreline," Proceeding of 9th Coastal Engineering Conference 1965, pp. 219–235.

[7] B. Le Mahute, and M. Soldate, "Mathematical Modeling of Shoreline Evolution," US Army Corps of Engineer Waterways Experiment Station, CERC, 1977.

[8] T. Waltonand, and T. Chiu, "A review of analytical technique to solve the sand transport equation and some simplified solution," Coastal Structure, pp. 809–837, 1979.

[9] H. Hanson, M. Larson, and N. C. Kraus, "Analytical Solution of the One-line Model for Shoreline Changel," US Army Corps of Engineer Waterways Experiment Station, CERC, 1987.

[10] US Army Corp of Engineers, "Shore Protection Manual," Coastal Engineering Research Centre, Washington, 1984.

[11] L. X. Hoan, "Some result of comparison between numerical and analytical solutions of the one-line model for shoreline change," Vietnam Journal of Mechanics., pp. 94–102, 2006.

[12] M. Mamat Subiyanto, M. F. Ahmad, and M. L. Husain, "Comparison of numerical method for forward and backward time centered space for long – term simulation of shoreline evolution," Applied Mathematical Sciences, vol. 7, pp. 5165–5173, 2013.

[13] N. Pochai, "Unconditional stable numerical techniques for a water-quality model in a non-uniform flow stream," Advances in Difference Equations, vol. 2017, Article ID 286, 13 pages, 2017.

[14] P. Samalerk, and N. Pochai, "Numerical Simulation of a One-Dimensional Water-Quality Model in a Stream Using a Saulyev Technique with Quadratic Interpolated Initial-Boundary Conditions," Abstract and Applied Analysis, vol. 2018, Article ID 1926519, 7 pages, 2018.

[15] Ben Wongsaijai, Kanyuta Poochinapan, and Thongchai Disyadej, "A Compact Finite Difference Method for Solving the General Rosenau-RLW Equation," IAENG International Journal of Applied Mathematics, vol. 44, no. 4, pp. 192-199, 2014.

[16] Shixiang Zhou, Fanwei Meng, Qinghua Feng, and Li Dong, "A Spatial Sixth Order Finite Difference Scheme for Time Fractional Sub-diffusion Equation with Variable Coefficient," IAENG International Journal of Applied Mathematics, vol. 47, no. 2, pp. 175-181, 2017.

[17] Kewalee Suebyat, and Nopparat Pochai, "A Numerical Simulation of a Three-dimensional Air Quality Model in an Area Under a Bangkok Sky Train Platform Using an Explicit Finite Difference Scheme," IAENG International Journal of Applied Mathematics, vol. 47, no. 4, pp. 471-476, 2017.

[18] Alia Khurram, and David W Kammler, "Numerical Generation of Images for the Gibbs Phenomenon Near a Corner in the Plane," IAENG International Journal of Applied Mathematics, vol. 44, no. 1, pp 15-22, 2014.

[19] Tata Sutardi, Linwei Wang, Manosh C. Paul, and Nader Karimi, "Numerical Simulation Approaches for Modelling a Single Coal Particle Combustion and Gasification," Engineering Letters, vol. 26, no. 2, pp. 257-266, 2018.

[20] Linna Li, Zhirou Wei, and Qiongdan Huang, "A Numerical Method for Solving Fractional Variational Problems by the Operational Matrix Based on Chelyshkov Polynomials," Engineering Letters, vol. 28, no. 2, pp. 486-491, 2020.

[21] Witsarut Kraychang, and Nopparat Pochai, "A Simple Numerical Model for Water Quality Assessment with Constant Absorption around Nok Phrao Island of Trang River," Engineering Letters, vol. 28, no. 3, pp. 912-922, 2020.

[22] Elvira Armenio, Francesca De Serio, Michele Mossa, and Antonio F. Petrillo, "Coastline evolution based on statistical analysis and modeling," Nat. Hazards Earth Syst. Sci., 19, pp. 1937–1953, 2019.

[23] C. Coelho, F. Celoso-Gomes, and R. Silva, "Shoreline coastal evolution model: two Portuguese case studies," Coastal Engineering, vol. 5, pp. 3430-3441, 2006.

[24] J. Guillen, M. J. F. Stive, and M. Capobianco, "Shoreline evolution of the holland coast on a decadal scale," Earth Surface Processes and Landforms, vol. 24, pp. 517-536, 1999.

[25] P. K. Mohanty, S. K. Patra, W. Bramha, B. Seth, U. Pradhan, B. Behera, P. Mishra, and U. S. Panda, "Impact of Groins on Beach Morphology: A Case Study near Gopalpur Port, East Coast of India," Journal of Coastal Research, vol. 28, pp. 132-142, 2012.

[26] Laura Lemke, J. K. Miller, A. Gorton, and E. Livermont, "EOF Analysis of Shoreline Changes Following an Alternative Beachfill within a Groin Field," Coastal Engineering Proceedings 2014, 12 pages, 2014.

[27] Le Xuan Roan, "Some results of comparison between numerical and analytic solutions of the one-line model for shoreline change," Vietnam Journal of Mechanics, VAST, vol. 28, pp. 94-102, 2006.

[28] Witsarut Kraychang and Nopparat Pochai, "Numerical Treatment to a Water-Quality Measurement Model in an Opened-Closed Reservoir," Thai Journal of Mathematics, vol. 13, pp. 775-788, 2015.
[29] A. R. Mitchell, "Computational Methods in Partial Differential Equations," John Wiley & Sons Ltd., London, 1969.
[30] Pidok Unyapoti and Nopparat Pochai, "A Shoreline Evolution Model with a Twin Groins Structure using Unconditionally Stable Explicit Finite Difference Techniques." Engineering Letters, vol. 29, no. 1, pp. 288-296, 2021.
[31] Pidok Unyapoti and Nopparat Pochai, "A One-Dimensional Mathematical Model of Long-Term Shoreline Evolution with Groin System using an Unconditionally Stable Explicit Finite Difference Method," International Journal of Simulation: Systems, Science and Technology, vol. 21, no.3, pp. 2.1-2.6, 2020.
[32] W. Kraychang, S. Meechowna, W. Welamas, and N. Pochai, "A Simple Mathematical Model of Water Quality Control for Recirculating Pond on A Shrimp Farm," Engineering Letters, vol 24, no 4, pp. 1470 – 1477, 2021.
[33] Pornpon Othata and Nopparat Pochai, "A Mathematical Model of Salinity Control in a River with an Effect of Internal Waves using Two Explicit Finite Difference Methods," Engineering Letters, vol 29, no 2, pp 689-696, 2021.
[34] Piyada Phosri and Nopparat Pochai, "A Couple Mathematical Models of the Water Quality Measurement in a Stream using Upwind Implicit Methods," IAENG International Journal of Applied Mathematics, Vol.51, No.1, pp. 237-249, 2021

N. Pochai is a researcher of Centre of Excellence in Mathematics, MHESI, Bangkok 10400, Thailand.

P. Unyapoti is an assistant researcher of Centre of Excellence in Mathematics, MHESI, Bangkok 10400, Thailand.

IAENG International Journal of Computer Science, 50:2, IJCS_50_2_01

A Combination of A Shoreline Evolution Model and A Wave Crest Model on T-Head Groin Structures With the Breaking Wave Effect

Pidok Unyapoti, Nopparat Pochai

Abstract—**Beach erosion is a naturally occurring phenomenon that occurs when the transfer of material away from the beach is not balanced by the deposit of new material on the shoreline. Beach erosion have always existed and have influenced the shoreline shape. This is a problem that contributes to the loss of shorelines. Structures invented to prevent beach erosion, such as seawalls, groins, and breakwaters. To avoid coastal erosion and sedimentation, a groin and a sea wall were constructed. Shoreline evolution analysis is being used to research the future topography of the beach. Beach erosion and beach deposition research requires a qualitative analysis of the model shoreline behavior with respect to the driving process. In this research, we focus on the effects of the T-head groin structure on shoreline evolution. The average wave crest impact is analyzed for eight sizes of T-head groin construction. An initial condition setting technique and boundary conditions techniques, as well as the structural impacts of the T-head groin, are discussed. Each year, the shoreline evolution is approximated using the traditional forward time centered space techniques and the unconditionally stable Saulyev finite differential techniques. The calculated impacts of shoreline evolution for eight different T-head groin sizes were consistent with the wave crest impact model.**

Index Terms— **shoreline evolution, T- head groin system, explicit finite method, wave crest impact, mathematical model**

I. Introduction

Beach erosion is a naturally occurring phenomenon by which local sea-level rise, strong wave action, and coastal flooding wear down or carry away rocks, soils, and sands along the beach. Beach erosion and accretion have always existed and have influenced the current shoreline's shape. In many countries, beach erosion is responsible for coastal property loss, including damage to structures and loss of land. This is a problem that contributes to the loss of shorelines.

Nowadays, various construction structures are being invented to prevent beach erosion, such as seawalls, groins, breakwaters, etc. In this paper, we focused on the groin structure in the shape of the T-head groin. They demonstrated a novel approach in [1] that combines citizen science with low-cost unmanned aerial vehicles to generate survey-grade morphological data that can be used to model sediment dynamics at event to annual scales. The high-energy wavedominated coast of Victoria in south-eastern Australia serves as a field laboratory for testing the reliability of our protocol and developing a set of indices for studying multi-scale erosional dynamics. In [2], they presented sediment transport and erosion-deposition patterns near a detached, low-crested breakwater protecting Carey Island's cohesive shore in Malaysia. Their study found that the conductivity of the breakwater structure is essential to reducing erosion issues on Carey Island's cohesive coasts and to the effectiveness of mangrove rehabilitation initiatives in the area. In [3], they predicted the most likely total water level scenarios that result in overtopping at Santos Bay beaches and examined overtopping events in 2016. The prediction shows that the wider and flatter profiles in the western portion of Santos and Itararé provide greater protection from storm events, while the steeper eastern stretch of Santos Beach is more vulnerable to overtopping events. Their research focuses on beaches in Santos and So Vicente (So Paulo, Brazil). A seawall surrounds the entire 7 kilometer stretch of shoreline. In [4], they presented a study on the effect of groin application on shoreline erosion. Bathymetry and topography data from the north beach of Balongan, West Java, were used in the procedure. GENESIS software was used to model the coastline change caused by groin installation. They concluded that in the research area of west Java's north beach, an I-groin with a length of 70 meters and a T-head groin with a length of 60 meters efficiently overcomes erosion and advances the shoreline by 6,3 meters.

Many authors have developed one-line theory, and several contributors to the analytical solution of the shoreline evolution include [5], [6], [7], [8], [9], [10], and [11]. Analytical solutions cannot be expected to provide quantitatively precise solutions to situations with complicated boundary conditions and wave inputs. In the case of complicated boundary conditions and wave inputs, a numerical model of shoreline evolution would be more fitting than analytical solutions. A numerical model of shoreline evolution would be more fitting in the actual case.

In [12], [13], they have examined and presented two numerical schemes of shoreline evolution for simplified

Manuscript received September 26, 2022; revised December 19, 2022.
This paper is supported by Centre of Excellence in Mathematics, Ministry of Higher Education, Science, Research and Innovation, Bangkok, Thailand.

N. Pochai is an Assistant Professor of Department of Mathematics, Faculty of Science, King Mongkut's Institute of Technology Ladkrabang, Bangkok, 10520, Thailand (corresponding author to provide phone: 662-329-8400; fax: 662-329-8400; e-mail: nop_math@yahoo.com).
P. Unyapoti is a PhD. candidate of Mathematics Department, Faculty of Science, King Mongkut's Institute of Technology Ladkrabang, Bangkok, 10520, Thailand (e-mail: pidokunyapoti@gmail.com).

configuration beach. In [14], [15], [16], [17], [18], they have used the conditionally stable explicit finite difference methods to approximate their model solutions. In [19], [20], [21], they have used the numerical methods to approximate their model solution.

In [22], they proposed the Equilibrium energy function (EEF) analytical method and the shoreline evolution model. Testing of the proposed model at Nova Icaria reveals the same capabilities with only one measurement parameter as state-of-the-art models with more than 4 free parameters. In [23], a basic coastline profile model behavioral template was proposed to be calibrated and tested against a 6-year coastline location time series derived from a shoreline imaging system on the Gold Coast, Australia. Monitoring the model on unknown data shows that it can reproduce the dominant different seasons coastline transition observed at this site and up to 77% of the degraded coastline variability.

In this paper, we introduce a one-dimensional shoreline evolution model, wave crest impact model to obtain the breaking wave crest, the initial condition, and boundary conditions setting when T-head groins structure is added, eight lengths of considered T-head groins. The model solution will be approximated using finite difference techniques. We are focused on predicting the efficiency of T-head groin structure on shoreline evolution.

II. Governing Equation

A. Shoreline evolution model

In a one-dimensional shoreline evolution model, all of the bottom outlines should become parallel while the beach form remains constant and moves toward the land and the sea. Consequently, as the beach reduces and increases, so should be doing the design and volume of the beach level. Sand is moved along the shore on a profile between two clearly specified limit heights, which is the model's core idea. Where there is a difference between the rate of longshore sand transfer on the side of the segment and the associated sand condition, the adjustment in volume is affected. The laws of mass conservation must regularly be modified for the system [24]:

$$\frac{\partial y}{\partial t} = D\frac{\partial^2 y}{\partial x^2}, \tag{1}$$

for all $(x,t) \in (L,T)$, where $D = \dfrac{2Q_0}{D_B + D_C}$.

where x is the alongshore coordinate (m), y is the shoreline positions (m) and perpendicular to the x-axis, t is time (day), Q_0 is the long-shore sand transport rate amplitude (m^3/day), D_B is the average berm height (m) and D_C is the average closure depth (m).

B. Shoreline evolution parameters

The physical parameters of the shoreline evolution model are illustrated in Fig. 1-2. which are listed below.

α_0 is the angle between breaking wave crests impact angle and x-axis.

Q_0 is the long-shore sand transport rate amplitude.

D_B is the average berm height.

D_C is the average closure depth.

L is the length of alongshore.

T is the Time of simulation.

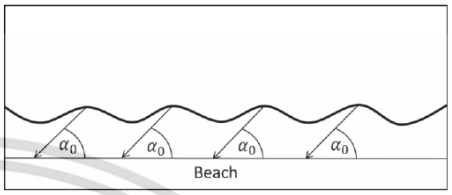

Fig. 1 Breaking wave crests impact angle when the beach is parallel to the x-axis

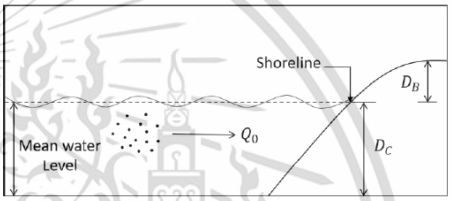

Fig. 2. Shoreline evolution parameters

C. The initial and boundary conditions for the shoreline evolution model

We assumed the initial beach to be parallel to the x-axis.

Assuming that, the angle between breaking wave crests impact angle and the shoreline is α_0. It follows that the sand transport rate along shoreline is consistent. The T-head groin is added on both side at $x=0$ and $x=L$ are illustrated in Fig. 3. Under this assumption, the initial condition becomes

$$y(x,t) = 0, \quad \text{at} \quad t = 0, \tag{2}$$

boundary conditions are also assumed by,

$$\frac{\partial y(x,t)}{\partial x} = -\tan(\alpha_0) \quad \text{at} \quad x = 0, \tag{3}$$

and

$$\frac{\partial y(x,t)}{\partial x} = -\tan(-\alpha_0) \quad \text{at} \quad x = L, \tag{4}$$

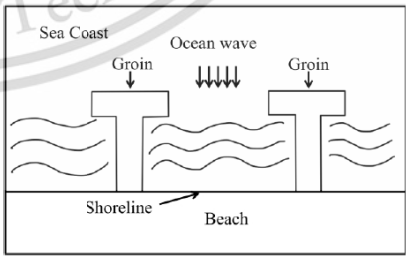

Fig. 3. Initial shoreline with configuration T-head groins.

D. Wave crest impact model

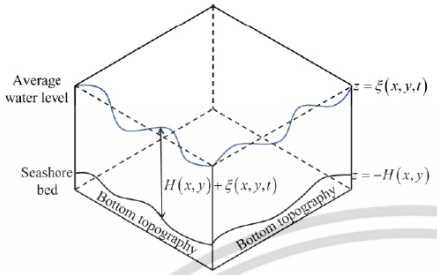

Fig. 4. Water elevation and bottom topography.

To achieve the wave crest impact in the shoreline evolution model, the hydrodynamic model is introduced [25].

A system of shallow water equations that takes into account momentum and mass conservation can be used to determine the two-dimensionally unstable water flows into and out of the coastline. The equations for this method should be derived from the depth-averaged Navier-Stokes equations in the vertical direction, omitting out the variables for the effects of friction, surface wind, Coriolis factor, and shear stress as well as the momentum diffusion caused by vibration. The equation of continuity is then expressed as follows:

$$\frac{\partial h}{\partial t}+\frac{\partial(uh)}{\partial x}+\frac{\partial(vh)}{\partial y}=0, \tag{5}$$

and the momentum equations are expressed as below:

$$\frac{\partial(uh)}{\partial t}+\frac{\partial\left(u^2h+\frac{1}{2}gh^2\right)}{\partial x}+\frac{\partial(uvh)}{\partial y}=0, \tag{6}$$

$$\frac{\partial(uh)}{\partial t}+\frac{\partial(uvh)}{\partial x}+\frac{\partial\left(v^2h+\frac{1}{2}gh^2\right)}{\partial y}=0, \tag{7}$$

where

$h(x,y,t)$ is the estimated depth from the average water surface to the seashore bed (m) $h=H+\xi$,

$\xi(x,y,t)$ is the elevation of the water surface above the average seashore water level (m),

$H(x,y)$ is the seashore's interpolated bottom topography function (m),

$u(x,y,t)$ is the velocity in the direction of x (m/s),

$v(x,y,t)$ is the velocity in the direction of y (m/s),

g is a gravity constant $(9.8\ m/s^2)$.

Such time (t), and two space coordinates, x and y are the independent variables. Likewise, the conserved quantities are mass, which is proportional to h, and momentum, which is proportional to (uh) and (vh). As taken with respect to the same term, the partial derivatives are grouped into vectors $(\partial x,\partial y,\partial t)$ and then rewritten as a partial differential hyperbolic equation as follows:

$$U=\begin{pmatrix}h\\uh\\vh\end{pmatrix},F(U)=\begin{pmatrix}uh\\u^2h+\frac{1}{2}gh^2\\uvh\end{pmatrix}, \tag{8}$$

$$G(U)=\begin{pmatrix}vh\\uvh\\v^2h+\frac{1}{2}gh^2\end{pmatrix}, \tag{9}$$

the hyperbolic PDE:

$$\frac{\partial U}{\partial t}+\frac{\partial F(U)}{\partial x}+\frac{\partial G(U)}{\partial y}=0. \tag{10}$$

E. The initial and boundary condition for wave crest impact model

The initial condition of the shoreline was as follows: the x and y velocity components, as well as the water elevation, were all zero: $u=0,v=0$ and $\xi=0$.

Assume that the T-head groin is not a perfect water barrier because of its rock composition, which has large gaps. Under this assumption, the boundary condition was as follows: *(i)* $u=0,\frac{\partial v}{\partial y}=0,\xi=f(x,y,t)$ for wave coming, *(ii)* $\frac{\partial u}{\partial x}=0,\mathrm{v}=0,\frac{\partial\xi}{\partial x}=0$ for left and right boundary, *(iii)* $u=0,\frac{\partial v}{\partial y}=0,\frac{\partial\xi}{\partial y}=0$ for along the beach, *(iv)* $u=0,\frac{\partial v}{\partial y}=0,\frac{\partial\xi}{\partial y}=0$ for top T-head groin structure, *(v)* $u=0,\frac{\partial v}{\partial y}=0,\frac{\partial\xi}{\partial y}=0$ for bottom T-head groin structure, and *(vi)* $\frac{\partial u}{\partial x}=0,\mathrm{v}=0,\frac{\partial\xi}{\partial x}=0$ for left and right T-head groin structure. The boundary conditions are illustrated in Fig. 5-7.

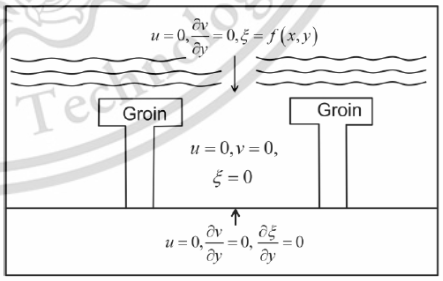

Fig. 5. Initial and boundary condition.

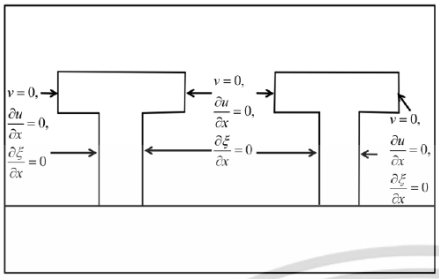

Fig. 6. Initial and boundary condition for T-head groin structure (1).

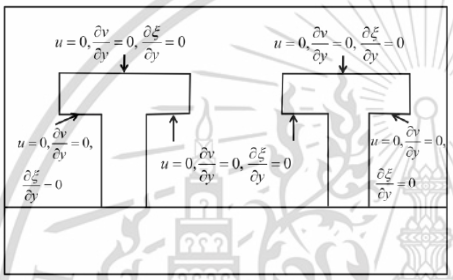

Fig. 7. Initial and boundary condition for T-head groin structure (2).

III. Numerical Techniques

A. Grid Spacing

We are discretizing (1) by splitting the interval $[0,L]$ into I subintervals such as $I\Delta x = L$ and the interval $[0,T]$ into N subintervals such as $N\Delta t = T$. Then we approximate $y(x_i,t_n)$ by y_i^n, at the points $x_i = i\Delta x$ and $t_n = n\Delta t$, where $0 \le i \le I$ and $0 \le n \le N$ are positive integers of I and N.

B. Traditional forward time centered space techniques

The forward time centered space techniques will also be used. We can obtain that the finite difference approximation is [26],

$$y \cong y_i^n, \tag{11}$$

$$\frac{\partial y}{\partial t} \cong \frac{y_i^{n+1} - y_i^n}{\Delta t}, \tag{12}$$

$$\frac{\partial y}{\partial x} \cong \frac{y_{i+1}^n - y_{i-1}^n}{2\Delta x}, \tag{13}$$

$$\frac{\partial^2 y}{\partial x^2} \cong \frac{y_{i+1}^n - 2y_i^n + y_{i-1}^n}{(\Delta x)^2}, \tag{14}$$

where $A = \dfrac{D\Delta t}{(\Delta x)^2}$.

Substituting (11) – (14), in (1), we are obtaining,

$$\frac{y_i^{n+1} - y_i^n}{\Delta t} = D\left(\frac{y_{i+1}^n - 2y_i^n + y_{i-1}^n}{(\Delta x)^2}\right), \tag{15}$$

for $1 \le i \le I-1$ and $0 \le n \le N-1$. (15), can be written in an explicit form of finite difference as follows,

$$y_i^{n+1} = Ay_{i+1}^n + (1-2A)y_i^n + Ay_{i-1}^n, \tag{16}$$

for $1 \le i \le I-1$ and $0 \le n \le N-1$.

C. An unconditionally Saulyev finite difference techniques

The Saulyev finite difference techniques will also be used. We can obtain that the finite difference approximation is

$$y \cong y_i^n, \tag{17}$$

$$\frac{\partial y}{\partial t} \cong \frac{y_i^{n+1} - y_i^n}{\Delta t}, \tag{18}$$

$$\frac{\partial^2 y}{\partial x^2} \cong \frac{y_{i+1}^n - y_i^n - y_i^{n+1} + y_{i-1}^{n+1}}{(\Delta x)^2}, \tag{19}$$

where $A = \dfrac{D\Delta t}{(\Delta x)^2}$.

Substituting (17) – (19), in (1), we are obtaining,

$$\frac{y_i^{n+1} - y_i^n}{\Delta t} = D\left(\frac{y_{i+1}^n - y_i^n - y_i^{n+1} + y_{i-1}^{n+1}}{(\Delta x)^2}\right), \tag{20}$$

for $1 \le i \le I-1$ and $0 \le n \le N-1$. (20), can be written in an explicit form of finite difference as follows,

$$y_i^{n+1} = \frac{1}{(1+A)}\left(Ay_{i+1}^n + (1-A)y_i^n + Ay_{i-1}^{n+1}\right), \tag{21}$$

for $1 \le i \le I-1$ and $0 \le n \le N-1$.

D. Numerical method for the wave crest impact model

The finite difference technique is

$$U_{i,j}^{n+1} = U_{i,j}^n - \frac{\Delta t}{\Delta x}\left(F_{i+\frac{1}{2},j}^{n+\frac{1}{2}} - F_{i-\frac{1}{2},j}^{n+\frac{1}{2}}\right) - \frac{\Delta t}{\Delta y}\left(G_{i,j+\frac{1}{2}}^{n+\frac{1}{2}} - G_{i,j-\frac{1}{2}}^{n+\frac{1}{2}}\right). \tag{22}$$

E. The averaged wave crest impact

We can determine that the wave crest impact is

$$\alpha(x_i, y_j, t) = \tan^{-1}\left(\frac{v(x_i, y_j, t)}{u(x_i, y_j, t)}\right), \tag{23}$$

We assume that the averaged wave crest impact is assumed by

$$\alpha_0(t) = \frac{\sum_{i=1}^{N_p} \alpha(x_i, 0, t)}{N_p}, \tag{24}$$

where N_p is several sample points along the shoreline for wave crest impact.

F. The application of finite difference techniques to the left and right boundary conditions

The forward time centered space techniques will also be used. We can obtain that the finite difference approximation

is,

$$y \cong y_i^n, \tag{25}$$

$$\frac{\partial y}{\partial t} \cong \frac{y_i^{n+1} - y_i^n}{\Delta t}, \tag{26}$$

$$\frac{\partial y}{\partial x} \cong \frac{y_{i+1}^n - y_{i-1}^n}{2\Delta x}, \tag{27}$$

where $A = \frac{D\Delta t}{(\Delta x)^2}$.

Substituting (25) - (27), in (1), we are obtaining,

$$\frac{y_i^{n+1} - y_i^n}{\Delta t} = D\left(\frac{y_{i+1}^n - 2y_i^n + y_{i-1}^n}{(\Delta x)^2}\right), \tag{28}$$

We approximated the substitution of the uncertain value of the left and right boundaries by using the center difference with the specified left and right boundary conditions.

For the left boundary i = 0, we are obtaining,

$$y_{-1}^n = y_1^n - 2(\Delta x)(-\tan(\alpha_0)), \tag{29}$$

substituting (29), in (28), we are obtaining,

$$y_i^{n+1} = (1-2A)y_i^n + 2Ay_{i+1}^n - 2A(\Delta x)(-\tan(\alpha_0)), \tag{30}$$

For the right boundary i = I, we are obtaining,

$$y_{I+1}^n = y_{M-1}^n + 2(\Delta x)(-\tan(-\alpha_0)), \tag{31}$$

substituting (31), in (28), we are obtaining,

$$y_i^{n+1} = 2Ay_{i-1}^n + (1-2A)y_i^n + 2A(\Delta x)(-\tan(-\alpha_0)), \tag{32}$$

(30), and (32), could be used to approximate the values y_i^n of the solution domain grid points.

IV. Groin Setting Techniques

We will consider eight lengths of considered T-head groin is 16, 18, 20, 22, 24, 26, 28, and 30 m. The consideration alongshore is illustrated in Fig 8.

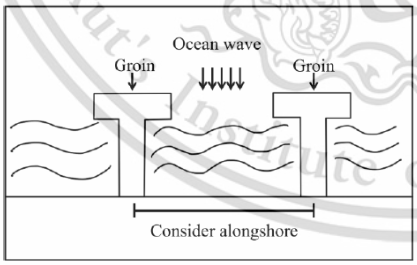

Fig. 8. Consider alongshore.

For eight lengths of the T-head groin that are being taken into consideration, the approximate wave crest impact model solution will be approximated using finite difference methods (22) are illustrated in Fig.9-16.

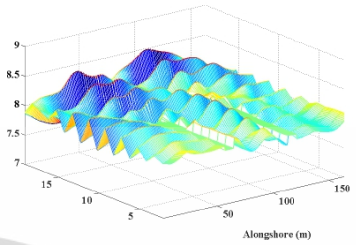

Fig. 9. Wave crest impact in 9 years when T-head groin 16 m.

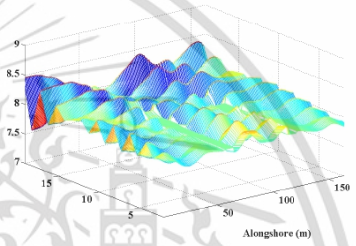

Fig. 10. Wave crest impact in 11 years when T-head groin 18 m.

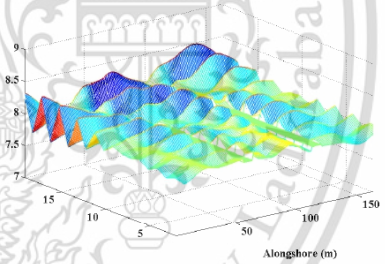

Fig. 11. Wave crest impact in 15 years when T-head groin 20 m.

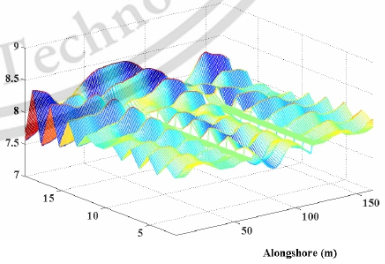

Fig. 12. Wave crest impact in 13 years when T-head groin 22 m.

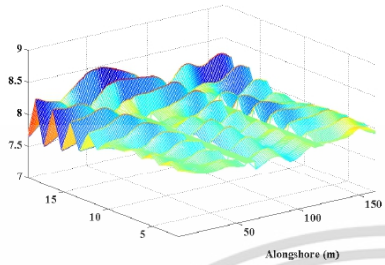

Fig. 13. Wave crest impact in 20 years when T-head groin 24 m.

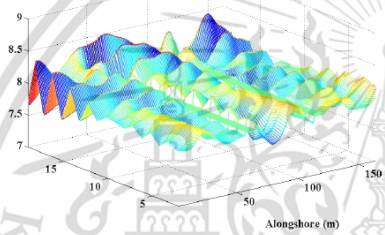

Fig. 14. Wave crest impact in 20 years when T-head groin 26 m.

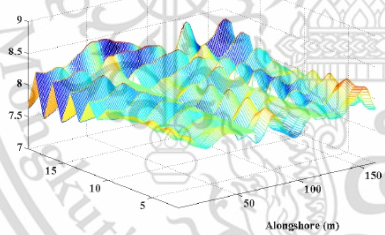

Fig. 15. Wave crest impact in 20 years when T-head groin 28 m.

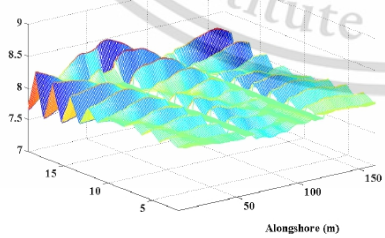

Fig. 16. Wave crest impact in 20 years when T-head groin 30 m.

Table 1-8 shows the averaged wave crest impact (α_0) obtained by (24) for eight lengths of the considered T-head groin.

TABLE I
THE AVERAGED WAVE CREST IMPACT 9 YEARS WHEN T-HEAD GROIN SIZE 16 M

Time (Years)	Minute					
	0-15	15-30	30-45	45-60	60-75	75-90
1	0.2635	0.2054	0.2100	0.2145	0.2189	0.2232
5	0.2645	0.2624	0.2604	0.2584	0.2564	0.2543
9	0.0264	0.0223	0.0181	0.0138	0.0093	0.0046

Time (Years)	Minute					
	…	1365-1380	1380-1395	1395-1410	1410-1425	1425-1440
1	…	-0.6192	-0.5621	-0.5047	-0.5098	-0.3890
5	…	0.0661	0.0633	0.0604	0.0575	0.0545
9	…	0.3304	0.3267	0.3859	0.3823	0.3786

TABLE II
THE AVERAGED WAVE CREST IMPACT 11 YEARS WHEN T-HEAD GROIN SIZE 18 M

Time (Years)	Minute					
	0-15	15-30	30-45	45-60	60-75	75-90
1	-0.0830	-0.0677	-0.0526	-0.1004	-0.0856	-0.0708
5	0.1572	0.1530	0.1488	0.1446	0.1404	0.1361
10	-0.1413	-0.1425	-0.2584	-0.0550	0.0099	0.1341
11	-0.0119	-0.0632	-0.0557	-0.0462	-0.0994	-0.0896

Time (Years)	Minute					
	…	1365-1380	1380-1395	1395-1410	1410-1425	1425-1440
1	…	-0.4803	-0.4885	-0.4339	-0.3791	-0.3242
5	…	0.0504	0.0493	0.0483	0.0472	0.0461
10	…	0.3557	0.3561	0.3564	0.3568	0.3572
11	…	-0.4077	-0.4091	-0.4107	-0.4123	-0.4769

TABLE III
THE AVERAGED WAVE CREST IMPACT 15 YEARS WHEN T-HEAD GROIN SIZE 20 M

Time (Years)	Minute					
	0-15	15-30	30-45	45-60	60-75	75-90
1	0.3146	0.3102	0.3052	0.2990	0.2906	0.3429
5	0.3369	0.3351	0.3333	0.3311	0.3284	0.3255
10	0.1009	0.1625	0.1610	0.1594	0.1577	0.1559
15	-0.4382	-0.3815	-0.3875	-0.3306	-0.2735	-0.2165

Time (Years)	Minute					
	…	1365-1380	1380-1395	1395-1410	1410-1425	1425-1440
1	…	-0.2437	-0.1238	-0.1295	-0.0096	-0.0154
5	…	0.1439	0.1422	0.1405	0.1388	0.1370
10	…	0.0145	0.0125	0.0104	0.0084	0.0062
15	…	0.2597	0.2581	0.2566	0.2551	0.2536

TABLE IV
THE AVERAGED WAVE CREST IMPACT 13 YEARS WHEN T-HEAD GROIN 22 M

Time (Years)	Minute					
	0-15	15-30	30-45	45-60	60-75	75-90
1	-0.2305	-0.1621	-0.1569	-0.1521	-0.1476	-0.1436
5	0.1447	0.1365	0.1287	0.1844	0.1782	0.1736
10	-0.0869	0.0900	0.1422	0.2579	0.3114	0.3654
13	0.1755	0.1749	0.1741	0.1733	0.1723	0.2340

Time (Years)	Minute					
	…	1365-1380	1380-1395	1395-1410	1410-1425	1425-1440
1	…	-0.3895	-0.3405	-0.3536	-0.3033	-0.2524
5	…	0.0922	0.0925	0.0928	0.0931	0.0934
10	…	0.3630	0.3630	0.3631	0.3631	0.3632
13	…	0.4394	0.4358	0.4324	0.4291	0.4260

TABLE V
THE AVERAGED WAVE CREST IMPACT 20 YEARS WHEN T-HEAD GROIN SIZE 24 M

Time (Years)	Minute					
	0-15	15-30	30-45	45-60	60-75	75-90
1	0.2364	0.2312	0.2260	0.2837	0.2785	0.2734
5	0.6124	0.6008	0.5904	0.5802	0.5703	0.5607
10	-0.3096	-0.3150	-0.2575	-0.2628	-0.2680	-0.1474
15	0.3091	0.2975	0.3488	0.4002	0.3888	0.4403
20	-0.3199	-0.3810	-0.3794	-0.3778	-0.3763	-0.4377

Time (Years)	Minute					
	…	1365-1380	1380-1395	1395-1410	1410-1425	1425-1440
1	…	0.0385	0.0926	0.1468	0.1381	0.1293
5	…	0.2496	0.2483	0.2470	0.2458	0.2445
10	…	-0.3180	-0.3202	-0.3224	-0.3246	-0.3268
15	…	0.3869	0.3849	0.3829	0.3809	0.3790
20	…	-0.2951	-0.2964	-0.2977	-0.2991	-0.3004

TABLE VI
THE AVERAGED WAVE CREST IMPACT 20 YEARS WHEN T-HEAD GROIN SIZE 26 M

Time (Years)	Minute					
	0-15	15-30	30-45	45-60	60-75	75-90
1	-0.2234	-0.1599	-0.2219	-0.2211	-0.2201	-0.2190
5	-0.1300	-0.1251	-0.1206	-0.1163	-0.1122	-0.0454
10	-0.2985	-0.2936	-0.2888	-0.2842	-0.2797	-0.2753
15	0.6864	0.7542	0.7602	0.7676	0.7130	0.5957
20	0.3344	0.3335	0.3324	0.3311	0.3926	0.3912

Time (Years)	Minute					
	…	1365-1380	1380-1395	1395-1410	1410-1425	1425-1440
1	…	0.3617	0.2390	0.2425	0.1210	0.1255
5	…	0.1702	0.1719	0.1736	0.1754	0.1771
10	…	-0.0298	-0.0289	-0.0280	-0.0272	-0.0263
15	…	0.1829	0.1846	0.1862	0.1879	0.1896
20	…	-0.1046	-0.1028	-0.1010	-0.0993	-0.0977

TABLE VII
THE AVERAGED WAVE CREST IMPACT 20 YEARS WHEN T-HEAD GROIN SIZE 28 M

Time (Years)	Minute					
	0-15	15-30	30-45	45-60	60-75	75-90
1	0.2891	0.3499	0.3478	0.3457	0.3436	0.3415
5	0.3573	0.4161	0.4121	0.4080	0.4040	0.4000
10	-0.4099	-0.4122	-0.4145	-0.3541	-0.3567	-0.2965
15	0.2809	0.2764	0.2720	0.3304	0.3260	0.3216
20	-0.5731	-0.5733	-0.5735	-0.5738	-0.5742	-0.6375

Time (Years)	Minute					
	…	1365-1380	1380-1395	1395-1410	1410-1425	1425-1440
1	…	-0.0372	-0.0400	-0.0428	0.0173	0.0146
5	…	0.2837	0.2812	0.2788	0.2764	0.2740
10	…	-0.2584	-0.2628	-0.2672	-0.2716	-0.2760
15	…	0.4681	0.4643	0.4606	0.4570	0.4534
20	…	-0.1795	-0.1837	-0.1879	-0.1921	-0.1963

TABLE VIII
THE AVERAGED WAVE CREST IMPACT 20 YEARS WHEN T-HEAD GROIN SIZE 30 M

Time (Years)	Minute					
	0-15	15-30	30-45	45-60	60-75	75-90
1	0.0787	0.0682	0.1205	0.1100	0.0995	0.1519
5	0.4851	0.4890	0.4296	0.4322	0.4338	0.4341
10	-0.3801	-0.3713	-0.3625	-0.4168	-0.4086	-0.4013
15	0.4475	0.5016	0.4929	0.4842	0.5385	0.5928
20	-0.1901	-0.1795	-0.1690	-0.2213	-0.2110	-0.2007

Time (Years)	Minute					
	…	1365-1380	1380-1395	1395-1410	1410-1425	1425-1440
1	…	0.5101	0.4583	0.4694	0.4804	0.4283
5	…	0.4199	0.4210	0.4222	0.4235	0.4248
10	…	-0.4248	-0.4256	-0.4266	-0.4276	-0.4286
15	…	0.4115	0.4115	0.4114	0.4115	0.4116
20	…	-0.4275	-0.4266	-0.4258	-0.4251	-0.4244

V. Numerical Experiment

In this section, the numerical results of the various beach scenarios of T-head groin structure are considered, and the solution to the idealized problem is introduced. Assuming, during the experiments, that the length of the shoreline (L) under consideration is 100 m and the averaged wave crest impact (α_0) for eight T-head groin sizes. Table 1-8 shows the averaged wave crest impact of eight T-head groin structure sizes. Table 9 shows the long-shore transport rate (D) [27]. The simulation setting is illustrated in Fig. 17.

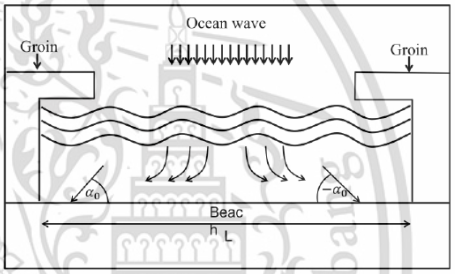

Fig. 17. Initial shoreline.

TABLE IX
THE LONG-SHORE TRANSPORT RATE

Month	$D\ (m/day)$
Jan	79.4659
Feb	62.1307
Mar	5.7869
Apr	61.4403
May	5.6420
Jun	5.4716
Jul	73.0227
Aug	83.071
Sep	121.7301
Oct	372.017
Nov	96.5710
Dec	101.1233

We are going to employ the traditional forward time centered space techniques (FTCS) (16), and the Saulyev finite difference techniques (21), to approximate the shoreline evolution model solution are illustrated in Fig. 18-25. Table 10-25 shows the calculated results.

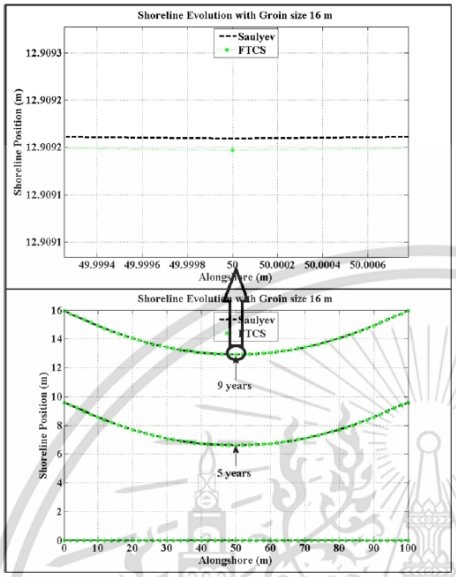

Fig. 18. Shoreline evolution in 9 years when T-head Groin size 16 m.

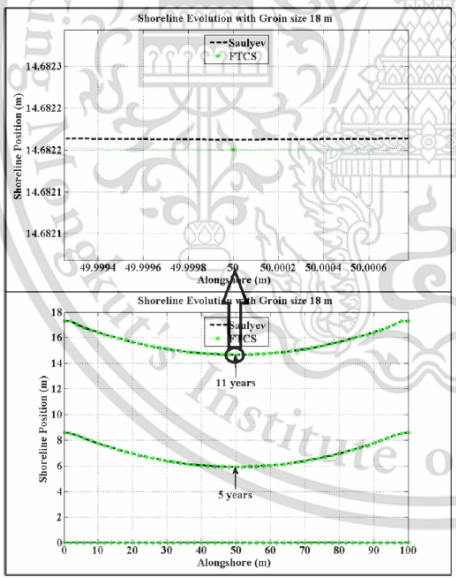

Fig. 19. Shoreline evolution in 11 years when T-head Groin size 18 m.

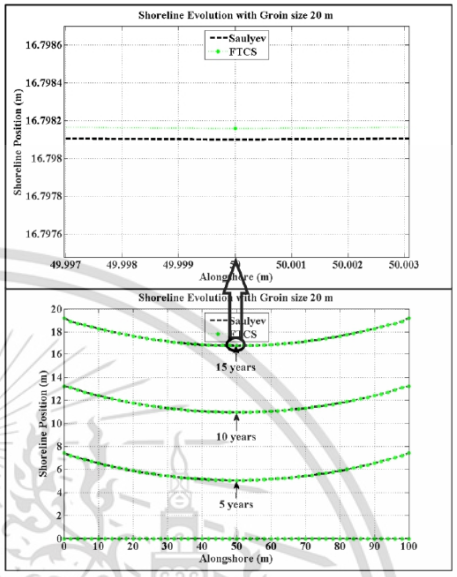

Fig. 20. Shoreline evolution in 15 years when T-head Groin size 20 m.

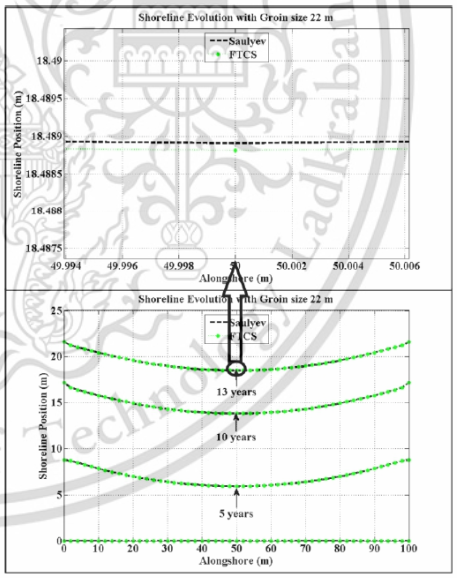

Fig. 21. Shoreline evolution in 13 years when T-head Groin size 22 m.

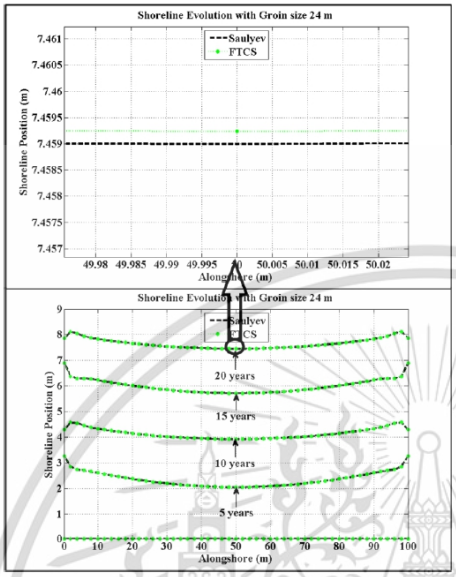

Fig. 22. Shoreline evolution in 20 years when T-head Groin size 24 m.

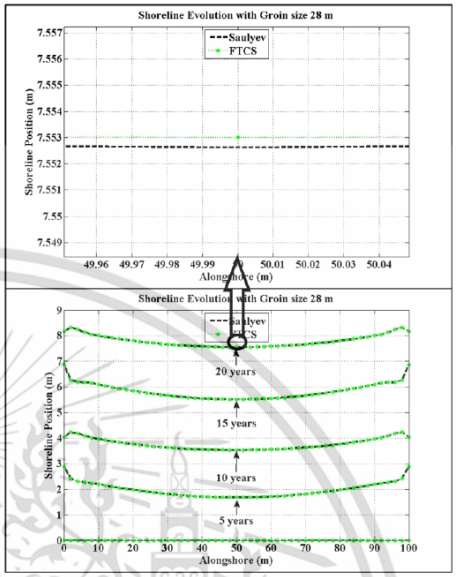

Fig. 24. Shoreline evolution in 20 years when T-head Groin size 28 m.

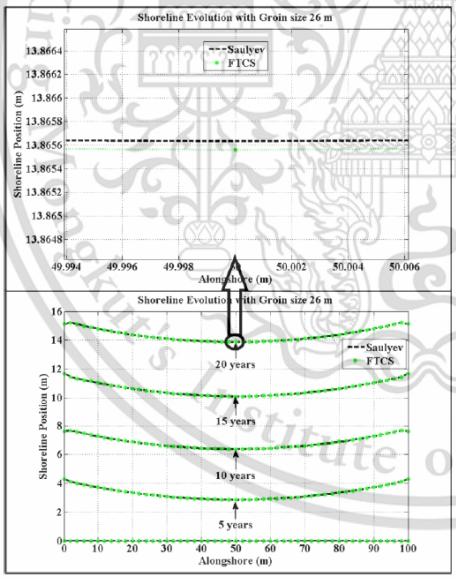

Fig. 23. Shoreline evolution in 20 years when T-head Groin size 26 m.

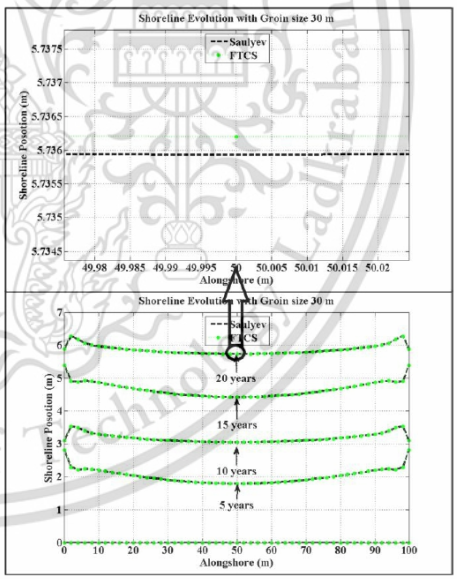

Fig. 25. Shoreline evolution in 20 years when T-head Groin size 30 m.

TABLE X
APPROXIMATED SHORELINE EVOLUTION ALONG 9 YEARS USING THE TRADITIONAL FORWARD TIME CENTERED SPACE TECHNIQUES WHEN T-HEAD GROIN SIZE 16 M

Time (Years)	Distance(m)					
	0	20	40	60	80	100
1	2.8710	1.4100	0.6302	0.6302	1.4100	2.8710
5	9.5859	7.7058	6.7258	6.7258	7.7058	9.5859
9	15.9610	14.0431	13.0345	13.0345	14.0431	15.9610

TABLE XI
APPROXIMATED SHORELINE EVOLUTION ALONG 9 YEARS USING THE SAULYEV FINITE DIFFERENCE TECHNIQUES WHEN T-HEAD GROIN SIZE 16 M

Time (Years)	Distance (m)					
	0	20	40	60	80	100
1	2.8718	1.4107	0.6305	0.6300	1.4094	2.8701
5	9.5859	7.7059	6.7259	6.7260	7.7059	9.5860
9	15.9615	14.0435	13.0346	13.0345	14.0429	15.9609

TABLE XII
APPROXIMATED SHORELINE EVOLUTION ALONG 11 YEARS USING THE TRADITIONAL FORWARD TIME CENTERED SPACE TECHNIQUES WHEN T-HEAD GROIN SIZE 18 M

Time (Years)	Distance(m)					
	0	20	40	60	80	100
1	2.4433	1.2654	0.5617	0.5617	1.2654	2.4433
5	8.5988	6.9462	6.0354	6.0354	6.9462	8.5988
10	16.3731	14.2624	13.3619	13.3619	14.2624	16.3731
11	17.2722	15.6527	14.7912	14.7912	15.6527	17.2722

TABLE XIII
APPROXIMATED SHORELINE EVOLUTION ALONG 11 YEARS USING THE SAULYEV FINITE DIFFERENCE TECHNIQUES WHEN T-HEAD GROIN SIZE 18 M

Time (Years)	Distance (m)					
	0	20	40	60	80	100
1	2.4436	1.2659	0.5619	0.5615	1.2649	2.4427
5	8.5988	6.9463	6.0353	6.0355	6.9464	8.5989
10	16.3738	14.2626	13.3621	13.3618	14.2622	16.3731
11	17.2720	15.6525	14.7911	14.7912	15.653	17.2724

TABLE XIV
APPROXIMATED SHORELINE EVOLUTION ALONG 15 YEARS USING THE TRADITIONAL FORWARD TIME CENTERED SPACE TECHNIQUES WHEN T-HEAD GROIN SIZE 20 M

Time (Years)	Distance(m)					
	0	20	40	60	80	100
1	2.2494	1.1606	0.5209	0.5209	1.1606	2.2494
5	7.4274	5.8894	5.1479	5.1479	5.8894	7.4274
10	13.2267	11.7631	11.0379	11.0379	11.7631	13.2267
15	19.2122	17.6409	16.8916	16.8916	17.6409	19.2122

TABLE XV
APPROXIMATED SHORELINE EVOLUTION ALONG 15 YEARS USING THE SAULYEV FINITE DIFFERENCE TECHNIQUES WHEN T-HEAD GROIN SIZE 20 M

Time (Years)	Distance(m)					
	0	20	40	60	80	100
1	2.2499	1.1610	0.5211	0.5207	1.1601	2.2488
5	7.4275	5.8894	5.1479	5.1479	5.8894	7.4273
10	13.2269	11.7631	11.0378	11.0379	11.7632	13.2268
15	19.2123	17.641	16.8916	16.8915	17.6408	19.2122

TABLE XVI
APPROXIMATED SHORELINE EVOLUTION ALONG 13 YEARS USING THE TRADITIONAL FORWARD TIME CENTERED SPACE TECHNIQUES WHEN T-HEAD GROIN SIZE 22 M

Time (Years)	Distance(m)					
	0	20	40	60	80	100
1	2.4577	1.1767	0.5171	0.5171	1.1767	2.4577
5	8.7941	7.0079	6.063	6.063	7.0079	8.7941
10	17.1728	14.9308	13.9419	13.9419	14.9308	17.1728
13	21.5783	19.5870	18.6116	18.6116	19.5870	21.5783

TABLE XVII
APPROXIMATED SHORELINE EVOLUTION ALONG 13 YEARS USING THE SAULYEV FINITE DIFFERENCE TECHNIQUES WHEN T-HEAD GROIN SIZE 22 M

Time (Years)	Distance(m)					
	0	20	40	60	80	100
1	2.4578	1.1770	0.5173	0.5169	1.1763	2.4574
5	8.7940	7.0079	6.0628	6.0629	7.0079	8.7940
10	17.1735	14.9311	13.942	13.9417	14.9306	17.1728
13	21.5774	19.5868	18.6117	18.6116	19.5870	21.5786

TABLE XVIII
APPROXIMATED SHORELINE EVOLUTION ALONG 20 YEARS USING THE TRADITIONAL FORWARD TIME CENTERED SPACE TECHNIQUES WHEN T-HEAD GROIN SIZE 24 M

Time (Years)	Distance(m)					
	0	20	40	60	80	100
1	1.0972	0.5544	0.2391	0.2391	0.5544	1.0972
5	3.2598	2.3726	2.0848	2.0848	2.3729	3.2598
10	4.285	4.1421	3.9454	3.9454	4.1421	4.285
15	6.8976	6.014	5.7506	5.7506	6.014	6.8976
20	7.8626	7.6623	7.4815	7.4815	7.6623	7.8626

TABLE XIX
APPROXIMATED SHORELINE EVOLUTION ALONG 20 YEARS USING THE SAULYEV FINITE DIFFERENCE TECHNIQUES WHEN T-HEAD GROIN SIZE 24 M

Time (Years)	Distance(m)					
	0	20	40	60	80	100
1	1.0975	0.5547	0.2392	0.2389	0.554	1.0968
5	3.2607	2.3731	2.0852	2.0848	2.3724	3.2596
10	4.2846	4.1417	3.945	3.9455	4.1424	4.2851
15	6.8987	6.0147	5.751	5.7506	6.0137	6.8975
20	7.8624	7.6618	7.4811	7.4815	7.6626	7.8627

TABLE XX
APPROXIMATED SHORELINE EVOLUTION ALONG 20 YEARS USING THE TRADITIONAL FORWARD TIME CENTERED SPACE TECHNIQUES WHEN T-HEAD GROIN SIZE 26 M

Time (Years)	Distance(m)					
	0	20	40	60	80	100
1	1.4976	0.5985	0.2596	0.2596	0.5985	1.4976
5	4.3015	3.3562	2.9214	2.9214	3.3562	4.3015
10	7.6055	6.8702	6.4288	6.4288	6.8702	7.6055
15	11.6917	10.6384	10.1618	10.1618	10.6384	11.6917
20	15.1301	14.3789	13.922	13.922	14.3789	15.1301

TABLE XXI
APPROXIMATED SHORELINE EVOLUTION ALONG 20 YEARS USING THE SAULYEV FINITE DIFFERENCE TECHNIQUES WHEN T-HEAD GROIN SIZE 26 M

Time (Years)	Distance(m)					
	0	20	40	60	80	100
1	1.4979	0.5988	0.2598	0.2595	0.5983	1.4974
5	4.3016	3.3563	2.9215	2.9213	3.3561	4.3014
10	7.6051	6.8701	6.4288	6.4289	6.8703	7.6056
15	11.6919	10.6386	10.1621	10.1619	10.6382	11.6916
20	15.1297	14.3787	13.922	13.9222	14.3791	15.1303

TABLE XXII
APPROXIMATED SHORELINE EVOLUTION ALONG 20 YEARS USING THE TRADITIONAL FORWARD TIME CENTERED SPACE TECHNIQUES WHEN T-HEAD GROIN SIZE 28 M

Time (Years)	Distance(m)					
	0	20	40	60	80	100
1	0.7186	0.3100	0.0987	0.0987	0.3100	0.7186
5	2.8822	1.9768	1.7127	1.7127	1.9768	2.8822
10	4.0363	3.7656	3.5555	3.5555	3.7656	4.0363
15	6.8627	5.8516	5.5533	5.5533	5.8516	6.8627
20	8.1678	7.800	7.5806	7.5806	7.800	8.1678

TABLE XXIII
APPROXIMATED SHORELINE EVOLUTION ALONG 20 YEARS USING THE SAULYEV FINITE DIFFERENCE TECHNIQUES WHEN T-HEAD GROIN SIZE 28 M

Time (Years)	Distance(m)					
	0	20	40	60	80	100
1	0.7189	0.3103	0.0989	0.0986	0.3095	0.718
5	2.8834	1.9772	1.7129	1.7125	1.9764	2.8819
10	4.0361	3.7650	3.5549	3.5555	3.7658	4.0364
15	6.8640	5.8523	5.5536	5.5532	5.8513	6.8625
20	8.1674	7.7994	7.5800	7.5805	7.8002	8.1679

TABLE XXIV
APPROXIMATED SHORELINE EVOLUTION ALONG 20 YEARS USING THE TRADITIONAL FORWARD TIME CENTERED SPACE TECHNIQUES WHEN T-HEAD GROIN SIZE 30 M

Time (Years)	Distance(m)					
	0	20	40	60	80	100
1	1.2549	0.4986	0.2042	0.2042	0.4986	1.2549
5	2.8227	2.0405	1.8249	1.8249	2.0405	2.8227
10	3.0897	3.1776	3.0660	3.0660	3.1776	3.0897
15	5.4009	4.6835	4.4527	4.4527	4.6835	5.4009
20	5.8824	5.8600	5.7502	5.7502	5.8600	5.8824

TABLE XXV
APPROXIMATED SHORELINE EVOLUTION ALONG 20 YEARS USING THE SAULYEV FINITE DIFFERENCE TECHNIQUES WHEN T-HEAD GROIN SIZE 30 M

Time (Years)	Distance(m)					
	0	20	40	60	80	100
1	1.2554	0.4992	0.2044	0.2041	0.4982	1.2546
5	2.8240	2.0415	1.8256	1.8249	2.0401	2.8224
10	3.0883	3.1765	3.0652	3.0660	3.1781	3.0900
15	5.4021	4.6844	4.4533	4.4527	4.6830	5.4006
20	5.8817	5.8593	5.7497	5.7502	5.8604	5.8824

VI. Discussion

In this paper, we considered the averaged wave crest impact (α_0) as obtained by (29) for eight T-head groin sizes as seen in Table 1-8. The long-shore transport rate (D) for each month as seen in Table 9.

We used numerical techniques, the traditional forward time centered space techniques (FTCS), and the Saulyev finite difference techniques to approximate the shoreline evolution for eight T-head groin sizes.

The approximated shoreline evolution for T-head groin size 16 m with a time duration of eight years is seen in Table 10, 11, and Fig 18. As a result of shoreline evolution, the longest distance is 15.9615 meters, and the shortest distance is 12.9092 meters.

The approximated shoreline evolution for T-head groin size 18 m with a time duration of 11 years is seen in Table 12, 13, and Fig 19. As a result of shoreline evolution, the longest distance is 14.6822 meters, and the shortest distance is 17.2724 meters.

The approximated shoreline evolution for T-head groin size 20 m with a time duration of 15 years is seen in Table 14, 15, and Fig 20. As a result of shoreline evolution, the longest distance is 19.2123 meters, and the shortest distance is 16.7981 meters.

The approximated shoreline evolution for T-head groin size 22 m with a time duration of 13 years is seen in Table 16, 17, and Fig 21. As a result of shoreline evolution, the longest distance is 21.5786 meters, and the shortest distance is 18.4889 meters.

The approximated shoreline evolution for T-head groin size 24 m with a time duration of 20 years is seen in Table 18, 19, and Fig 22. As a result of shoreline evolution, the longest distance is 7.8627 meters, and the shortest distance is 7.4590 meters.

The approximated shoreline evolution for T-head groin size 26 m with a time duration of 20 years is seen in Table 20, 21, and Fig 23. As a result of shoreline evolution, the longest distance is 15.1303 meters, and the shortest distance is 13.8656 meters.

The approximated shoreline evolution for T-head groin size 28 m with a time duration of 20 years is seen in Table 22, 23 and Fig 24. As a result of shoreline evolution, the longest distance is 8.1679 meters, and the shortest distance is 7.5526 meters.

The approximated shoreline evolution for T-head groin size 30 m with a time duration of 9 years is seen in Table 24, 25, and Fig 25. As a result of shoreline evolution, the longest distance is 5.8824 meters, and the shortest distance is 5.7362 meters.

Approximate shoreline evolutions of all numerical approaches in eight sizes of the considered T-head groin are compatible.

The approximate shoreline evolution of T-head groin sizes of 16, 18, 20, and 22 m is used over time durations of 9, 11, 15, and 13 years, respectively, making the approximate shoreline comparable in size to the T-head groin. Other approximate T-head groin sizes are used over a time duration of 20 years. The approximate shoreline is still in the T-head groin area. The approximate shoreline tends to decrease with T-head groin sizes of 26, 28, and 30 m.

VII. Conclusion

In this paper, we introduce a shoreline evolution model was created in this research to adjust for the T-head groin structure. The nonuniform breaking wave crest impact is estimated using the wave crest impact model. The average wave crest impact for eight sizes of T-head groin structures is considered. The shoreline evolution in areas where T-head groins are installed on both sides. The initial condition setting approach and boundary conditions techniques, as well as the structural impacts of the T-head groin, are discussed. The traditional forward time centered space techniques (FTCS) and the unconditionally stable Saulyev finite differential techniques are used to approximate shoreline evolution each year. The estimated impacts of shoreline evolution were consistent with the wave crest impact model for eight different T-head groin sizes. As a result, the size of T-head groin influences the approximated shoreline evolution. The time duration of the approximate shoreline comparable in size to the T-head groin increases as the size of the T-head groin increases. But the size of the T-head groin is too large, the approximate shoreline evolution rate is lower, and the approximate shoreline evolution has resulted in a smaller shoreline area.

References

[1] 1 C. Netzold and I. Mohamed, "Seawalls as a response to coastal erosion and flooding: a case study from Grande Comore, Comoros (West Indian Ocean)," Regional Environmental Change 17, pp. 1077–1087, 2017.

[2] 2 A. Fitri. R. Hashim, S. Abolfathi, and Khairul Nizam Abdul Maulud, "Dynamics of Sediment Transport and Erosion-Deposition Patterns in the Locality of a Detached Low-Crested Breakwater on a Cohesive Coast," Water, Vol. 11, 28 pages, 2019.

[3] 3 Le Xuan Roan, "Some results of comparison between numerical and analytic solutions of the one-line model for shoreline change," Vietnam Journal of Mechanics, VAST, Vol. 28, pp. 94-102, 2006.

[4] 4 Alia Khurram, and David W Kammler, "Numerical Generation of Images for the Gibbs Phenomenon Near a Corner in the Plane," IAENG International Journal of Applied Mathematics, vol. 44, no. 1, pp. 15-22, 2014.

[5] 5 W. T. Bakker, "The dynamics of coast with a groin system," Proceeding of 11th Coastal Engineering Conference 1969, pp. 492–517.

[6] 6 W. T. Bakker, and T. Edelman, "The coastline of river deltas," Proceeding of 9th Coastal Engineering Conference 1965, pp. 199–218.

[7] 7 W. Grijimr, "Theoretical form of shoreline," Proceeding of 7th Coastal Engineering Conference 1961, pp. 197–202.

[8] 8 W. Grijimr, "Theoretical form of shoreline," Proceeding of 9th Coastal Engineering Conference 1965, pp. 219–235.

[9] 9 B. Le Mahute, and M. Soldate, "Mathematical Modeling of Shoreline Evolution," US Army Corps of Engineer Waterways Experiment Station, CERC, 1977.

[10] 10 H. Hanson, M. Larson, and N. C. Kraus, "Analytical Solution of the One-line Model for Shoreline Changel," US Army Corps of Engineer Waterways Experiment Station, CERC, 1987.

[11] 11 T. Waltonand, and T. Chiu, "A review of analytical technique to solve the sand transport equation and some simplified solution," Coastal Structure, pp. 809–837, 1979.

[12] 12 M. Mamat Subiyanto, M. F. Ahmad, and M. L. Husain, "Comparison of numerical method for forward and backward time centered space for long – term simulation of shoreline evolution," Applied Mathematical Sciences, Vol. 7, pp. 5165–5173, 2013.

[13] 13 Pidok Unyapoti and Nopparat Pochai, "A One-Dimensional Mathematical Model of Long-Term Shoreline Evolution with Groin System using an Unconditionally Stable Explicit Finite Difference Method," International Journal of Simulation: Systems, Science and Technology, vol. 21, no.3, pp. 2.1-2.6, 2020.

[14] 14 N. Pochai, "Unconditional stable numerical techniques for a water-quality model in a non-uniform flow stream," Advances in Difference Equations, vol. 2017, Article ID 286, 13 pages, 2017.

[15] 15 P. Samalerk, and N. Pochai, "Numerical Simulation of a One-Dimensional Water-Quality Model in a Stream Using a Saulyev Technique with Quadratic Interpolated Initial-Boundary Conditions," Abstract and Applied Analysis, vol. 2018, Article ID 1926519, 7 pages, 2018.

[16] 16 Shixiang Zhou, Fanwei Meng, Qinghua Feng, and Li Dong, "A Spatial Sixth Order Finite Difference Scheme for Time Fractional Sub-diffusion Equation with Variable Coefficient," IAENG International Journal of Applied Mathematics, vol. 47, no. 2, pp. 175-181, 2017.

[17] 17 Kewalee Suebyat, and Nopparat Pochai, "A Numerical Simulation of a Three-dimensional Air Quality Model in an Area Under a Bangkok Sky Train Platform Using an Explicit Finite Difference Scheme," IAENG International Journal of Applied Mathematics, vol. 47, no. 4, pp. 471-476, 2017.

[18] 18 Tata Sutardi, Linwei Wang, Manosh C. Paul, and Nader Karimi, "Numerical Simulation Approaches for Modelling a Single Coal Particle Combustion and Gasification," Engineering Letters, vol. 26, no. 2, pp. 257-266, 2018.

[19] 19 Ben Wongsaijai, Kanyuta Poochinapan, and Thongchai Disyadej, "A Compact Finite Difference Method for Solving the General Rosenau-RLW Equation," IAENG International Journal of Applied Mathematics, vol. 44, no. 4, pp. 192-199, 2014.

[20] 20 Linna Li, Zhirou Wei, and Qiongdan Huang, "A Numerical Method for Solving Fractional Variational Problems by the Operational Matrix Based on Chelyshkov Polynomials," Engineering Letters, vol. 28, no. 2, pp. 486-491, 2020.

[21] 21 Pompon Othata and Nopparat Pochai, "A Mathematical Model of Salinity Control in a River with an Effect of Internal Waves using Two Explicit Finite Difference Methods," Engineering Letters, vol 29, no 2, pp.689-696, 2021.

[22] 22 M. S. Jara, M. González, and R. Medina, "Shoreline evolution model from a dynamic equilibrium beach profile," Coastal Engineering, vol. 99, pp. 1-14, 2015.

[23] 23 L. P. Stein, and E. Siegle, "Overtopping events on seawall-backed beaches: Santos Bay, SP, Brazil," Regional Studies in Marine Science, Vol. 40, 101492, 2020.

[24] 24 Dalrino, R. Herdianto and D. B. Silitonga, "Study of groin structures effectiveness for against abrasion in Padang Beach," IOP Conference Series: Earth and Environmental Science, vol. 708, pp. 012035, 2021.

[25] 25 Witsarut Kraychang, and Nopparat Pochai, "A Simple Numerical Model for Water Quality Assessment with Constant Absorption around Nok Phrao Island of Trang River," Engineering Letters, vol. 28, no. 3, pp. 912-922, 2020.

[26] 26 Witsarut Kraychang and Nopparat Pochai, "Numerical Treatment to a Water-Quality Measurement Model in an Opened-Closed Reservoir," Thai Journal of Mathematics, vol.13, pp. 775-788, 2015.

[27] 27 Pidok Unyapoti and Nopparat Pochai, "A Shoreline Evolution Model with a Twin Groins Structure using Unconditionally Stable Explicit Finite Difference Techniques." Engineering Letters, vol. 29, no. 1, pp. 288-296, 2021.

N. Pochai is a researcher of Centre of Excellence in Mathematics, MHESI, Bangkok 10400, Thailand.

P. Unyapoti is an assistant researcher of Centre of Excellence in Mathematics, MHESI, Bangkok 10400, Thailand.

Author Biography

Name	Mr. Pidok Unyapoti
Date of Birth	21 July 1995
Address	151/1, Nakhon Nayok Province, Wangkrajom District, 26000
Education	2017 Bachelor of Science in Applied Mathematics GPA 3.55 King Mongkut's Institute of Technology Ladkrabang
	2020 Master of Science in Applied Mathematics GPA 3.78 King Mongkut's Institute of Technology Ladkrabang
	2022 Doctoral of Science in Applied Mathematics GPA 3.8x King Mongkut's Institute of Technology Ladkrabang
Scholarship(s)	Assistant Researcher by Centre of Excellence in Mathematics(CEM) Mahidol university.

Academic Publication(s)

Pidok Unyapoti and Nopparat Pochai, "A one-dimensional mathematical model of long-term shoreline evolution with groin system using an unconditionally stable explicit finite difference method", International Journal of Simulation: Systems, Science and Technology, Vol. 21, No.3, (2020), pp. 2.12.6

Pidok Unyapoti and Nopparat Pochai, "A Shoreline Evolution Model with a Twin Groins Structure using Unconditionally Stable Explicit Finite Difference Techniques." Engineering Letters, vol. 29, no. 1, pp. 288-296, 2021.

Pidok Unyapoti and Nopparat Pochai, "A Shoreline Evolution Model with a Groin Structure under Non-Uniform Breaking Wave Crest Impact." Computation, 2021, 9, 42.

Pidok Unyapoti and Nopparat Pochai, "A Shoreline Evolution Model With the Wavelength Effect of Breaking Waves on Groin Structures." International Journal of Computer Science, vol. 49, no. 3, 12 pages, 2022.

Pidok Unyapoti and Nopparat Pochai, "A Combination of A Shoreline Evolution Model and A Wave Crest Model on T-Head Groin Structures with the Breaking Wave Effect."

International Journal of Computer Science, vol. 50, no. 2, 12 pages, 2023.